Data Summary Report for the Monitoring Survey at the Isles of Shoals Disposal Site North - September 2015

Disposal Area Monitoring System DAMOS

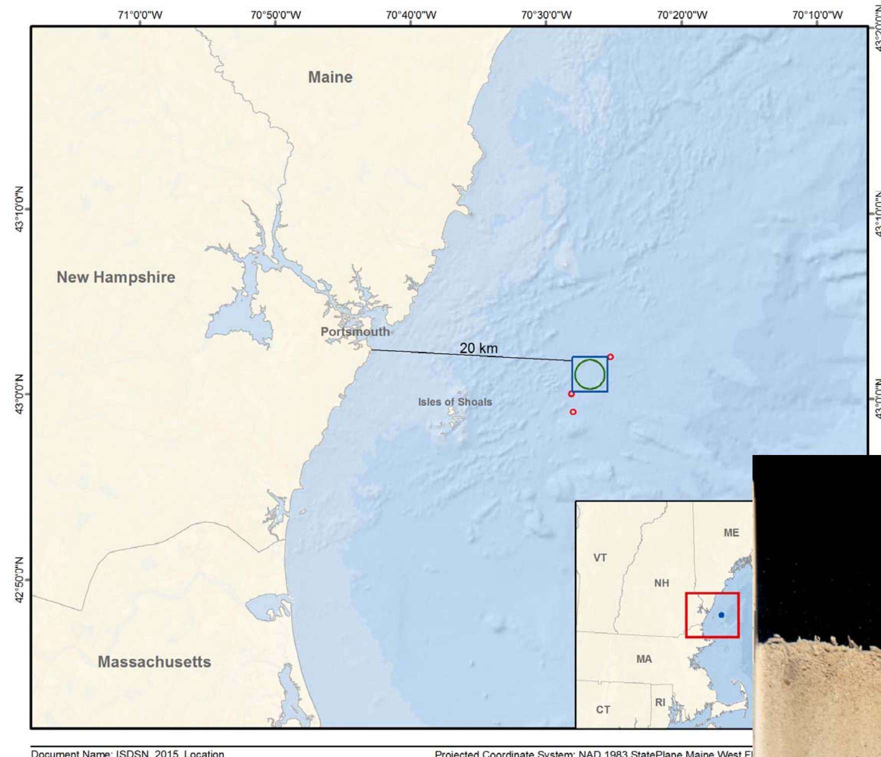

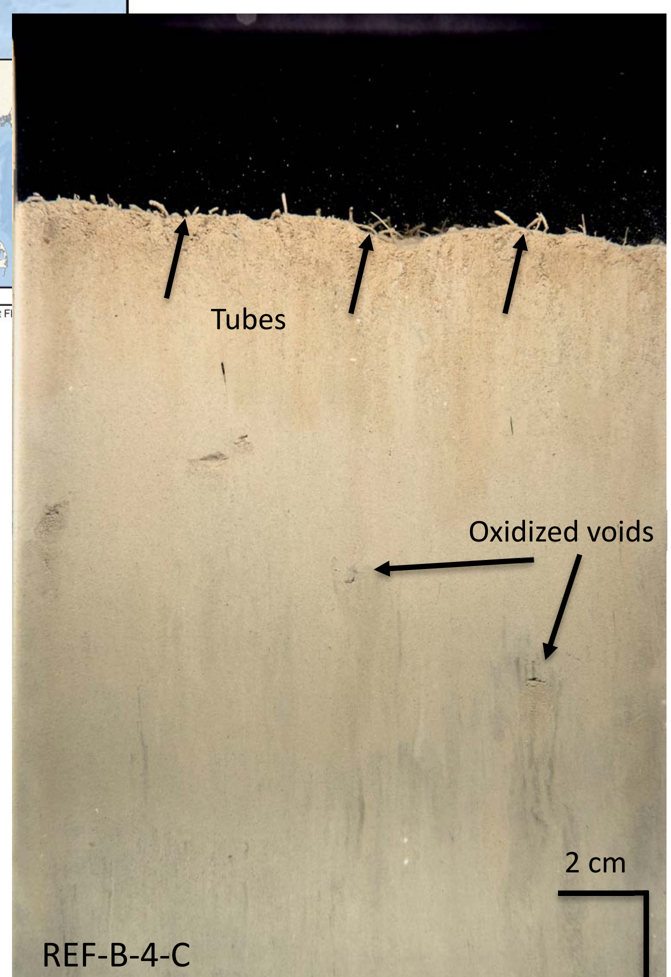

D A M O S

DISPOSAL AREA MONITORING SYSTEM

Data Summary Report 2015-D-01

June 2016

US Army Corps of Engineers®

New England District

This report should be cited as:

Guarinello, M. L.; Carey, D. A.; Wright, C. 2016. Data Summary Report for the Monitoring Survey at the Isles of Shoals Disposal Site North, September 2015. U.S. Army Corps of Engineers, New England District, Concord, MA, 63 pp.

Note on units of this report: As a scientific data summary, information and data are presented in the metric system. However, given the prevalence of English units in the dredging industry of the United States, conversions to English units are provided for general information in Section 1. A table of common conversions can be found in Appendix A.

TABLE OF CONTENTS

Page

LIST OF TABLES iii
LIST OF FIGURES iv
LIST OF ACRONYMS vii

1.0 INTRODUCTION 1
1.1 Overview of the DAMOS Program 1
1.2 Introduction to the Isles of Shoals Disposal Site North 2
1.3 2015 Survey Objectives 2
2.0 METHODS 5
2.1 Navigation and On-Board Data Acquisition 5
2.2 Acoustic Survey 5
2.2.1 Acoustic Survey Planning 5
2.2.2 Acoustic Data Collection 6
2.2.3 Bathymetric Data Processing 6
2.2.4 Backscatter Data Processing 7
2.2.5 Side-Scan Sonar Data Processing 8
2.2.6 Acoustic Data Analysis 8
2.3 Sediment-Profile and Plan-View Imaging Survey 8
2.3.1 SPI and PV Survey Planning 8
2.3.2 Sediment-Profile Imaging 8
2.3.3 Plan-View Imaging 9
2.3.4 SPI and PV Data Collection 10
2.3.5 Image Conversion and Calibration 10
2.3.6 SPI and PV Data Analysis 11
2.3.7 Statistical Methods 12
3.0 RESULTS 23
3.1 Acoustic Survey 23
3.1.1 Bathymetry 23
3.1.2 Acoustic Backscatter and Side-Scan Sonar 23
3.1.3 Comparison with Previous Bathymetry 24
3.2 Sediment-Profile and Plan-View Imaging 24
3.2.1 Reference Areas 24
3.2.2 Proposed Disposal Site 25
3.2.3 Comparison to Reference Areas 27
4.0 SUMMARY 60
5.0 REFERENCES 61
6.0 DATA TRANSMITTAL 63

APPENDICES

A Table of Common Conversions

B ISDSN 2015 Survey Actual SPI/PV Replicate Locations

C Sediment-Profile and Plan-View Image Analysis Results for ISDSN Survey, September 2015

D Grain Size Scale for Sediments

LIST OF TABLES

Page

Table 2-1. Accuracy and Uncertainty Analysis of Bathymetric Data 16

Table 2-2. ISDSN 2015 Survey Target SPI/PV Station Locations....................................... 17

Table 3-1. Summary of ISDSN Reference Stations Sediment-Profile Imaging Results (station means), September 2015 28

Table 3-2. Summary of ISDSN Site Stations Sediment-Profile Imaging Results (station means), September 2015 29

Table 3-3. Summary of Station Means for aRPD and Successional Stage by Sampling Location 31

Table 3-4. Summary Statistics and Results of Inequivalence Hypothesis Testing for aRPD Values 31

LIST OF FIGURES

Page

Figure 1-1. Location of Isles of Shoals Disposal Site North (ISDSN) 3

Figure 1-2. ISDSN site boundary and reference areas on existing bathymetry from an NOS 1947 data set 4

Figure 2-1. ISDSN acoustic survey area and tracklines 19

Figure 2-2. ISDSN proposed disposal site and reference areas with target SPI/PV stations 20

Figure 2-3. Schematic diagram of the SPI/PV camera deployment 21

Figure 2-4. The stages of infaunal succession as a response of soft-bottom benthic communities to (A) physical disturbance or (B) organic enrichment; from Rhoads and Germano (1982) 22

Figure 3-1. Bathymetric contour map of ISDSN – September 2015..................................... 32

Figure 3-2. Bathymetric depth data over acoustic relief model of ISDSN – September 2015.. 33

Figure 3-3. Mosaic of unfiltered backscatter data of ISDSN – September 2015 34

Figure 3-4. Filtered backscatter over acoustic relief model of ISDSN – September 2015.. 35

Figure 3-5. Side-scan mosaic of ISDSN – September 2015.. 36

Figure 3-6. Bathymetric depth data at ISDSN proposed reference areas with SPI/PV stations indicated... 37

Figure 3-7. Sediment grain size major mode (phi units) at the ISDSN reference areas.......... 38

Figure 3-8. Mean station camera prism penetration depths (cm) at the ISDSN reference areas 39

Figure 3-9. Sediment-profile images from (A) Station REF-B-2 and (B) Station REF-C-4 where camera penetration depths were shallower and where there was evidence of possible dredged material at depth 40

Figure 3-10. Mean station small-scale boundary roughness values (cm) at the ISDSN reference areas 41

Figure 3-11. Sediment-profile images depicting small-scale boundary roughness created by biological activity of surface and subsurface dwelling infauna at (A) Station REF-B-4 and (B) Station ISDSN-18 42

Figure 3-12. Mean station aRPD depths (cm) at the ISDSN reference areas 43

Figure 3-13. Mean aRPD depths (cm) were shallower at (A) Station REF-C-2, compared to the other reference areas, e.g., (B) Station REF-A-1. Note: The sloughing of sediment particles near the surface of (A) is an occasional artifact of the camera action. 44

Figure 3-14. Infaunal successional stages found at stations at the ISDSN reference areas 45

Figure 3-15. Infaunal successional stages found at the ISDSN reference areas: Stage 1 on 3 at (A) Station REF-B-4 with small tubes at surface and oxidized voids at depth; (B) Station REF-A-1 with fecal pellets, small tubes at surface, clear subsurface burrows, polychaetes (worm), and a large void 46

Figure 3-16. Maximum subsurface feeding void depth at ISDSN reference areas 47

Figure 3-17. Plan-view images depicting small to medium burrows and small tubes at (A) Station REF-C-3 and (B) ISDSN-29 48

Figure 3-18. Plan-view images depicting tracks indicative of a mobile epifauna community at (A) Station REF-B-3-A and (B) ISDSN-24-A 49

Figure 3-19. ISDSN with SPI/PV stations indicated 50

Figure 3-20. Sediment grain size major mode (phi) at ISDSN 51

Figure 3-21. Mean station camera prism penetration depth (cm) at ISDSN 52

Figure 3-22. Sediment-profile images with evidence of possible dredged material at (A) Station ISDSN-5 and (B) Station ISDSN-12 53

Figure 3-23. Mean station small-scale boundary roughness values (cm) at ISDSN 54

Figure 3-24. Mean station aRPD depth (cm) at ISDSN 55

Figure 3-25. Mean aRPD depths (cm) and infaunal successional stages found at ISDSN: Stage 1 on 3 at (A) Station ISDSN-22 with small tubes at surface, shallow burrowing, and oxidized voids at depth; (B) Station ISDSN-3 with small tubes at surface, shallow burrowing, and subsurface void; and (C) Station ISDSN-14 with small to medium tubes at surface, shallow burrowing, in-filled voids at depth 56

Figure 3-26. Infaunal successional stages found at ISDSN 57

Figure 3-27. Maximum subsurface feeding void depth at ISDSN reference areas 58

Figure 3-28. Boxplot showing distribution of station mean aRPD depths (cm) for 2015 ISDSN and each of the reference areas.. 59

LIST OF ACRONYMS

aRPD	Apparent redox potential discontinuity
ASCII	American Standard Code for Information Interchange
CCOM	Center for Coastal and Ocean Mapping
CI	Confidence interval
CTD	Conductivity-temperature-depth
DAMOS	Disposal Area Monitoring System
DGPS	Differential global positioning system
GIS	Graphic information system
GPS	Global positioning system
ISDSN	Isles of Shoals Disposal Site North
JHC	Joint Hydrographic Center
JPEG	Joint Photographic Experts Group
MBES	Multibeam echosounder
MLLW	Mean lower low water
MPRSA	Marine Protection Research and Sanctuaries Act
NAE	New England District
NEF	Nikon Electronic Format
NOAA	National Oceanic and Atmospheric Administration
NOS	National Ocean Service
NTRIP	Network transport of RTCM data over IP
PV	Plan-view
RGB	Red green blue (file format)
RTCM	Radio Technical Commission for Maritime Services
RTK	Real time kinematic GPS
SHP	Shapefile or geospatial data file
SOP	Standard Operating Procedures
SPI	Sediment-profile imaging
TVG	time-varied gain
TIF	Tagged image file
USACE	U.S. Army Corps of Engineers

1.0 INTRODUCTION

A monitoring survey was conducted at a potential new open water dredged material disposal site, the Isles of Shoals Disposal Site North (ISDSN), in September 2015 as part of the U.S. Army Corps of Engineers (USACE) New England District (NAE) Disposal Area Monitoring System (DAMOS) Program. DAMOS is a comprehensive monitoring and management program designed and conducted to address environmental concerns surrounding the placement of dredged material at aquatic disposal sites throughout the New England region. An overview of the DAMOS Program and ISDSN is provided below.

1.1 Overview of the DAMOS Program

The DAMOS Program features a tiered management protocol designed to ensure that any potential adverse environmental impacts associated with dredged material disposal are promptly identified and addressed (Germano et al. 1994). For over 35 years, the DAMOS Program has collected and evaluated disposal site data throughout New England. Based on these data, patterns of physical, chemical, and biological responses of seafloor environments to dredged material disposal activity have been documented (Fredette and French 2004).

DAMOS monitoring surveys fall into two general categories: confirmatory studies and focused studies. The data collected and evaluated during these studies provide answers to strategic management questions in determining the next step in the disposal site management process to guide the management of disposal activities at existing sites, plan for use of future sites, and evaluate the long-term status of historic sites.

Confirmatory studies are designed to test hypotheses related to expected physical and ecological response patterns following placement of dredged material on the seafloor at established, active disposal sites. Two primary goals of DAMOS confirmatory monitoring surveys are to document the physical location and stability of dredged material placed into the aquatic environment and to evaluate the biological recovery of the benthic community following placement of dredged material. Several survey techniques are employed in order to characterize these responses to dredged material placement. Sequential acoustic monitoring surveys (including bathymetric, acoustic backscatter, and side-scan sonar data collection) are performed to characterize the height and spread of discrete dredged material deposits or mounds created at open water sites as well as the accumulation/consolidation of dredged material into confined aquatic disposal cells.

Sediment-profile (SPI) and plan-view (PV) imaging surveys are often performed in both confirmatory and focused studies to provide further physical characterization of the material and to support evaluation of seafloor (benthic) habitat conditions and recovery over time. Each type of data collection activity is conducted periodically at disposal sites and the conditions found after a defined period of disposal activity are compared with the long-term data set at specific sites to determine the next step in the disposal site management process (Germano et al. 1994).

Focused studies are periodically undertaken within the DAMOS Program to evaluate inactive or historical disposal sites and contribute to the development of dredged material placement and management techniques. Focused DAMOS monitoring surveys may also feature additional types of data collection activities as deemed appropriate to achieve specific survey objectives, such as subbottom profiling, towed video, sediment coring, or grab sampling. The 2015 ISDSN investigation was considered a confirmatory/reconnaissance study for possible designation of the site as a formal disposal site by the U.S. Environmental Protection Agency (USEPA) under Section 103 of the Marine Protection Research and Sanctuaries Act (MPRSA). This survey included a baseline acoustic survey and a SPI/PV imaging survey.

1.2 Introduction to the Isles of Shoals Disposal Site North

ISDSN is located in the Gulf of Maine, approximately 20 km (10.8 nmi) east of Portsmouth, New Hampshire (Figure 1-1). ISDSN is being considered by NAE for selection as a dredged material disposal site and for possible designation by USEPA under Section 103 of MPRSA. This potential disposal site is currently defined as a 3000-m (9840-ft) diameter circle on the seafloor with its center located at 70° 26.680' W and 43° 1.309' N. Three potential reference areas (REF-A, REF-B, and REF-C) were defined as 250-m radius circles located at 70° 25.165' W, 42° 59.282' N; 70° 28.039' W, 43° 0.257' N; and 70° 27.895' W, 43° 2.280' N, respectively (Figure 1-2). Reference areas were selected based on a review of existing data prior to the survey to represent areas of the seafloor with similar bathymetric characteristics. Previous work at the site has included side-scan sonar performed by USEPA from their ocean survey vessel *BOLD* and grab sampling for grain size and benthic biology analysis performed by NAE (all unpublished data).

Water depths at ISDSN vary from 78 m (255 ft) to 104 m (340 ft) and gradually slope from approximately 90 m (295 ft) on the western boundary to 100 m (328 ft) in the southeastern portion of the site (Figure 1-2). Topographic highs are present in the northwest, southeast, and northeast corners of the site (Figure 1-2). In 2015 the Center for Coastal and Ocean Mapping Joint Hydrographic Center at the University of New Hampshire (UNH/NOAA CCOM) published composite bathymetric and backscatter data for the Western Gulf of Maine, an area that includes ISDSN (UNH/NOAA CCOM 2015). These data were used for comparison purposes.

1.3 2015 Survey Objectives

An acoustic survey was conducted at ISDSN to characterize the seafloor topography and surface features. Additionally, a sediment-profile/plan-view (SPI/PV) imaging survey was conducted to further define the physical characteristics of surface sediment and to assess the benthic status over the proposed site and potential reference areas (Figure 1-2).

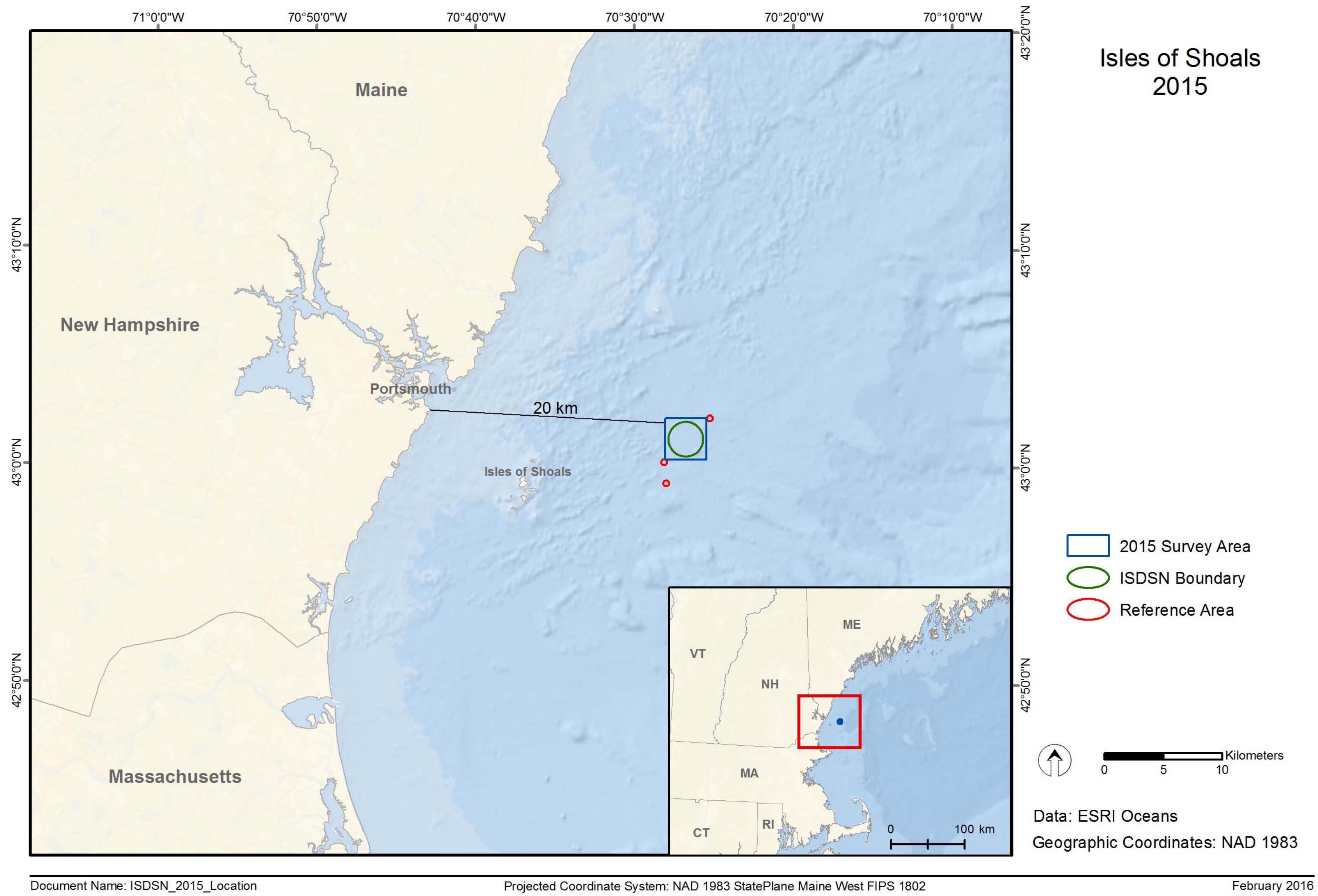

Figure 1-1. Location of Isles of Shoals Disposal Site North (ISDSN)

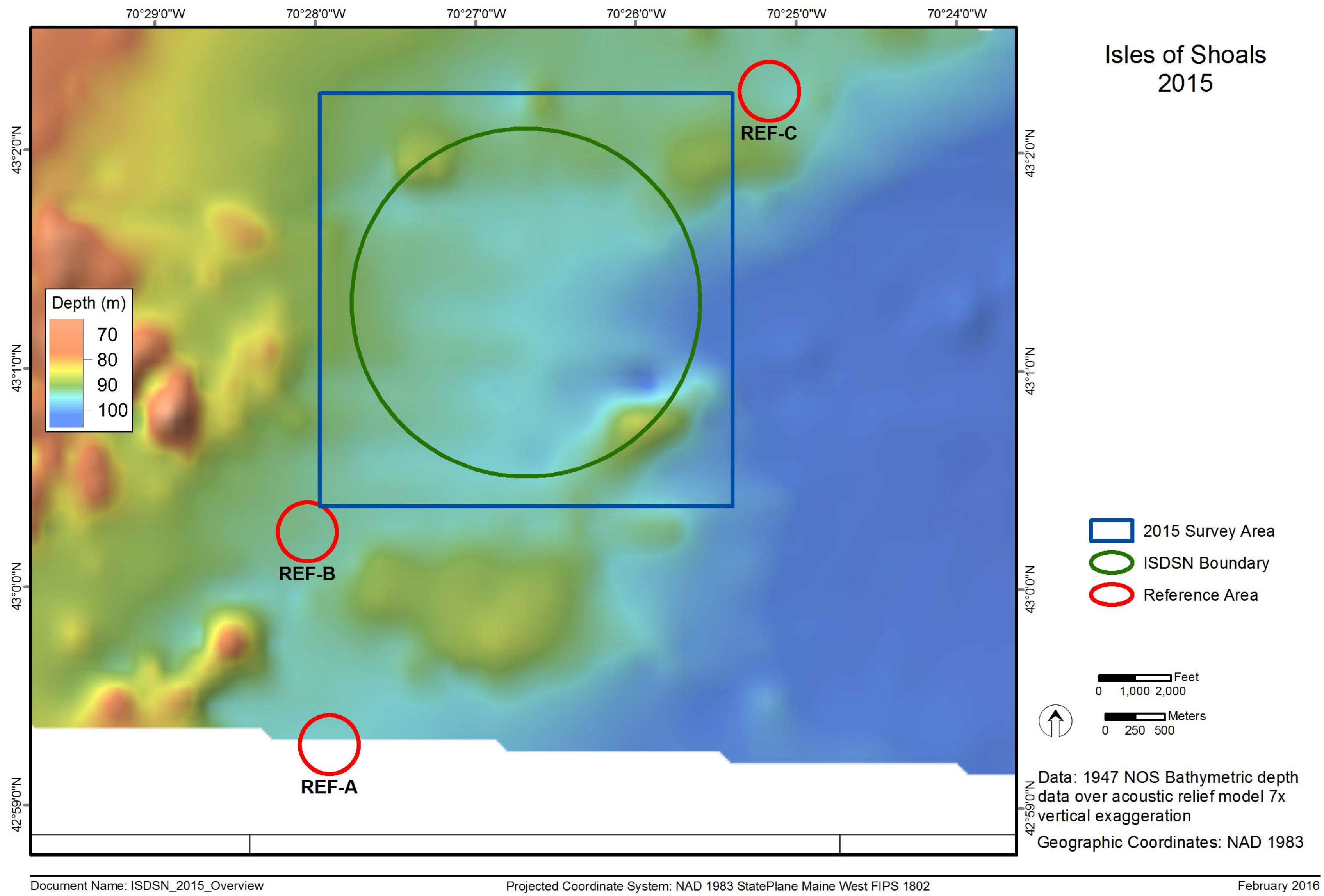

Figure 1-2. ISDSN site boundary and reference areas on existing bathymetry from an NOS 1947 data set

2.0 METHODS

The September 2015 survey at ISDSN was conducted by a team of investigators from DAMOSVision (CoastalVision, CR Environmental, and Germano & Associates) aboard the 55-foot R/V *Jamie Hanna*. The acoustic survey was conducted 15-16 September 2015 and the SPI/PV survey was conducted 25-27 September 2015. An overview of the methods used to collect, process, and analyze the survey data is provided below. Detailed Standard Operating Procedures (SOPs) for data collection and processing are available in Carey et al. (2013).

2.1 Navigation and On-Board Data Acquisition

Navigation for the acoustic survey was accomplished using a Hemisphere VS-330 Real-time kinematic Global Positioning System (RTK GPS) which received base station correction through the Keynet NTRIP broadcast. Horizontal position accuracy in fixed RTK mode was approximately 2 cm. A dual-antennae Hemisphere VS110 differential GPS (DGPS) was available if necessary as a backup. The GPS system was interfaced to a desktop computer running HYPACK MAX® hydrographic survey software. HYPACK MAX® continually recorded vessel position and GPS satellite quality and provided a steering display for the vessel captain to accurately maintain the position of the vessel along pre-established survey transects and targets. Vessel heading measurements were provided by an IxBlue Octans III fiber optic gyrocompass.

Navigation for the SPI survey was accomplished using a Hemisphere R110 sub-meter DGPS.

2.2 Acoustic Survey

The acoustic survey included bathymetric, backscatter, and side-scan sonar data collection. The bathymetric data provided measurements of water depth that, when processed, were used to map the seafloor topography. Backscatter and side-scan sonar data provided images that supported the characterization of surface sediment texture and roughness. Each of these acoustic data types is useful for assessing dredged material placement and surface sediment features.

2.2.1 Acoustic Survey Planning

The acoustic survey featured a high spatial resolution survey of ISDSN. DAMOSVision hydrographers coordinated with USACE NAE scientists and reviewed alternative survey designs. For ISDSN, a 3500 × 3500 m area was selected. Hydrographers obtained site coordinates, imported them to graphic information system (GIS) software, and created maps to aid planning. Base bathymetric data were obtained from the National Ocean Service Hydrographic Data Base to estimate the transect separation required to obtain full bottom coverage using an assumed beam angle limit of 90-degrees (45 degrees to port, 45 degrees to starboard). Transects spaced 150 m apart and cross-lines spaced 500 m apart were created to meet conservative beam angle constraints (Figure 2-1). The proposed survey area and design were then reviewed and approved by NAE scientists. Additional transects were added to the southwest and northeast of the primary survey area to characterize potential reference areas.

2.2.2 Acoustic Data Collection

The 2015 multibeam bathymetric survey of ISDSN was conducted 15-16 September 2015. Data layers generated by the survey included bathymetric, acoustic backscatter, and side-scan sonar and were collected using an R2Sonic 2022 broadband multibeam echosounder (MBES). This 200-400 kHz system forms up to 256 1-2° beams (frequency dependent) distributed equiangularly or equidistantly across a 10-160° swath. The MBES transducer was mounted amidships to the port rail of the survey vessel using a high strength adjustable boom. The primary GPS antenna was mounted on the transducer boom. The transducer depth below the water surface (draft) and antenna height were checked and recorded at the beginning and end of data acquisition, and the draft was confirmed using the "bar check" method.

An IxBlue Octans III motion reference unit (MRU) was interfaced to the MBES topside processor and to the acquisition computer. Precise linear offsets between the MRU and MBES were recorded and applied during acquisition. Depth and backscatter data were synchronized using pulse-per-second timing and transmitted to the HYPACK MAX® acquisition computer via Ethernet communications. Several patch tests were conducted during the survey to allow computation of angular offsets between the MBES system components.

The system was calibrated for local water mass speed of sound by performing sound velocity profile (SVP) casts at frequent intervals throughout the survey day using a Seabird, Inc. SBE-19 CTD.

2.2.3 Bathymetric Data Processing

Bathymetric data were processed using HYPACK HYSWEEP® software. Processing components are described below and included:

- Adjustment of data for tidal elevation fluctuations
- Correction of ray bending (refraction) due to density variation in the water column
- Removal of spurious points associated with water column interference or system errors
- Development of a grid surface representing depth solutions
- Statistical estimation of sounding solution uncertainty
- Generation of data visualization products

Tidal adjustments were accomplished using RTK GPS. Water surface elevations derived using RTK were adjusted to Mean Lower Low Water (MLLW) elevations using NOAA's VDATUM Model. Processed RTK tide data were successfully ground-truthed against a data series acquired at NOAA's Fort Point Tide Station (#8423898). While tidal amplitudes from RTK data and NOAA data were similar, the comparison documented a high tide time offset of approximately -15 minutes between the NOAA Station and the survey area.

Correction of sounding depth and position (range and azimuth) for refraction due to water column stratification was conducted using a series of fourteen sound-velocity profiles acquired by the survey team. Data artifacts associated with refraction remain in the bathymetric surface model at a relatively fine scale (generally less than 5 to 10 cm) relative to the survey depth.

Data acquired in the disposal site portion of the survey area were filtered to accept only beams falling within an angular limit of 45° to minimize refraction artifacts. Spurious sounding solutions were rejected based on the careful examination of data on a sweep-specific basis.

The R2Sonics 2022 MBES system was operated at 200 kHz. At this frequency the system has a published beam width of 2.0°. Assuming an average depth of 94 m and a maximum beam angle of 45°, the average diameter of the beam footprint was calculated at approximately 3.8 × 3.6 m (13.7 m^2). Data were reduced to a cell (grid) size of 5.0 × 5.0 m, acknowledging the system's fine range resolution while accommodating beam position uncertainty. This data reduction was accomplished by calculating and exporting the average elevation for each cell in accordance with USACE recommendations (USACE 2013).

Statistical analysis of data as summarized on Table 2-1 showed negligible tide bias and vertical uncertainty substantially lower than values recommended by USACE (2013) or NOAA (2015). Note that the most stringent National Ocean Service (NOS) standard for this project depth (Special Order 1A) would call for a 95^{th} percentile confidence interval (95% CI) of 0.82 m at the maximum site depth (103.8 m) and 0.75 m at the average site depth (94.1 m).

Reduced data were exported in ASCII text format with fields for Easting, Northing, and MLLW Elevation (meters). All data were projected to the Maine State Plane (West), NAD83 (metric). A variety of data visualizations were generated using a combination of ESRI ArcMap (V.10.1) and Golden Software Surfer (V.13). Visualizations and data products included:

- ASCII data files of all processed soundings including MLLW depths and elevations
- Contours of seabed elevation (50-cm and 1.0-m intervals) in a geospatial data file (SHP) format suitable for plotting using GIS and computer-aided design software
- 3-dimensional surface maps of the seabed created using 5× vertical exaggeration and artificial illumination to highlight fine-scale features not visible on contour layers delivered in grid and tagged image file (TIF) formats, and
- An acoustic relief map of the survey area created using 2× vertical exaggeration, delivered in georeferenced TIF format.

2.2.4 Backscatter Data Processing

Backscatter data were extracted from cleaned MBES TruePix formatted files then used to provide an estimation of surface sediment texture based on seabed surface roughness. Mosaics of backscatter data were created using HYPACK®'s implementation of GeoCoder software developed by scientists at the University of New Hampshire's NOAA Center for Coastal and Ocean Mapping (UNH/NOAA CCOM). A seamless mosaic of unfiltered backscatter data was developed and exported in grayscale TIF format. Backscatter data were also exported in ASCII format with fields for Easting, Northing, and backscatter (dB). A Gaussian filter was applied to backscatter data to minimize nadir artifacts and the filtered data were used to develop backscatter values on a 2-m grid. The grid was exported as an ESRI binary GRD format to facilitate comparison with other data layers.

2.2.5 Side-Scan Sonar Data Processing

Side-scan sonar data were processed using both Chesapeake Technology, Inc. Sonar Wiz software and HYPACK®'s implementation of GeoCoder software to generate a database of images that maximized both textural information and structural detail.

A seamless mosaic of side-scan sonar data was developed using GeoCoder and exported in grayscale TIF format using a resolution of 0.35 m per pixel. This mosaic optimized textural information but is less well suited for analysis of fine seabed structures due to blending of overlapping data. Three additional mosaics of side-scan data were created using SonarWiz to facilitate detailed inspection of sonar imagery. Mosaic versions included raw swath data, data with a customized time-varied gain (TVG) curve developed to normalize across-track signal attenuation, and a version that utilized an automatic gain adjustment algorithm.

2.2.6 Acoustic Data Analysis

The processed bathymetric grids were converted to rasters, and bathymetric contour lines and acoustic relief models were generated and displayed using GIS. The backscatter mosaics and filtered backscatter grid were combined with acoustic relief models in GIS to facilitate visualization of relationships between acoustic datasets. This is done by rendering images and color-coded grids with sufficient transparency to allow three-dimensional acoustic relief model to be visible underneath.

2.3 Sediment-Profile and Plan-View Imaging Survey

SPI/PV imaging are monitoring techniques used to provide data on the physical characteristics of the seafloor and the status of the benthic biological community (Germano et al. 2011).

2.3.1 SPI and PV Survey Planning

For the ISDSN survey, a total of 45 SPI/PV stations were planned with 30 stations located in the proposed disposal site, and 5 stations in each of the three proposed reference areas (REF-A, REF-B, and REF-C). A random location generator was used to select the locations of all the SPI/PV stations (Figure 2-2). SPI/PV station locations are provided in Table 2-1 and actual SPI/PV station replicate locations are provided in Appendix B.

2.3.2 Sediment-Profile Imaging

The SPI technique involves deploying an underwater camera system to photograph a cross-section of the sediment-water interface. In the 2015 survey at ISDSN, high-resolution SPI images were acquired using a Nikon® D7100 digital single-lens reflex camera mounted inside an Ocean Imaging® Model 3731 pressure housing. The pressure housing sat atop a wedge-shaped steel prism with a glass front faceplate and a back mirror. The mirror was mounted at a 45° angle to reflect the profile of the sediment-water interface. As the prism penetrated the seafloor, a trigger activated a time-delay circuit that fired an internal strobe to obtain a cross-sectional image of the upper 15–20 cm of the sediment column (Figure 2-3).

The camera remained on the seafloor for approximately 20 seconds to ensure that a successful image had been obtained. Details of the camera settings for each digital image are available in the associated parameters file embedded in each electronic image file. For this survey, the ISO-equivalent was set at 640, shutter speed was 1/250, f-stop was f9, and storage was in compressed raw Nikon Electronic Format (NEF) files (approximately 30 MB each).

Test exposures of the X-Rite Color Checker Classic Color Calibration Target were made on deck at the beginning of the survey to verify that all internal electronic systems were working to design specifications and to provide a color standard against which final images could be checked for proper color balance. After deployment of the camera at each station, the frame counter was checked to ensure that the requisite number of replicates had been obtained. In addition, a prism penetration depth indicator on the camera frame was checked to verify that the optical prism had actually penetrated the bottom to a sufficient depth. If images were missed or the penetration depth was insufficient, the camera frame stop collars were adjusted and/or weights were added or removed, and additional replicate images were taken. Changes in prism weight amounts, the presence or absence of mud doors, and frame stop collar positions were recorded for each replicate image.

Each image was assigned a unique time stamp in the digital file attributes by the camera's data logger and cross-checked with the time stamp in the navigational system's computer data file. In addition, the field crew kept redundant written sample logs. Images were downloaded periodically to verify successful sample acquisition and/or to assess what type of sediment/depositional layer was present at a particular station. Digital image files were renamed with the appropriate station names immediately after downloading as a further quality assurance step.

2.3.3 Plan-View Imaging

An Ocean Imaging® Model DSC24000 plan-view underwater camera (PV) system with two Ocean Imaging® Model 400-37 Deep Sea Scaling lasers was attached to the sediment-profile camera frame and used to collect plan-view photographs of the seafloor surface; both SPI and PV images were collected during each "drop" of the system. The PV system consisted of a Nikon D-7100 encased in an aluminum housing, a 24 VDC autonomous power pack, a 500 W strobe, and a bounce trigger. A weight was attached to the bounce trigger with a stainless steel cable so that the weight hung below the camera frame; the scaling lasers projected two red dots that are separated by a constant distance (26 cm) regardless of the field-of-view of the PV system. The field-of-view can be varied by increasing or decreasing the length of the trigger wire and thereby the camera height above the bottom when the picture is taken. As the camera apparatus was lowered to the seafloor, the weight attached to the bounce trigger contacted the seafloor prior to the camera frame hitting the bottom and triggered the PV camera (Figure 2-3). Details of the camera settings for each digital image are available in the associated parameters file embedded in each electronic image file; for this survey, the ISO-equivalent was set at 640. The additional camera settings used were as follows: shutter speed 1/250, f14, white balance set to flash, color mode set to Adobe RGB, sharpening set to none, noise reduction off, and storage in compressed raw NEF files (approximately 30 MB each).

Prior to field operations, the internal clock in the digital PV system was synchronized with the GPS navigation system and the SPI camera. Each PV image acquired was assigned a time stamp in the digital file and redundant notations in the field and navigation logs. Throughout the survey, PV images were downloaded at the same time as the SPI images after collection and evaluated for successful image acquisition and image clarity.

The ability of the PV system to collect usable images was dependent on the clarity of the water column. Water conditions at ISDSN allowed use of a 0.9-m trigger wire, resulting in an area of bottom visualization approximately 1.0 m × 0.5 m in size.

2.3.4 SPI and PV Data Collection

The SPI/PV survey was conducted at ISDSN from 25-27 September 2015 aboard the R/V *Jamie Hanna*. At each station, the vessel was positioned at the target coordinates and the camera was deployed within a defined station tolerance of 10 m. Four replicate SPI and PV images were collected at each of the stations (Appendix B). The three replicates with the best quality images from each station were chosen for analysis (Appendix C).

The DGPS described above was interfaced to HYPACK® software via laptop serial ports to provide a method to locate and record sampling locations. Throughout the survey, the HYPACK® data acquisition system received DGPS data. The incoming data stream was digitally integrated and stored on the PC's hard drive. The system provided a steering display to enable the vessel captain to navigate to the pre-established survey target locations. The navigator electronically recorded the vessel's position when the equipment contacted the seafloor and the winch wire went slack. Each replicate SPI/PV position was recorded and time stamped. Actual SPI/PV sampling locations were recorded using this system.

2.3.5 Image Conversion and Calibration

Following completion of the field operations, the raw image files were color calibrated in Adobe Camera Raw® by synchronizing the raw color profiles to an X-Rite Color Checker Classic Color Calibration Target that was photographed on-site with the SPI camera. The raw images were then converted to high-resolution Photoshop Document (PSD) format files, using a lossless conversion file process, maintaining an Adobe RGB (1998) color profile. The PSD images were then calibrated and analyzed in Adobe Photoshop®. Image calibration was achieved by measuring the pixel length of a 5 cm scale bar printed on the X-Rite Color Checker Target, providing a pixel per centimeter calibration. This calibration information was applied to all SPI images analyzed. Linear and area measurements were recorded as the number of pixels and converted to scientific units using the calibration information.

Measured parameters were recorded on a Microsoft Excel© spreadsheet. Germano and Associates' senior scientist Dr. Joseph D. Germano subsequently checked these data as an independent quality assurance/quality control review of the measurements before final interpretation was performed. Spatial distributions of SPI parameters from stations within the study area were mapped using ArcGIS.

2.3.6 SPI and PV Data Analysis

Computer-aided analysis of the resulting images provided a set of standard measurements to allow comparisons between different locations and different surveys. The DAMOS Program has successfully used this technique for over 30 years to map the distribution of disposed dredged material and to monitor benthic recolonization at disposal sites.

2.3.6.1 SPI Data Analysis

Analysis of each SPI image was performed to provide measurement of the following standard set of parameters:

<u>Sediment Type</u>– The sediment grain size major mode and range were estimated visually from the images using a grain size comparator at a similar scale. Results were reported using the phi scale. Conversion to other grain size scales is provided in Appendix D. The presence and thickness of disposed dredged material were also assessed by inspection of the images.

<u>Penetration Depth</u>– The depth to which the camera penetrated into the seafloor was measured to provide an indication of the sediment density or bearing capacity. The penetration depth can range from a minimum of 0 cm (i.e., no penetration on hard substrata) to a maximum of 20 cm (full penetration on very soft substrata).

<u>Surface Boundary Roughness</u>– Surface boundary roughness is a measure of the vertical relief of features at the sediment-water interface in the sediment-profile image. Surface boundary roughness was determined by measuring the vertical distance between the highest and lowest points of the sediment-water interface. The surface boundary roughness measured over the width of sediment-profile images typically ranges from 0 to 4 cm and may be related to physical structures (e.g., ripples, rip-up structures, mud clasts) or biogenic features (e.g., burrow openings, fecal mounds, foraging depressions).

<u>Apparent Redox Potential Discontinuity (aRPD) Depth</u>– The aRPD depth provides a measure of the integrated time history of the balance between near-surface oxygen conditions and biological reworking of sediments. Sediment particles exposed to oxygenated waters oxidize and lighten in color to brown or light gray. As the particles are buried or moved down by biological activity, they are exposed to reduced oxygen concentrations in subsurface pore waters and their oxic coating slowly reduces, changing color to dark gray or black. When biological activity is high, the aRPD depth increases; when it is low or absent, the aRPD depth decreases. The aRPD depth was measured by visually assessing color and reflectance boundaries within the images, and for each image a mean aRPD was calculated.

<u>Infaunal Successional Stage</u>– Infaunal successional stage is a measure of the biological community inhabiting the seafloor. Current theory holds that organism-sediment interactions in fine-grained sediments follow a predictable sequence of development after a major disturbance (such as dredged material disposal) and this sequence has been divided subjectively into four

stages (Rhoads and Germano 1982, 1986). Successional stage was assigned by assessing which types of species or organism-related activities were apparent in the images (Figure 2-4).

Additional components of the SPI analysis included calculation of means and ranges for the parameters listed above and mapping of means of replicate values from each station. Station means were calculated from three replicates from each station and used in statistical analysis.

2.3.6.2 PV Data Analysis

The PV images provided a much larger field-of-view than the SPI images and provided valuable information about the landscape ecology and sediment topography in the area where the pinpoint "optical core" of the sediment profile was taken. Unusual surface sediment layers, textures, or structures detected in any of the sediment-profile images can be interpreted in light of the larger context of surface sediment features; i.e., is a surface layer or topographic feature a regularly occurring feature and typical of the seafloor in this general vicinity or just an isolated anomaly? The scale information provided by the underwater lasers allows for accurate density counts (number per square meter) of attached epifaunal colonies, sediment burrow openings, or larger macrofauna or fish which may have been missed in the sediment-profile cross section. Information on sediment transport dynamics and bedform wavelength were also available from PV image analysis. Analysts calculated the image size and field-of-view and noted sediment type; recorded the presence of bedforms, burrows, tubes, tracks, trails, epifauna, mud clasts, and debris; and included descriptive comments (Appendix C).

2.3.7 Statistical Methods

In order to meet the objective of this survey to assess the baseline status of benthic community at the proposed disposal site relative to reference area conditions, statistical analyses were conducted to compare key SPI variables between the proposed disposal site and reference areas (REF-A, REF-B, REF-C). The aRPD depth and successional stage measured in each image are the best indicators of infaunal activity measured by SPI and were, therefore, used in this comparative analysis. Standard boxplots were generated for visual assessment of the central tendency and variation in each of these variables within the proposed disposal site and each reference area. Tests rejecting the inequivalence between the reference areas and disposal site were conducted, as described in detail below.

The objective to look for differences is conventionally addressed using a point null hypothesis of the form, "There is no significant difference in benthic conditions between the reference area and the disposal site." However, there is always some difference (perhaps only to a very small decimal place) between groups, but the statistical significance of this difference may or may not be ecologically meaningful. On the other hand, differences may not be detected due to insufficient statistical power. Without a power analysis and specification of what constitutes an ecologically meaningful difference, the results of conventional point null hypothesis testing often provide inadequate information for ecological assessments (Germano 1999). An approach using an inequivalence null hypothesis will identify when groups are statistically similar, within a specified interval, which is more suited to the objectives of the DAMOS monitoring program.

For an inequivalence test, the null hypothesis presumes the difference is great; this is recognized as a "proof of safety" approach because rejection of the inequivalence null hypothesis requires sufficient proof that the difference was actually small (e.g., McBride 1999). The null and alternative hypotheses for the inequivalence hypothesis test are:

$$H_0: \ d < -\delta \text{ or } d > \delta \text{ (presumes the difference is great)}$$

$$H_A: \ -\delta < d < \delta \text{ (requires proof that the difference is small)}$$

where d is the difference between a reference mean and a site mean. If the inequivalence null hypothesis is rejected, then it is concluded that the two means are equivalent to one another within ±δ units. The size of δ should be determined from historical data, and/or best professional judgment, to identify a maximum difference that is within background variability and is therefore not ecologically meaningful. Primarily differences greater than δ are of ecological interest. Previously established δ values of 1 cm for aRPD depth, and 0.5 for successional stage rank (on the 0–3 scale) were used.

The test of this inequivalence (interval) hypothesis can be broken down into two one-sided tests, TOST (McBride 1999, Schuirmann 1987). Assuming a symmetric distribution, the inequivalence hypothesis is rejected at α of 0.05 if the 90% confidence interval for the measured difference (or, equivalently, the 95% upper limit *and* the 95% lower limit for the difference) is wholly contained within the equivalence interval [-δ, +δ]. The statistics used to test the interval hypotheses shown here are based on the Central Limit Theorem (CLT) and basic statistical properties of random variables. A simplification of the CLT states that the mean of any random variable is normally distributed. Linear combinations of normal random variables are also normal so a linear function of means is also normally distributed. When a linear function of means is divided by its standard error the ratio follows a t-distribution with degrees of freedom associated with the variance estimate. Hence, the t-distribution can be used to construct a confidence interval around any linear function of means.

In this survey, four distinct locations were sampled, three were categorized as reference areas (REF-A, REF-B, REF-C) and one was the proposed disposal location. The difference equation of interest was the linear contrast of the average of the three reference means minus the disposal site mean, or

$$\hat{d} = [1/3 \text{ x } (\text{Mean}_{\text{REF-A}} + \text{Mean}_{\text{REF-B}} + \text{Mean}_{\text{REF-C}}) - (\text{Mean}_{\text{Disposal}})] \qquad \text{[Eq. 1]}$$

where $\text{Mean}_{\text{Disposal}}$ was the mean for all samples within the proposed disposal site. The three reference areas collectively represented ambient conditions, but if the means were different among these three areas, then pooling them into a single reference group would inflate the variance estimate because it would include the variability between areas, rather than only the variability between stations within each single homogeneous area. The effect of keeping the three reference areas separate has no effect on the grand reference mean when sample size is equal among these areas, but it ensures that the variance is truly the residual variance within a single population with a constant mean.

The difference equation, $\hat{d}$, for the comparison of interest was specified in Eq. 1 and the standard error of this difference equation uses the fact that the variance of a sum is the sum of the variances for independent variables, or:

$$SE(\hat{d}) = \sqrt{\sum_j \left(S_j^2 c_j^2 / n_j\right)} \qquad \text{[Eq. 2]}$$

where:

c_j = coefficients for the j means in the difference equation, $\hat{d}$ [Eq. 1] (i.e., for equation 1 shown above, the coefficients were 1/3 for each of the 3 reference areas, and -1 for the proposed disposal site).

S_j^2 = variance for the jth area. If equal variances are assumed, the pooled residual variance estimate equal to the mean square error from an ANOVA based on all groups involved, can be used for each S_j^2.

n_j = number of stations for the jth area.

The inequivalence null hypothesis is rejected (and equivalence concluded) if the confidence interval on the difference of means, $\hat{d}$, is fully contained within the interval [–δ , + δ]. Thus the decision rule was to reject H_0 (the two groups are inequivalent) if:

$$D_L = \hat{d} - t_{\alpha,\upsilon} SE(\hat{d}) > -\delta \quad \text{and} \quad D_U = \hat{d} + t_{\alpha,\upsilon} SE(\hat{d}) < \delta \qquad \text{[Eq. 3]}$$

where:

$\hat{d}$ = observed difference in means between the reference areas and disposal site.

$t_{\alpha,\upsilon}$ = upper (1-α)*100th percentile of a Student's t-distribution with υ degrees of freedom (α = 0.05)

$SE(\hat{d})$ = standard error of the difference ([Eq. 2])

υ = degrees of freedom for the standard error. If a pooled residual variance estimate was used, this was the residual degrees of freedom from an ANOVA on all groups (total number of stations minus the number of groups); if separate variance estimates were used, degrees of freedom were calculated based on the Welch-Sattherthwaite estimation (Satterthwaite 1946, Welch 1947, with the results nicely summarized on the Wikipedia page for 'Welch-Satterthwaite equation'; a two sample example is found in Zar 1996).

Validity of normality and equal variance assumptions was tested using Shapiro-Wilk's test for normality on the area residuals ($\alpha = 0.05$) and Levene's test for equality of variances among the 4 areas ($\alpha = 0.05$). If normality was not rejected but equality of variances was, then normal parametric confidence bounds were calculated, using separate variance estimates for each group. If normality was rejected, then non-parametric bootstrapped estimates of the confidence bounds were calculated.

Table 2-1.

Accuracy and Uncertainty Analysis of Bathymetric Data

		Results (m)		
Survey Date(s)	**Quality Control Metric**	**Mean**	**95% Uncertainty**	**Range**
9/15-16/2015	Cross-Line Swath Comparisons	0.01	0.22	
	Within Cell Uncertainty	0.05	0.11	0.00 - 2.76
	Beam Angle Uncertainty (0 - 45d)	0.01	0.24	0.18 - 0.34

Notes:
1. The mean of cross-line nadir and full swath comparisons are indicators of tide bias.
2. 95% uncertainty values were calculated using the sums of mean differences and standard deviations expressed at the 2-sigma level.
3. Within cell uncertainty values include biases and random errors.
4. Beam angle uncertainty was assessed by comparing cross-line data (45-degree swath limit) with a reference surface created using mainstay transect data.
5. Swath and cell based comparisons were conducted using 5 m x 5 m cell averages. These analyses do not exclude sounding variability associated with terrain slopes. Uncertainties associated with slope are depicted on maps within the report.

Table 2-2.

ISDSN 2015 Survey Target SPI/PV Station Locations

Station Name	Easting	Northing	Latitude (N)	Longitude (W)
1	875912.3	22183.2	43° 1.958'	70° 27.734'
2	876412.2	22524.9	43° 2.144'	70° 27.367'
3	877234.2	22130.5	43° 1.933'	70° 26.761'
4	877545.5	22478.6	43° 2.121'	70° 26.533'
5	877941.7	22565.0	43° 2.168'	70° 26.241'
6	878791.4	22387.7	43° 2.074'	70° 25.615'
7	875969.1	21497.3	43° 1.588'	70° 27.691'
8	876584.5	21520.4	43° 1.602'	70° 27.238'
9	877339.6	21411.6	43° 1.544'	70° 26.681'
10	877728.6	21485.9	43° 1.585'	70° 26.396'
11	877985.3	21553.2	43° 1.622'	70° 26.207'
12	879052.3	21994.4	43° 1.862'	70° 25.422'
13	875832.2	20694.7	43° 1.154'	70° 27.790'
14	876554.8	21230.5	43° 1.445'	70° 27.259'
15	877289.0	20785.4	43° 1.206'	70° 26.717'
16	877801.4	21117.6	43° 1.387'	70° 26.341'
17	878404.0	21208.7	43° 1.437'	70° 25.898'
18	878830.8	20720.2	43° 1.174'	70° 25.582'
19	875797.3	20486.5	43° 1.042'	70° 27.815'
20	876498.9	20371.9	43° 0.982'	70° 27.298'
21	876919.1	20552.2	43° 1.079'	70° 26.989'
22	877888.8	20380.9	43° 0.989'	70° 26.275'
23	878195.8	20359.4	43° 0.977'	70° 26.049'
24	878642.4	20506.2	43° 1.058'	70° 25.721'
25	876075.3	19586.3	43° 0.556'	70° 27.608'
26	876515.2	19306.1	43° 0.406'	70° 27.283'
27	877318.7	19706.0	43° 0.623'	70° 26.693'
28	877533.2	19591.3	43° 0.562'	70° 26.535'
29	878431.0	19305.2	43° 0.409'	70° 25.873'
30	878971.3	19320.4	43° 0.418'	70° 25.476'
REF-A-01	875836.9	17199.6	43° -0.733'	70° 27.777'
REF-A-02	875624.1	17210.3	43° -0.728'	70° 27.934'
REF-A-03	875561.9	17012.4	43° -0.835'	70° 27.979'
REF-A-04	875537.4	17332.6	43° -0.662'	70° 27.998'
REF-A-05	875605.9	17165.6	43° -0.752'	70° 27.947'
REF-B-01	875644.3	18929.2	43° 0.200'	70° 27.923'

Station Name	Easting	Northing	Latitude (N)	Longitude (W)
REF-B-02	875339.8	19183.8	43° 0.337'	70° 28.148'
REF-B-03	875391.3	18874.4	43° 0.170'	70° 28.109'
REF-B-04	875358.0	19172.3	43° 0.331'	70° 28.135'
REF-B-05	875543.7	19033.2	43° 0.257'	70° 27.997'
REF-C-01	879365.9	22613.4	43° 2.197'	70° 25.193'
REF-C-02	879444.2	22982.5	43° 2.396'	70° 25.136'
REF-C-03	879499.2	22702.5	43° 2.245'	70° 25.095'
REF-C-04	879216.8	22819.3	43° 2.308'	70° 25.303'
REF-C-05	879286.3	22806.2	43° 2.301'	70° 25.252'

Notes
1. Grid coordinates are State Plane Maine West FIPS 1802 (NAD83), metric
2. Geographic coordinates are NAD83 degrees decimal minute

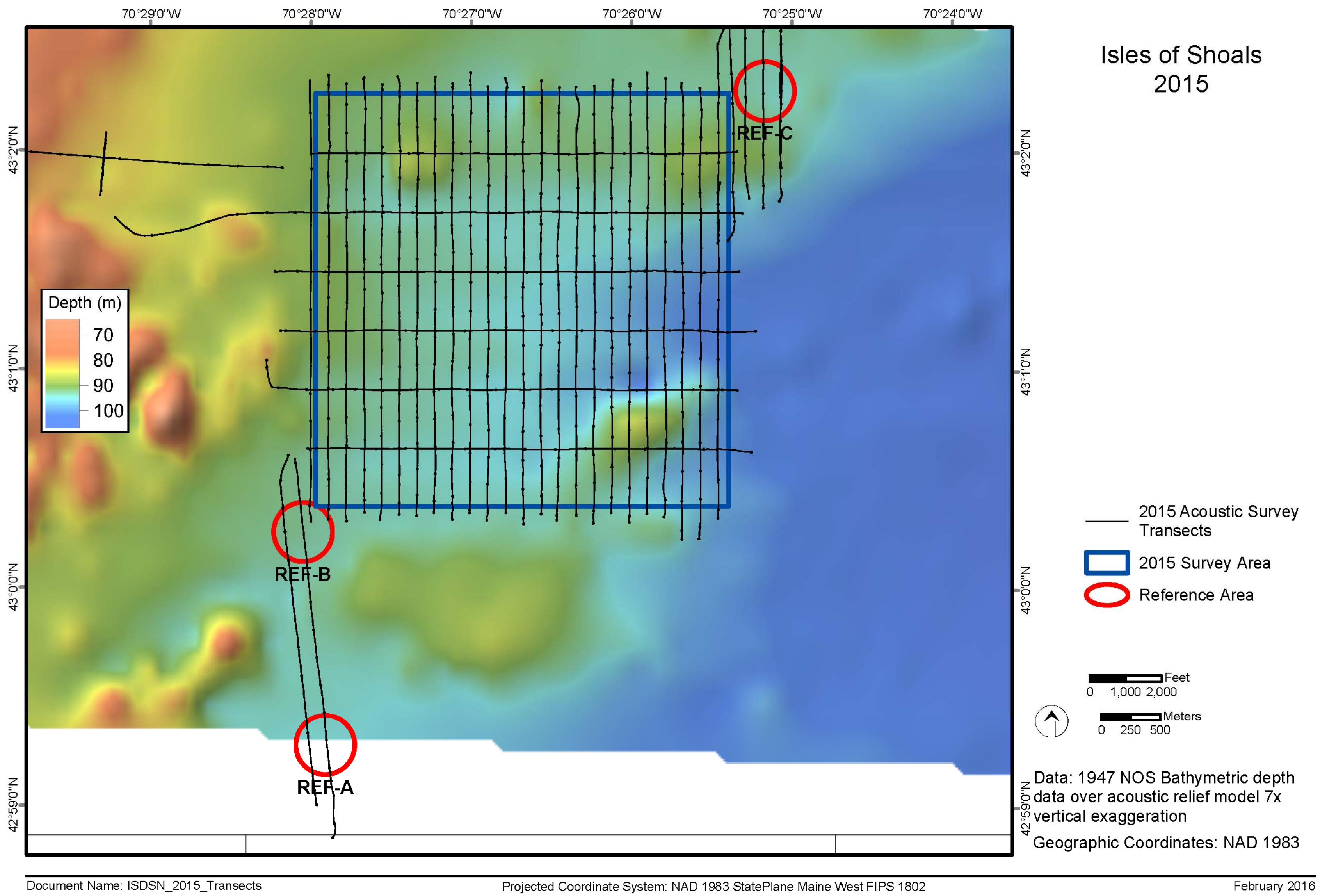

Figure 2-1. ISDSN acoustic survey area and tracklines

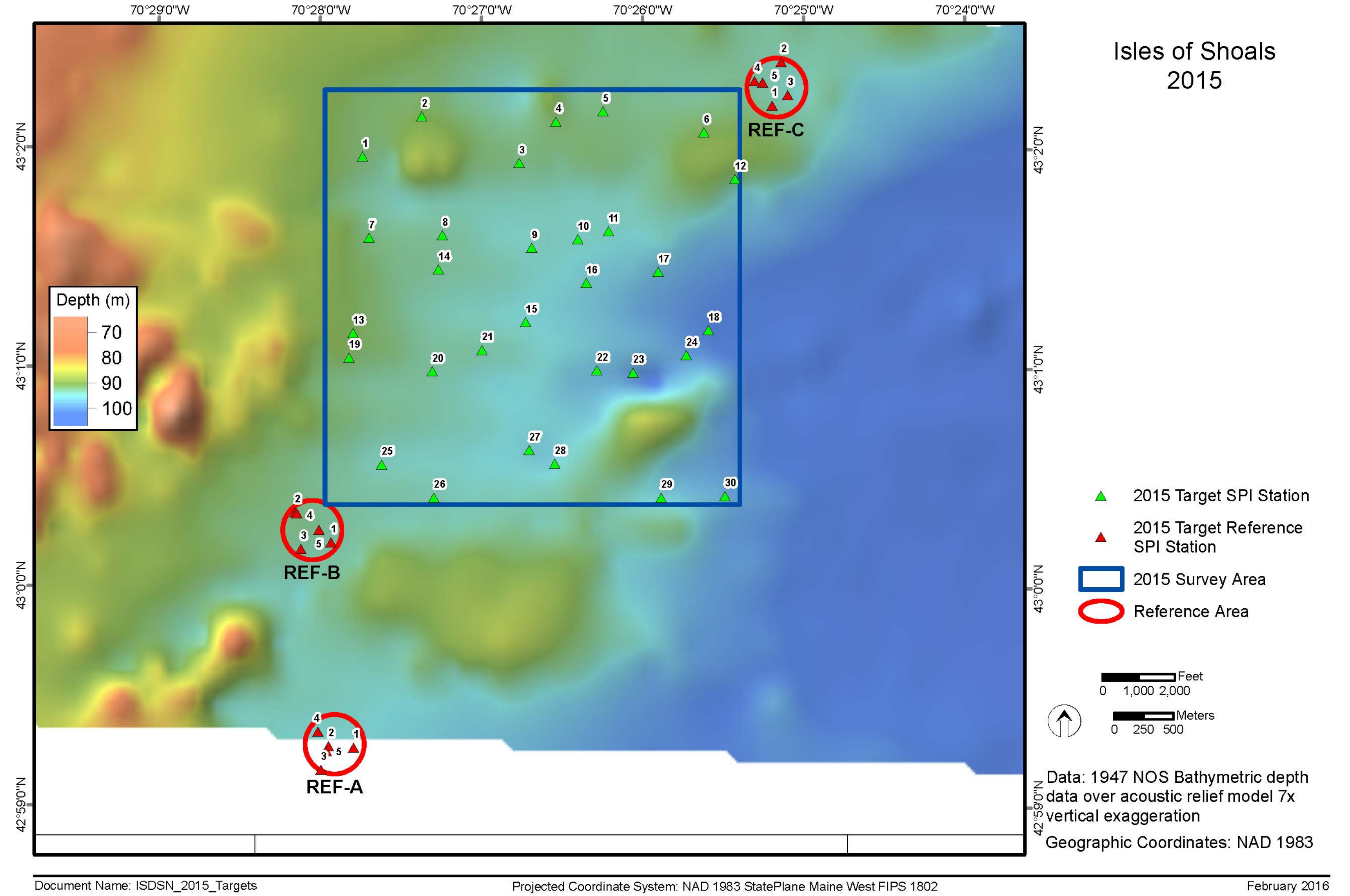

Figure 2-2. ISDSN proposed disposal site and reference areas with target SPI/PV stations

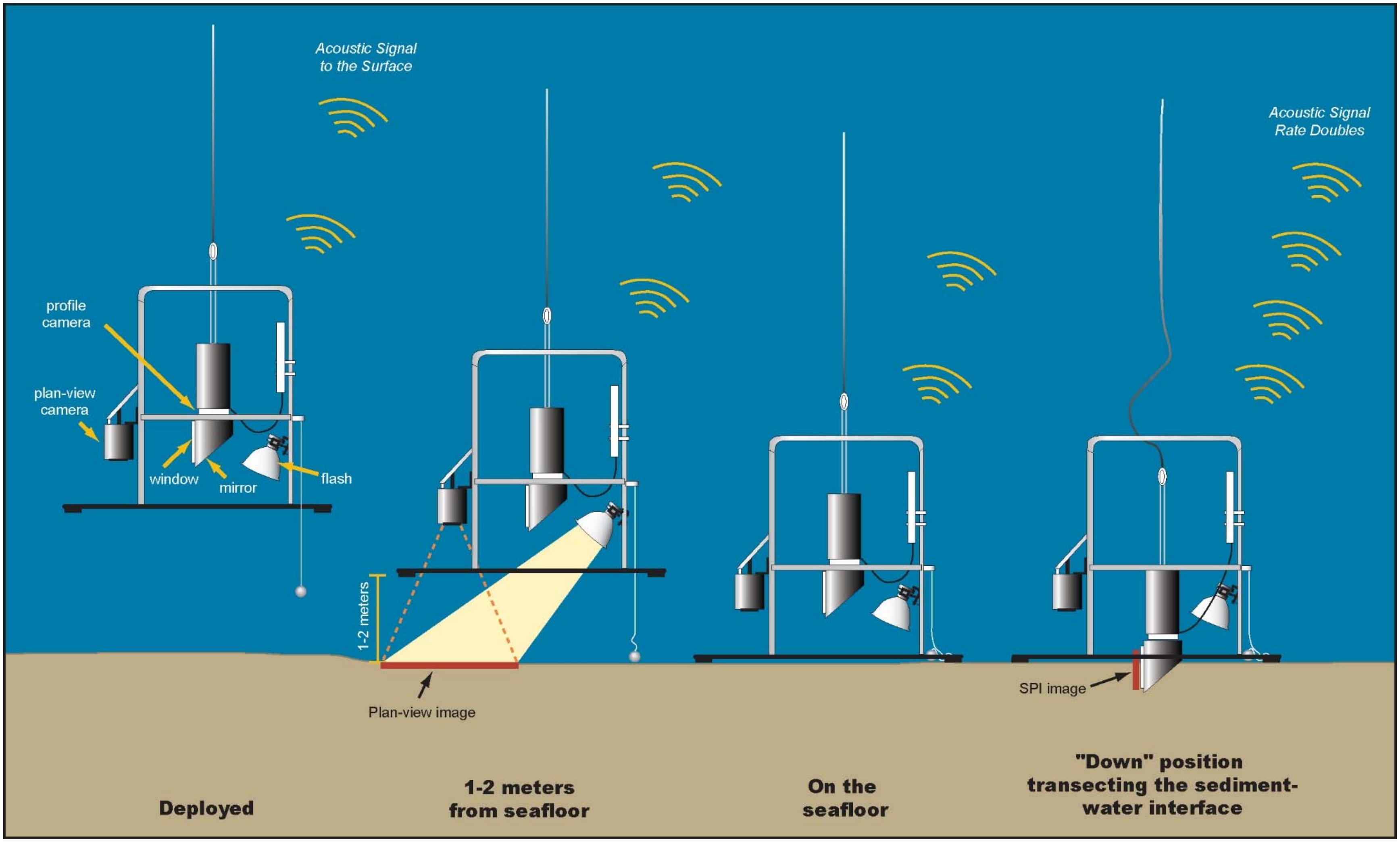

Figure 2-3. Schematic diagram of the SPI/PV camera deployment

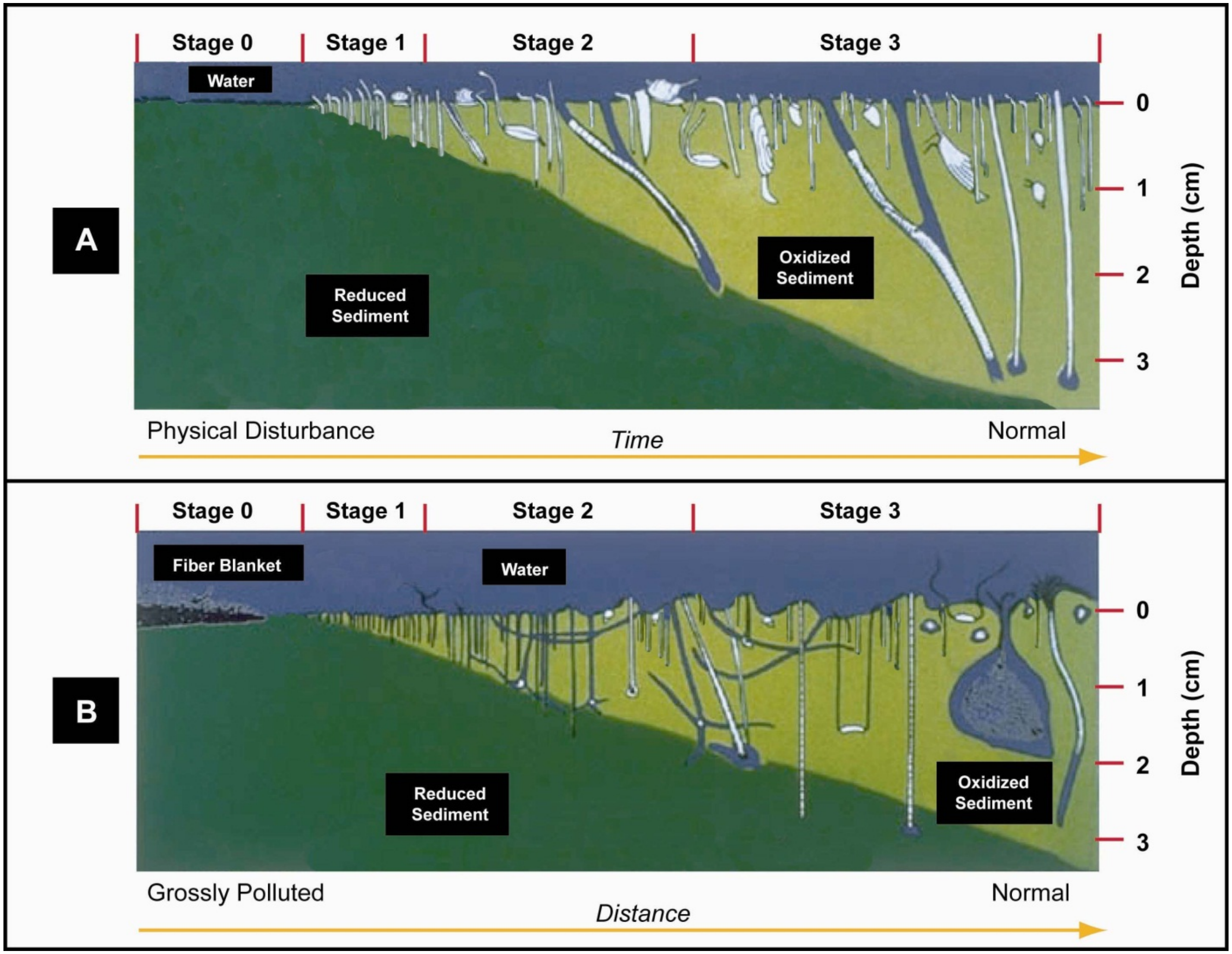

Figure 2-4. The stages of infaunal succession as a response of soft-bottom benthic communities to (A) physical disturbance or (B) organic enrichment; from Rhoads and Germano (1982)

3.0 RESULTS

3.1 Acoustic Survey

An acoustic survey was conducted in September 2015 to characterize seafloor topography and surface features over the entire ISDSN site and reference areas.

3.1.1 Bathymetry

Water depths at ISDSN varied from 77.7 m to 103.8 m and gradually sloped from approximately 90 m on the western boundary to 100 m in the southeastern portion of the site (Figure 3-1). Depths ranged from 90 to 95 m in the northeast portion of the site. The shallowest depths were on two distinct topographic highs in the southeast corner and northwest corners of ISDSN, rising from 10 to 20 m off the surrounding seafloor. The northeast quadrant of the site also had a noticeable topographic high, rising from 3 to 10 m from the surrounding seafloor (Figure 3-1).

Multibeam bathymetric data rendered as a color scale by depth over an acoustic relief model (grayscale with hill-shading) provided a more detailed representation of these topographic highs and of the entire site (Figure 3-2). These data also revealed several depressions near the center of the site, as well as a group of circular features in the northeast quadrant of the site (Figure 3-2). The small craters in the northeast quadrant are consistent with dredged material disposal features seen at other disposal sites and may indicate the presence of historical dredged material placement (Carey et al. 2013). Stations in this region and to the northeast in REF-C also had evidence of possible dredged material in SPI images (discussed below in section 3.2).

3.1.2 Acoustic Backscatter and Side-Scan Sonar

Acoustic backscatter data provided an estimate of surface sediment texture (hard, soft, rough, and smooth). Side-scan sonar data are higher resolution and more responsive to minor surface textural features and slope than backscatter results and can reveal additional information about topographic and textural properties of the seafloor.

A mosaic of unfiltered backscatter data for ISDSN (Figure 3-3) generally revealed the shallower areas as harder surfaces having a stronger acoustic return (lighter gray in Figure 3-3) and deeper areas as soft sediment having a weaker acoustic return (darker gray). Filtered backscatter results were processed into a grid file and presented in a quantitative form where backscatter intensity values were assigned a color (Figure 3-4). In this filtered and gridded display, the finer-scale details were less visible, but the relative intensity of backscatter returns were easier to discern.

Areas with stronger returns (-37 to -28 db) were the topographic highs in the northwest, southeast, and northeast corners of the site (Figure 3-3). Those in the northwest and southeast may be glacial outcrops based on their sharp topographic profiles, hard backscatter returns, and the textural differences evident in the side-scan sonar data (Figure 3-5).

Filtered backscatter data showed the larger depressions toward the center of the site clearly (Figure 3-4). These depressions had weaker return signals than surrounding sediments indicating softer sediments and the potential to serve as depositional areas for fine-grained sediments. The circular features in the northeast quadrant were also clearly visible in both the unfiltered backscatter (Figure 3-3) and side-scan sonar data (Figure 3-5). These results indicated that the small craters that make up the circular features were both softer than surrounding sediments (based on backscatter) and had different surface topographical/textural properties compared to surrounding sediments (based on side-scan sonar).

3.1.3 Comparison with Previous Bathymetry

The bathymetry data of ISDSN as surveyed in 2015 were consistent with existing bathymetric data, which were collected and aggregated at a regional scale (UNH/NOAA CCOM 2015). These data reveal the same topographic highs and lows as the 2015 survey data, as well as the area of circular features in the northeastern quadrant of the site.

3.2 Sediment-Profile and Plan-View Imaging

The primary purposes of the SPI/PV survey at ISDSN were to characterize the physical features of the surface sediment throughout the study area and to assess the status of benthic communities within the proposed disposal site. A station summary of some measured parameters can be found in Tables 3-1 and 3-2 with a complete set of results in Appendix C.

3.2.1 Reference Areas

There are three areas proposed as reference areas, REF-A located 2 km south of the southwest corner of the 2015 survey area, REF-B located at the southwest corner of the 2015 survey area, and REF-C located just outside the 2015 survey area at the northeast corner (Figure 3-6).

Physical Sediment Characteristics

Depth of reference area stations ranged from 92.7 m to 97.5 m with a mean of 95.2 m. All stations were characterized by soft muds (e.g., silt/clay) with a major grain size mode of >4 phi (Table 3-1, Figure 3-7). Camera penetration depths also indicated soft sediments with a mean penetration depth of 14.3 cm and a range from 8.9 to 16.9 cm (Table 3-1, Figure 3-8). The shallowest camera penetration depths were in REF-C, just to the northeast of the topographic rise found in the northeast corner of the survey area (Figure 2-2). Camera penetrations at REF-C were all shallower than 12.2 cm; in contrast, the minimum penetration depth at the other reference areas was 15.2 cm (Table 3-1, Figure 3-9).

Possible dredged material was visible at all stations in REF-C (Figure 3-9). Neither of the other references areas showed signs of dredged material. There was no evidence of low dissolved oxygen or sedimentary methane in the reference areas.

Boundary roughness ranged from 0.9 to 1.5 cm, with a mean of 1.2 cm (Figure 3-10). All of this small-scale topography can be attributed to the surface and subsurface activity of benthic organisms evidenced as small burrowing openings, pits, mounds, etc. (e.g., Figure 3-11).

Biological Conditions

The average station aRPD depths ranged from 4.6 to 8.2 cm with an overall mean of 7.0 cm (SD±1.1) across all reference stations (Table 3-1, Figure 3-12 and Appendix C). Mean aRPD depths at REF-C were all shallower than 6.7 cm; in contrast the minimum aRPD depth at the other reference areas was 7.2 cm (Figure 3-13). This is consistent with the shallower penetration depths observed at REF-C (Table 3-1). Overall the aRPD depths at the reference area stations were relatively deep, indicative of a healthy seafloor and were biologically modified by infaunal reworking.

Stage 3 infauna were present across all three reference areas with the predominant stage at all three reference areas being Stage 1 on 3 (Table 3-1, Figure 3-14). Evidence for the presence of Stage 3 fauna included large-bodied infauna, deep subsurface burrows, and/or deep feeding voids (Figure 3-15); opportunistic Stage 1 taxa were indicated by the presence of small tubes at the sediment water interface (Figure 3-15). Subsurface feeding voids, indicating Stage 3 fauna, were present in at least 1 replicate of all but 1 station surveyed (Table 3-1). The mean of maximum subsurface feeding void depth ranged from 2.5 to 12.0 cm with an overall mean of 8.7 cm (SD±2.7) (Table 3-1; Figures 3-16).

Plan-View Imaging

The plan-view area of seafloor imaged ranged from 0.44 to 0.67 m^2. Oxidized silt/clay surface sediments with varying degrees of biological activity were seen in all PV images taken at the reference areas. Many images included small tubes and small to medium burrows, indicating the presence of deposit-feeding infauna (Figure 3-17). Tubes were generally sparse in their frequency, as were medium to large burrows, whereas small burrows were more frequent.

Small shrimp were seen at the seafloor surface in approximately half of the images. Anemones were seen at two locations in Reference Area C (C1-A, C2-D). All stations had tracks indicative of mobile epifauna (e.g., crab, shrimp, gastropods). These tracks often covered much of the visible seafloor in the images, indicating an active mobile epifaunal community at the reference areas (Figure 3-18). At the reference areas, plan-view images confirmed the physical and biological observations from the acoustic and SPI surveys.

3.2.2 Proposed Disposal Site

Physical Sediment Characteristics

Depth of the proposed disposal site stations ranged from 93.9 m to 103.6 m with a mean of 96.9 m (Figure 3-19). All stations were characterized by soft muds (e.g., silt/clay) with a major grain size mode of >4 phi (Table 3-2; Figure 3-20). Camera penetration depths throughout the site also indicated soft sediments with a mean penetration depth of 15.2 cm and a range from 9.3 to 18.7 cm (Table 3-2; Figure 3-21). The shallowest camera penetration depths were seen in stations along the north boundary and in the northeast and southeast corners of the proposed disposal site, in the vicinity of topographic rises in this portion of the proposed disposal site (Figure 3-21).

Possible dredged material was visible at Stations 5, 6, 12, 28, 29, 30, stations in the northeast and southeast corners of the survey area (Figure 3-22). There was no evidence of low dissolved oxygen or sedimentary methane within the proposed disposal site.

Boundary roughness ranged from 0.6 to 2.4 cm, with a mean of 1.1 cm (Figure 3-23). All of this small-scale topography can be attributed to the surface and subsurface activity of benthic organisms evidenced as small burrowing openings, pits, mounds, etc. (e.g., Figure 3-11).

Biological Conditions

The average station aRPD depths ranged from 4.8 to 9.5 cm with an overall mean of 7.3 cm (SD±1.1) across all the proposed disposal site stations (Table 3-2; Figure 3-24 and Appendix C). Only Station 6, in the northeast corner of the site was less than 5.0 cm (Figure 3-24). Overall the aRPD depths at the proposed disposal site stations were relatively deep, indicative of a healthy seafloor and were biologically modified by infaunal reworking (Figure 3-25).

Stage 3 infauna were present across the proposed disposal site with the predominant stage at all stations being Stage 1 on 3 (Table 3-2, Figure 3-26). Evidence for the presence of Stage 3 fauna included large-bodied infauna, deep subsurface burrows, and/or deep feeding voids (Figure 3-25); opportunistic Stage 1 taxa were indicated by the presence of small tubes at the sediment water interface (Figure 3-25). Subsurface feeding voids, indicating Stage 3 fauna, were present in at least 1 replicate of all but 2 stations surveyed (Table 3-2). The mean of maximum subsurface feeding void depth ranged from 5.7 to 15.9 cm with an overall mean of 9.9 cm (SD±2.6) (Table 3-2; Figure 3-27).

Plan-View Imaging

The plan-view area of seafloor imaged ranged from 0.42 to 0.72 m^2. Oxidized silt/clay surface sediments with varying degrees of biological activity were seen in all PV images taken at the proposed disposal site. Many images included small tubes and small to medium burrows, indicating the presence of deposit-feeding infauna (Figure 3-17). Tubes were generally sparse in their frequency, as were medium to large burrows. Small burrows were more frequent across much of the site.

Small shrimp were seen at the seafloor surface at 19 of the stations. Other epifauna were rarely seen (crab at 17-A, gastropod at 7-A, and anemone at 30-A), however, all but one station (1) had tracks indicative of these and other mobile epifauna. These tracks often covered much of the visible seafloor in the images, indicating an active mobile epifaunal community at ISDSN (Figure 3-18). A small fish was seen at Station 15. Within ISDSN, plan-view images confirmed both the physical and biological observations from the acoustic and SPI surveys.

3.2.3 Comparison to Reference Areas

3.2.3.1 Mean aRPD Variable

The mean aRPD depth for the proposed disposal site was 7.29 cm, comparable to the grand mean of the reference areas (7.01 cm). Area mean aRPD depths in the reference area ranged from 5.72 to 7.82 cm and were the shallowest at reference area C (Table 3-3; Figure 3-28). The standard deviation among stations for aRPD depths across all sampling areas ranged from 0.28 to 1.07 cm (Table 3-3).

A statistical inequivalence test was performed to determine whether or not the difference observed in mean aRPD values between the three reference areas and the proposed disposal site was statistically significant. The station mean aRPD data from all four locations were combined to assess normality and estimate pooled variance. Results for the normality test indicated that the area residuals (i.e., each observation minus the area mean) were not significantly different from a normal distribution (Shapiro-Wilk's test p-value = 0.53, with alpha = 0.05). Levene's test for equality for variances could not be rejected (p-value = 0.08, with alpha = 0.05). These results indicate that normally distributed data with equal variances can be assumed. Therefore, normal equations and a pooled variance estimate were used to construct the confidence interval for the difference equation.

The confidence region for the difference between the reference areas versus the proposed disposal site mean was contained within the interval [-1, +1] (Table 3-4). The conclusion was that the three reference areas and proposed disposal site did have significantly equivalent aRPD values in the 2015 survey, with a difference in means of approximately -0.28 cm, with reference areas having shallower aRPD values than proposed disposal locations (Table 3-4).

3.2.3.2 Successional Stage Rank Variable

Across the reference and disposal areas, Stage 3 fauna were consistently found, often along with Stage 1 fauna (Table 3-1, 3-2). To evaluate these successional stages numerically, a successional stage rank variable was applied to each image. A value of 3 was assigned to Stage 3, 2 on 3, or 1 on 3 designations, a value of 2 was applied to Stage 2 or 1 on 2, a value of 1 was applied to Stage 1, and images from which the stage could not be determined were excluded from calculations. The maximum successional stage rank among replicates was used to represent the station value.

The successional stage rank variable was uniformly 3 across all three reference areas and the proposed disposal site (Table 3-3). Therefore, no statistics were required to conclude that these areas were statistically equivalent.

Table 3-1.

Summary of ISDSN Reference Stations Sediment-Profile Imaging Results (station means), September 2015

Station	Water Depth (m)	Grain Size Major Mode (phi) [a]	Mean Prism Penetration Depth (cm)	Mean Boundary Roughness (cm)	Predominant Type of Boundary Roughness	Mean aRPD (cm)	Dredged Material Present	Mean # of Subsurface Feeding Voids	Mean of Maximum Subsurface Feeding Void Depth (cm)	Predominant Successional Stage [b]
REF-A-01	95.7	>4	16.2	1.0	Biological	8.2	No	1.3	10.2	1 on 3
REF-A-02	96.0	>4	16.9	1.0	Biological	7.9	No	1.3	8.3	1 on 3
REF-A-03	94.5	>4	15.9	1.4	Biological	7.6	No	3.7	12.0	1 on 3
REF-A-04	94.8	>4	15.5	1.5	Biological	7.9	No	2.3	12.0	1 on 3
REF-A-05	95.1	>4	16.9	1.3	Biological	7.5	No	2.0	11.9	1 on 3
REF-B-01	92.7	>4	15.7	1.2	Biological	8.1	No	0.3	2.5	1 on 3
REF-B-02	93.3	>4	15.2	1.1	Biological	7.6	No	1.7	10.3	1 on 3
REF-B-03	93.0	>4	16.6	0.9	Biological	7.4	No	1.7	9.4	1 on 3
REF-B-04	94.5	>4	15.5	1.1	Biological	7.2	No	2.0	8.8	1 on 3
REF-B-05	93.3	>4	16.0	1.4	Biological	7.2	No	2.0	9.0	1 on 3
REF-C-01	96.9	>4	10.5	1.2	Biological	6.1	Possible	1.7	7.5	1 on 3
REF-C-02	96.9	>4	8.9	1.0	Biological	4.6	Possible	0.0	--	1 on 3
REF-C-03	97.5	>4	10.8	1.0	Biological	5.8	Possible	2.3	8.8	1 on 3
REF-C-04	96.9	>4	12.0	1.2	Biological	5.4	Possible	0.3	5.8	1 on 3
REF-C-05	96.9	>4	12.2	1.2	Biological	6.7	Possible	0.3	5.2	1 on 3
Max	97.5		16.9	1.5		8.2		3.7	12.0	
Min	92.7		8.9	0.9		4.6		0.0	2.5	
Mean	95.2		14.3	1.2		7.0		1.5	8.7	

Ind = Indeterminate
a Grain Size: "/" indicates layer of one phi size range over another (see Appendix D)
b Successional Stage: "on" indicates one Stage is found on top of another Stage (i.e., 1 on 3);"→" indicates one Stage is progressing to another Stage (i.e., 2→3)

Table 3-2.

Summary of ISDSN Site Stations Sediment-Profile Imaging Results (station means), September 2015

Station	Water Depth (m)	Grain Size Major Mode (phi) [a]	Mean Prism Penetration Depth (cm)	Mean Boundary Roughness (cm)	Predominant Type of Boundary Roughness	Mean aRPD (cm)	Dredged Material Present	Mean # of Subsurface Feeding Voids	Mean of Maximum Subsurface Feeding Void Depth (cm)	Predominant Successional Stage [b]
01	94.5	>4	17.3	0.8	Biological	7.1	No	2.0	8.9	1 on 3
02	93.9	>4	14.0	1.8	Biological	6.2	No	0.7	7.1	1 on 3
03	97.2	>4	15.9	0.6	Biological	7.4	No	1.0	9.1	1 on 3
04	96.3	>4	14.2	0.7	Biological	5.7	No	1.3	6.8	1 on 3
05	96.0	>4	12.9	1.3	Biological	6.3	Possible	0.3	12.4	1 on 3
06	96.6	>4	11.9	2.4	Biological	4.8	Possible	4.0	8.7	1 on 3
07	94.5	>4	15.9	0.9	Biological	6.4	No	1.7	9.7	1 on 3
08	95.1	>4	17.6	1.0	Biological	7.9	No	2.3	15.9	1 on 3
09	98.1	>4	16.8	0.7	Biological	6.8	No	2.0	11.4	1 on 3
10	98.1	>4	14.9	0.9	Biological	6.6	No	0.0	--	1 on 3
11	98.1	>4	16.3	1.3	Biological	6.1	No	0.7	9.1	1 on 3
12	95.1	>4	9.4	0.9	Biological	7.1	Possible	0.7	9.2	1 on 3
13	93.9	>4	15.3	1.5	Biological	7.4	No	2.3	6.3	1 on 3
14	95.1	>4	15.3	1.4	Biological	7.3	No	1.3	9.5	1 on 3
15	97.5	>4	16.5	1.2	Biological	8.0	No	1.3	12.3	1 on 3
16	99.1	>4	15.9	1.3	Biological	9.5	No	0.7	7.6	1 on 3
17	101.2	>4	17.1	1.1	Biological	8.8	No	2.0	14.0	1 on 3
18	103.6	>4	17.9	0.8	Biological	8.0	No	2.3	11.6	1 on 3
19	94.5	>4	18.7	0.7	Biological	9.0	No	2.3	13.5	1 on 3
20	96.0	>4	16.1	1.3	Biological	8.1	No	1.3	11.8	1 on 3

Ind = Indeterminate
a Grain Size: "/" indicates layer of one phi size range over another (see Appendix D)
b Successional Stage: "on" indicates one Stage is found on top of another Stage (i.e., 1 on 3);"→" indicates one Stage is progressing to another Stage (i.e., 2→3)

Table 3-2. (continued)

Summary of ISDSN Site Stations Sediment-Profile Imaging Results (station means), September 2015

Station	Water Depth (m)	Grain Size Major Mode (phi) [a]	Mean Prism Penetration Depth (cm)	Mean Boundary Roughness (cm)	Predominant Type of Boundary Roughness	Mean aRPD (cm)	Dredged Material Present	Mean # of Subsurface Feeding Voids	Mean of Maximum Subsurface Feeding Void Depth (cm)	Predominant Successional Stage [b]
21	96.6	>4	16.4	1.4	Biological	7.8	No	0.7	7.4	1 on 3
22	99.1	>4	17.2	0.8	Biological	8.2	No	2.3	7.5	1 on 3
23	100.9	>4	16.4	1.3	Biological	7.8	No	0.7	13.0	1 on 3
24	99.4	>4	15.5	0.8	Biological	7.3	No	2.7	11.1	1 on 3
25	93.9	>4	15.4	0.7	Biological	7.2	No	3.3	11.1	1 on 3
26	94.8	>4	15.9	0.8	Biological	9.0	No	1.7	10.2	1 on 3
27	96.0	>4	16.1	0.6	Biological	7.4	No	0.0	--	1 on 3
28	95.7	>4	11.1	1.1	Biological	6.3	Possible	1.3	6.7	1 on 3
29	98.1	>4	12.6	1.1	Biological	7.3	Possible	2.3	8.3	1 on 3
30	98.1	>4	9.3	1.5	Biological	6.0	Possible	0.3	5.7	1 on 3
Max	103.6		18.7	2.4		9.5		4.0	15.9	
Min	93.9		9.3	0.6		4.8		0.0	5.7	
Mean	96.9		15.2	1.1		7.3		1.5	9.8	

Ind = Indeterminate
a Grain Size: "/" indicates layer of one phi size range over another (see Appendix D)
b Successional Stage: "on" indicates one Stage is found on top of another Stage (i.e., 1 on 3);"→" indicates one Stage is progressing to another Stage (i.e., 2→3)

Table 3-3.

Summary of Station Means for aRPD and Successional Stage by Sampling Location

	Mean aRPD (cm)		Successional Stage Rank	
Location	**Mean**	**Standard Deviation**	**Mean**	**Standard Deviation**
Disposal	7.29	1.07	3.0	0.00
REF-A	7.82	0.28	3.0	0.00
REF-B	7.50	0.37	3.0	0.00
REF-C	5.72	0.79	3.0	0.00

Table 3-4.

Summary Statistics and Results of Inequivalence Hypothesis Testing for aRPD Values

Difference Equation	**Observed Difference (d)**	$SE(\hat{d})$	***df* for SE**	**Confidence Bounds (D_L to D_U)[1]**	**Results[2]**
$Mean_{REF} - Mean_{ISDSN}$	-0.28	0.30	41	-0.78 to +0.22	s

[1] D_L and D_U as defined in [Eq. 3]
[2] s = Reject the null hypothesis of inequivalence: the two group means are significantly equivalent, within ± 1 cm.
d = Fail to reject the null hypothesis of inequivalence between the two group means, the two group means are different.

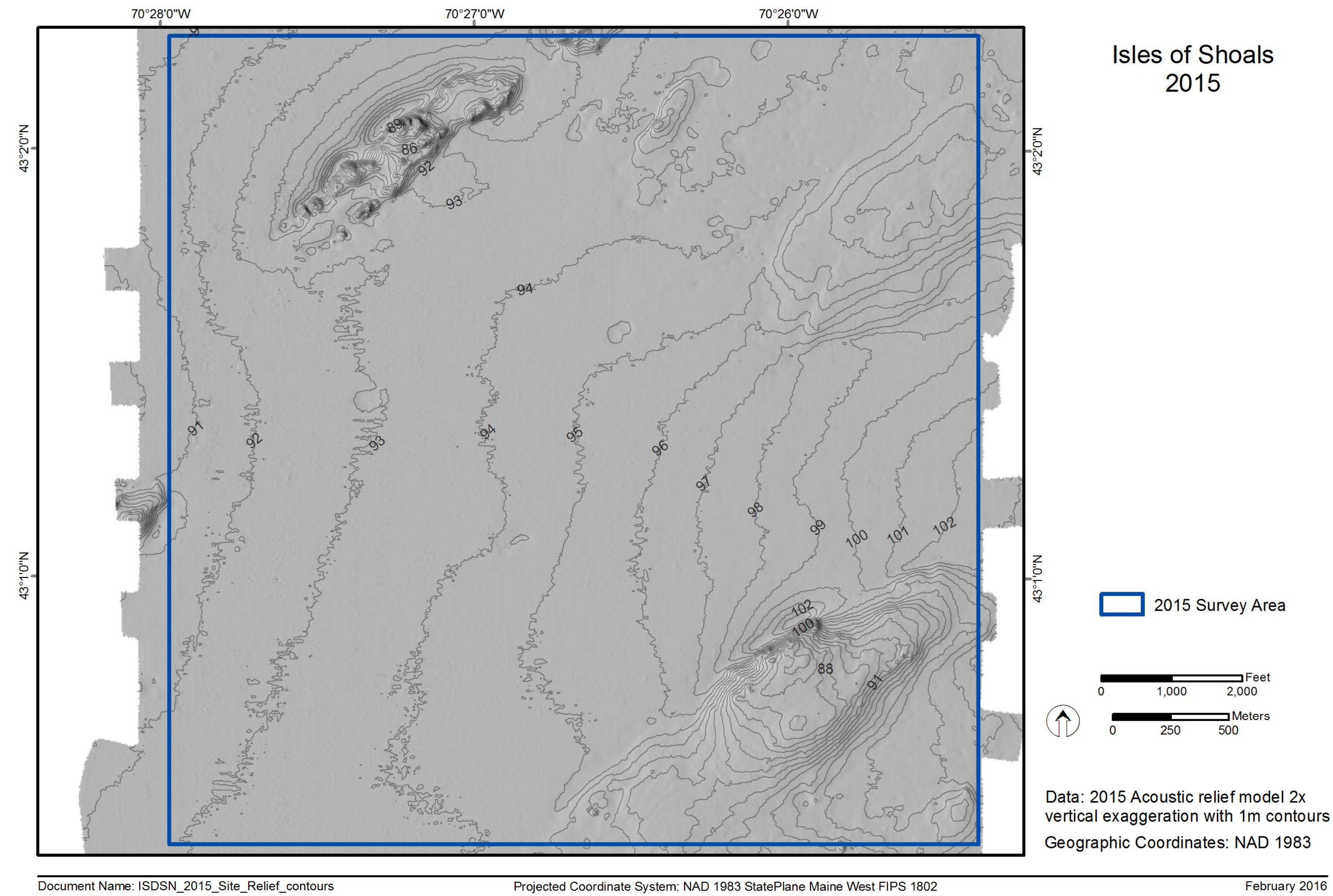

Figure 3-1. Bathymetric contour map of ISDSN – September 2015

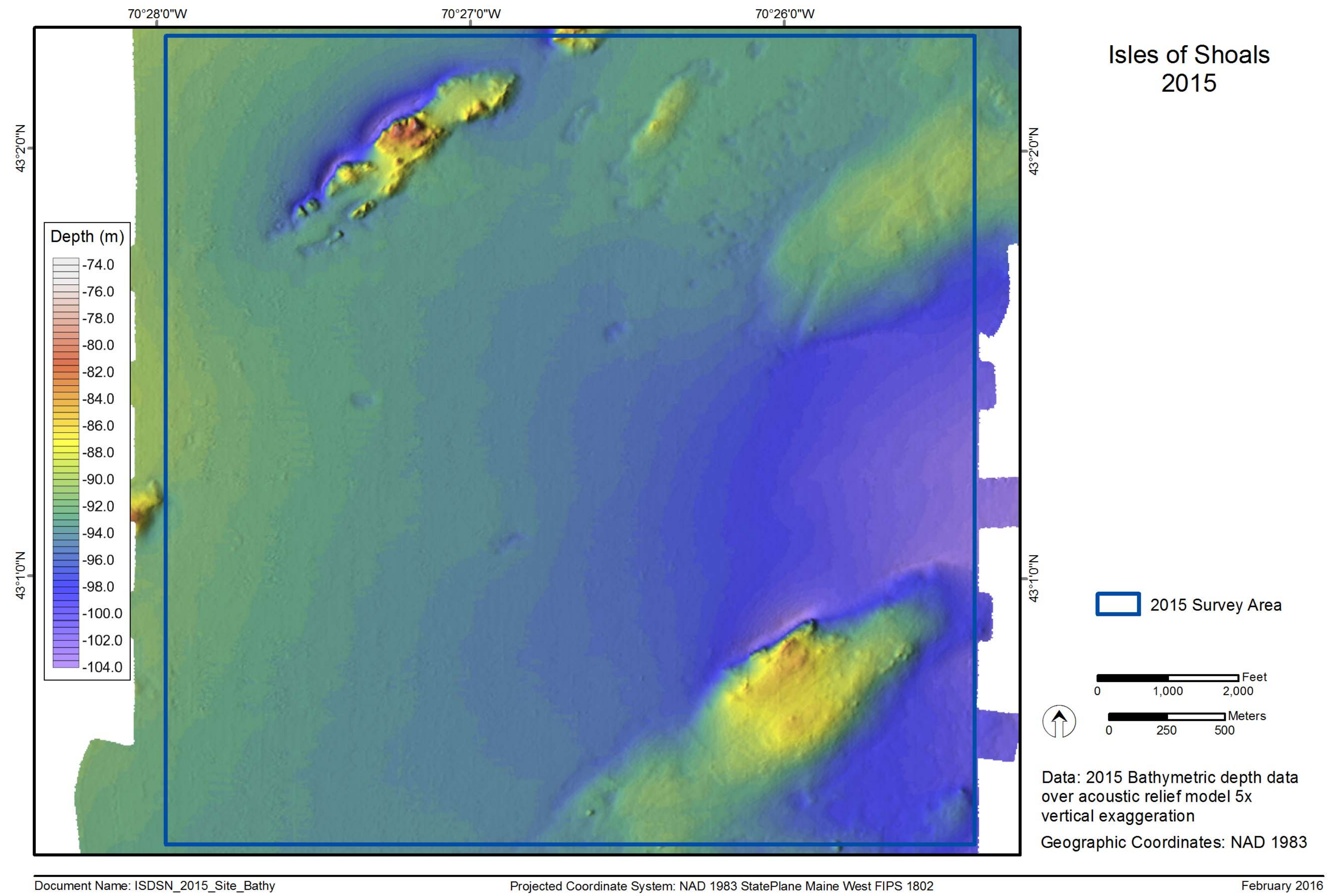

Figure 3-2. Bathymetric depth data over acoustic relief model of ISDSN – September 2015

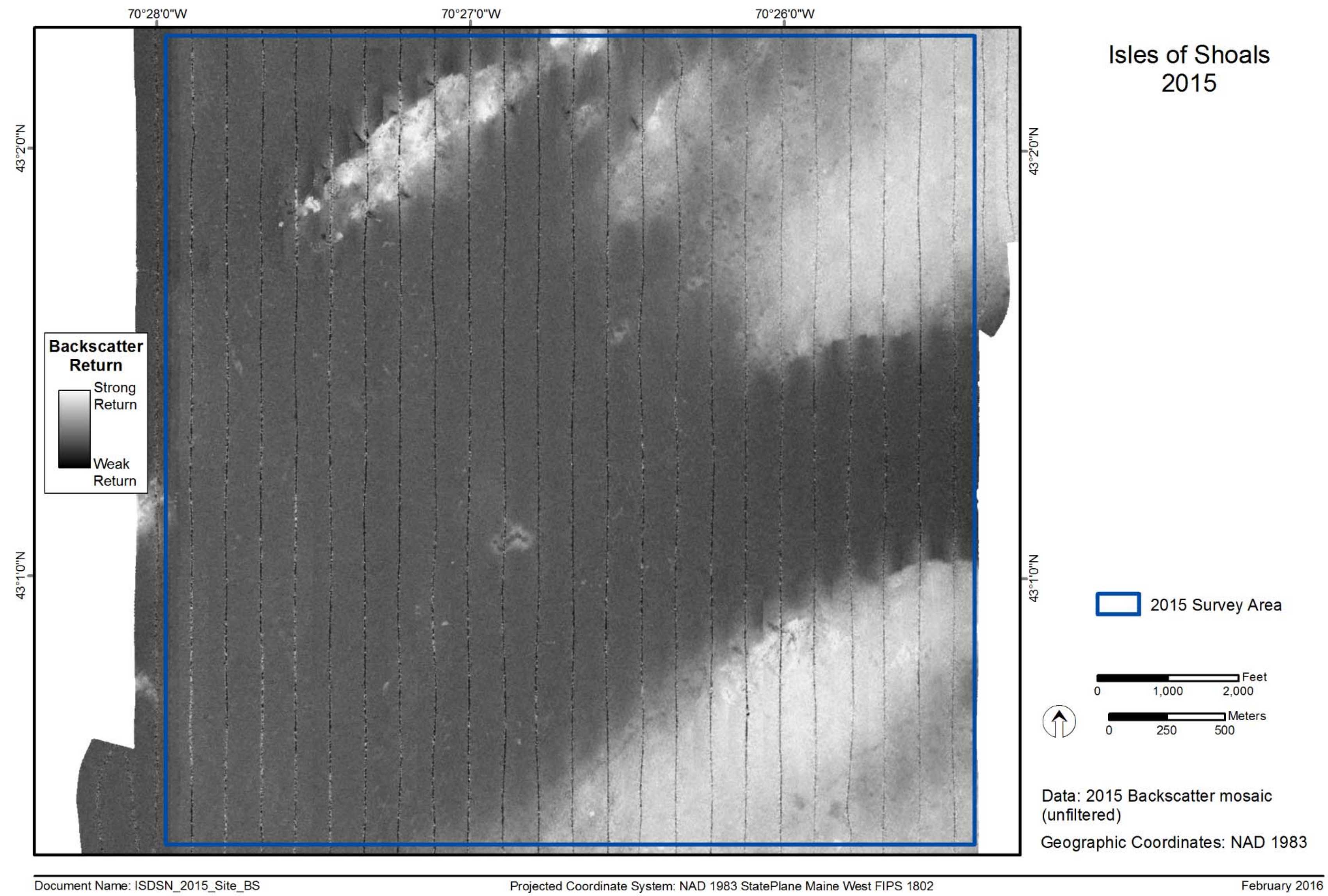

Figure 3-3. Mosaic of unfiltered backscatter data of ISDSN – September 2015

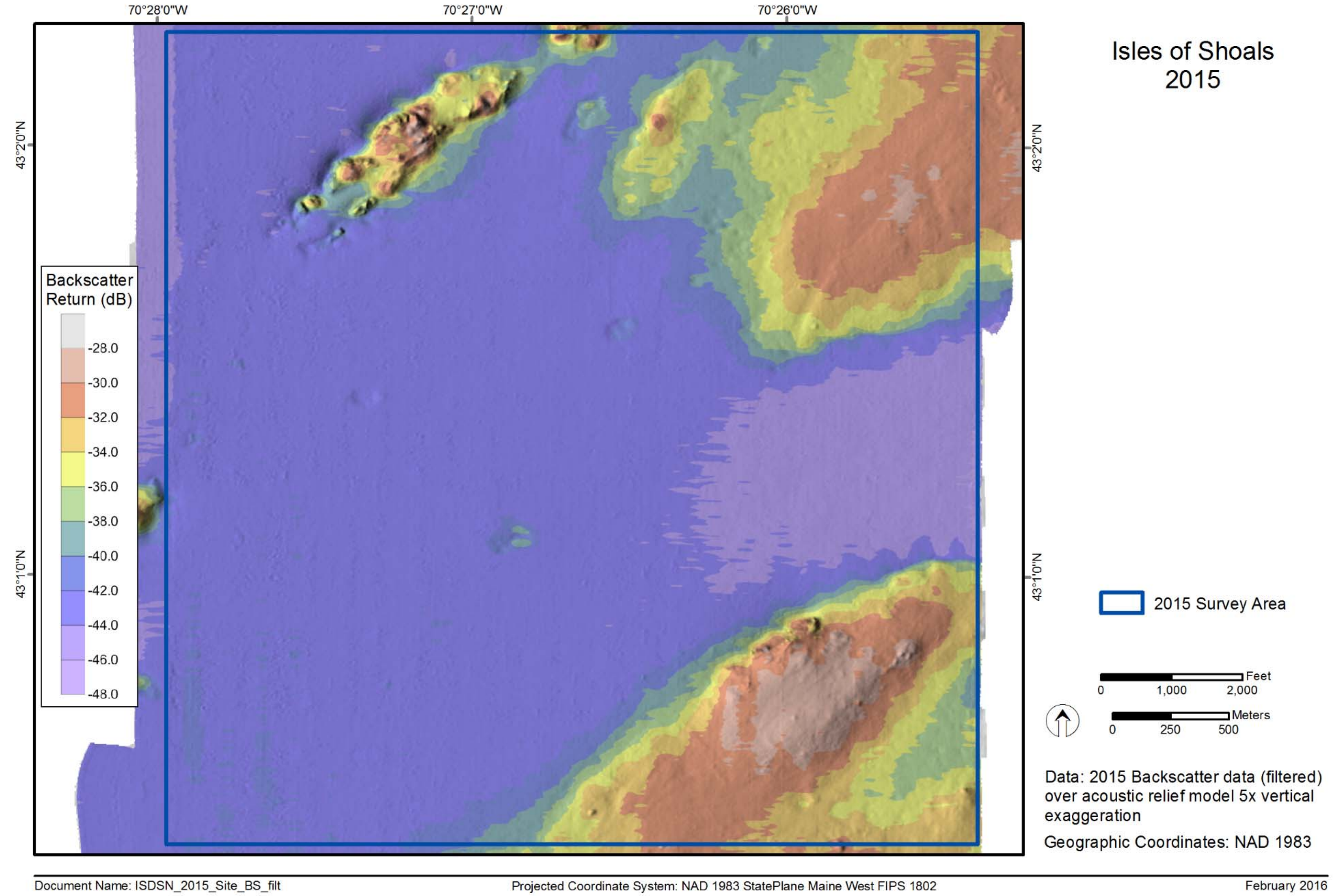

Figure 3-4. Filtered backscatter over acoustic relief model of ISDSN – September 2015

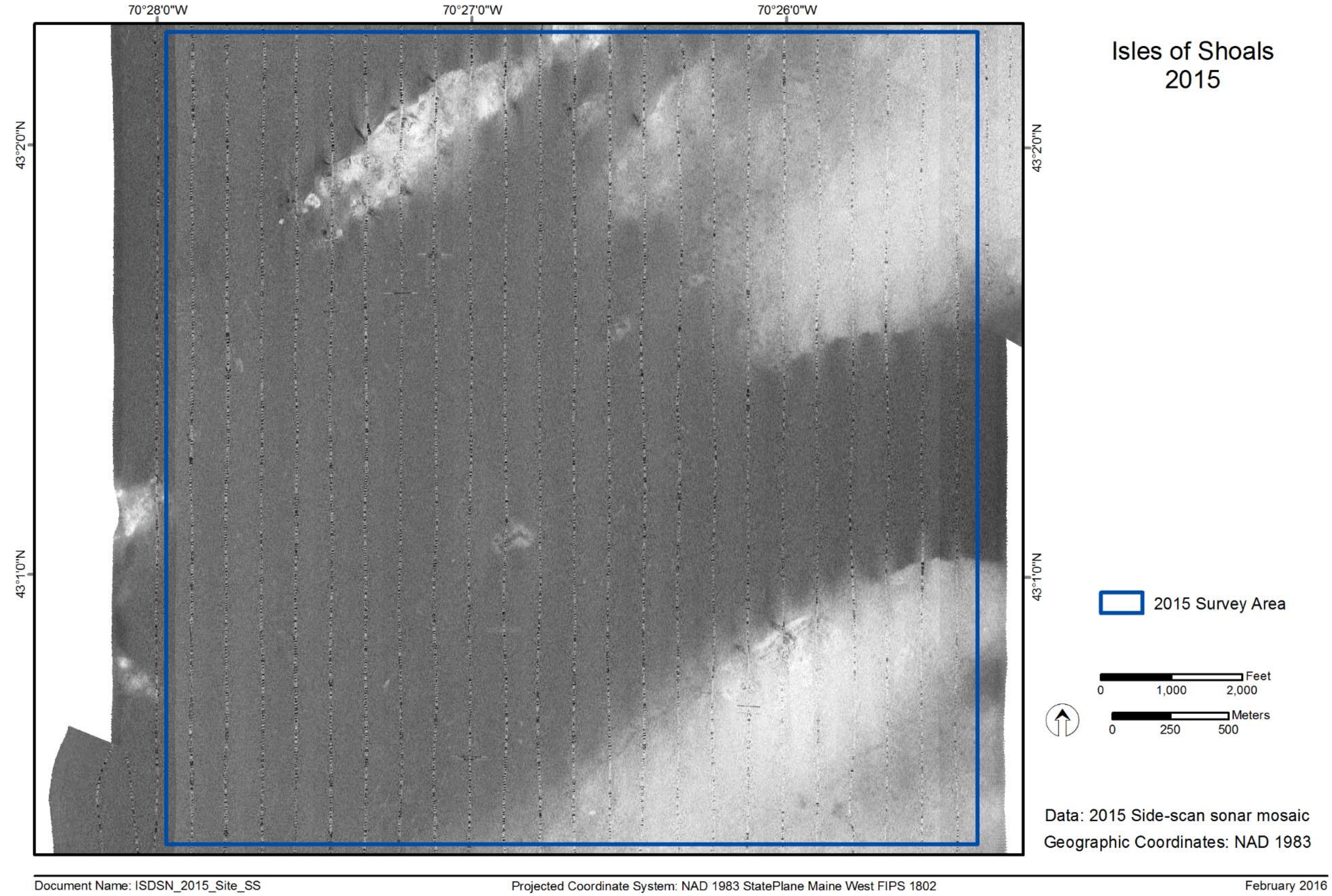

Figure 3-5. Side-scan mosaic of ISDSN – September 2015

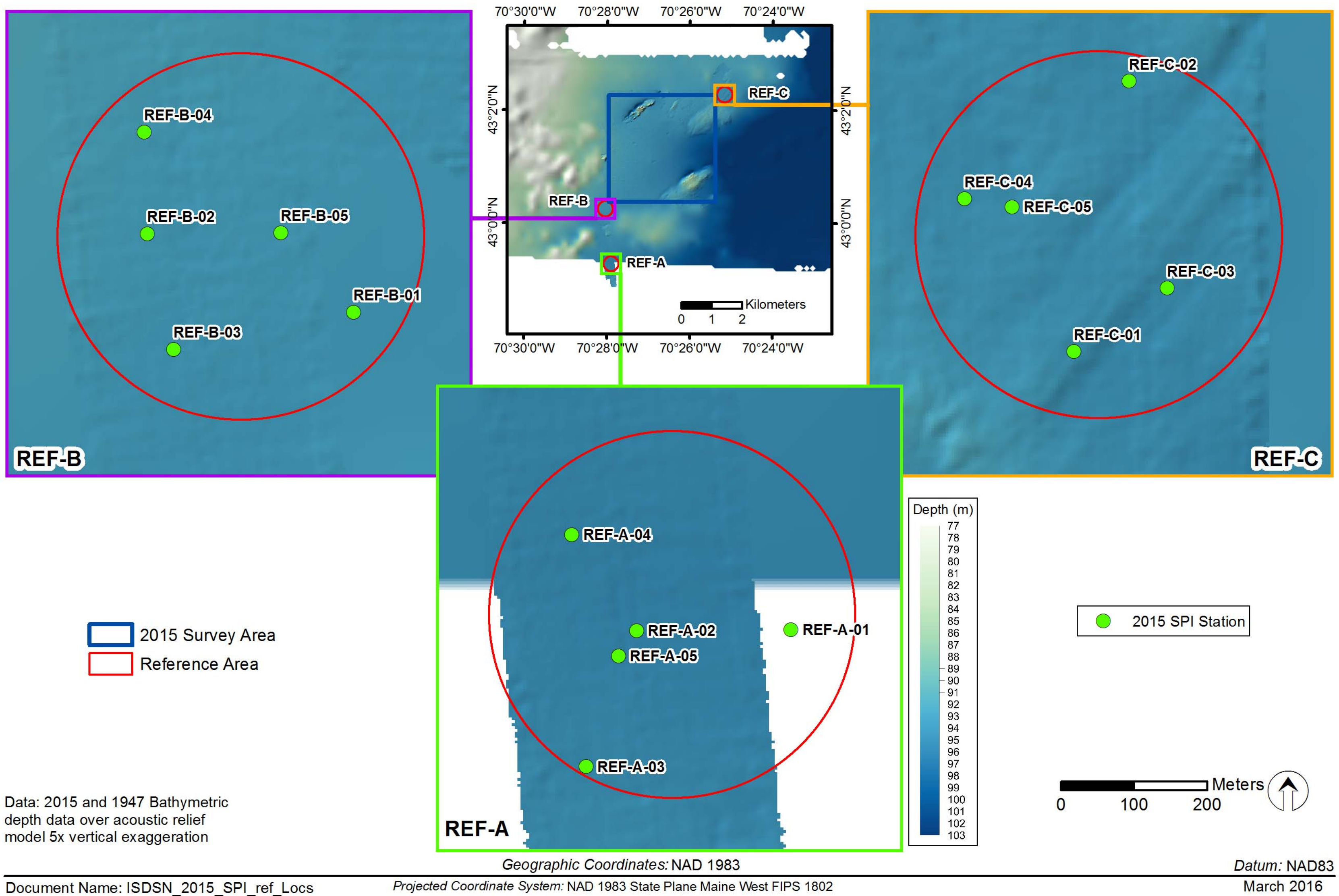

Figure 3-6. Bathymetric depth data at ISDSN proposed reference areas with SPI/PV stations indicated

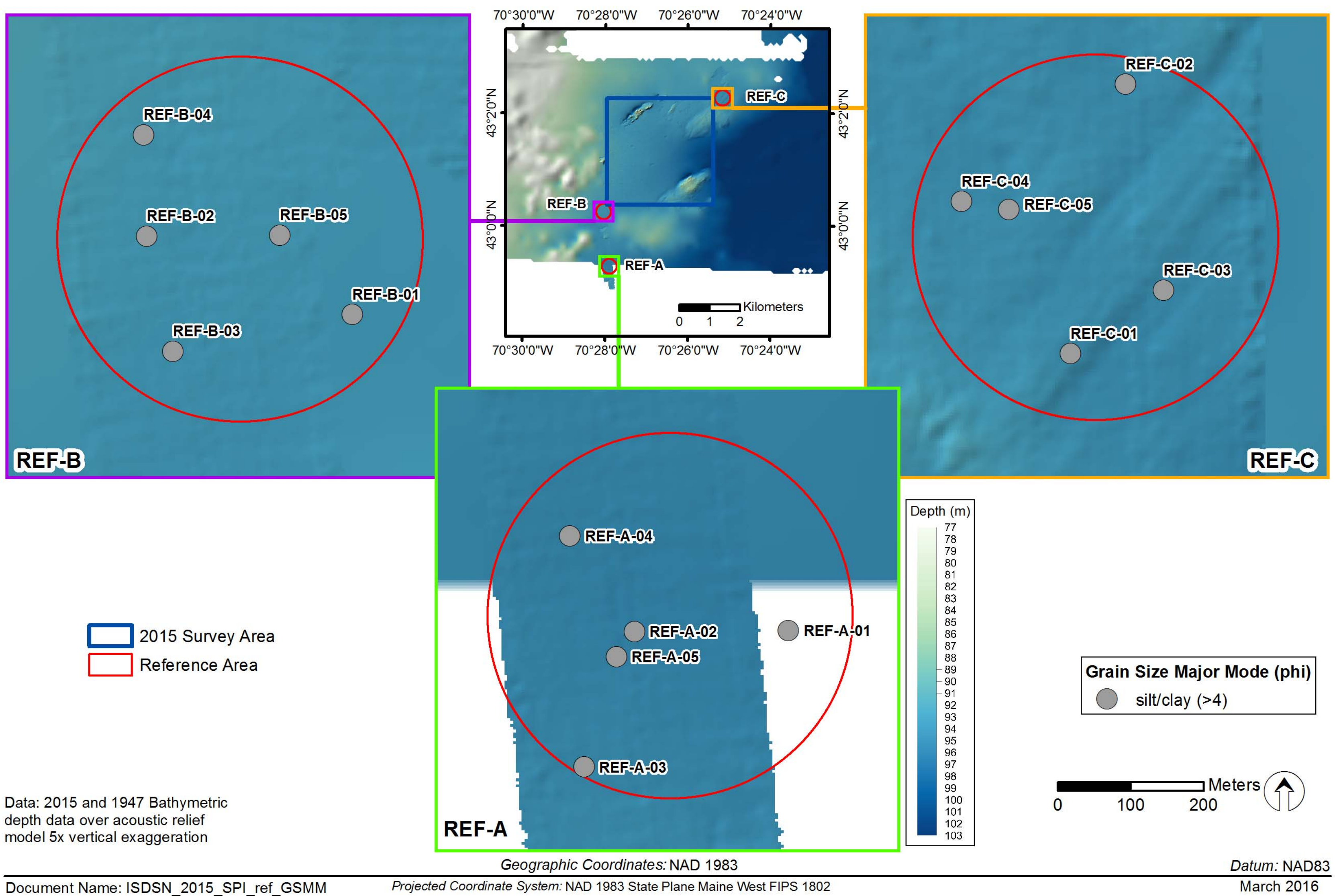

Figure 3-7. Sediment grain size major mode (phi units) at the ISDSN reference areas

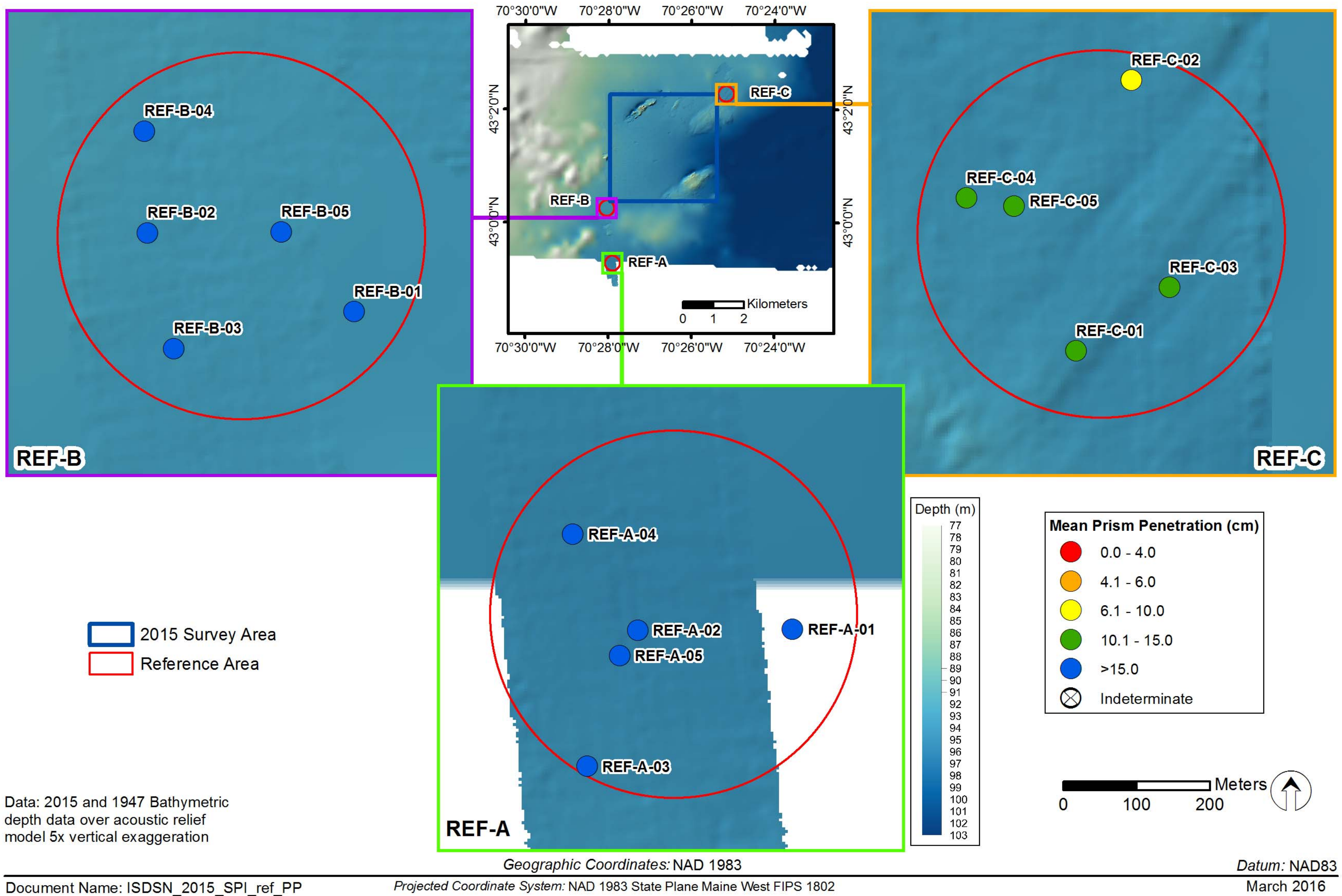

Figure 3-8. Mean station camera prism penetration depths (cm) at the ISDSN reference areas

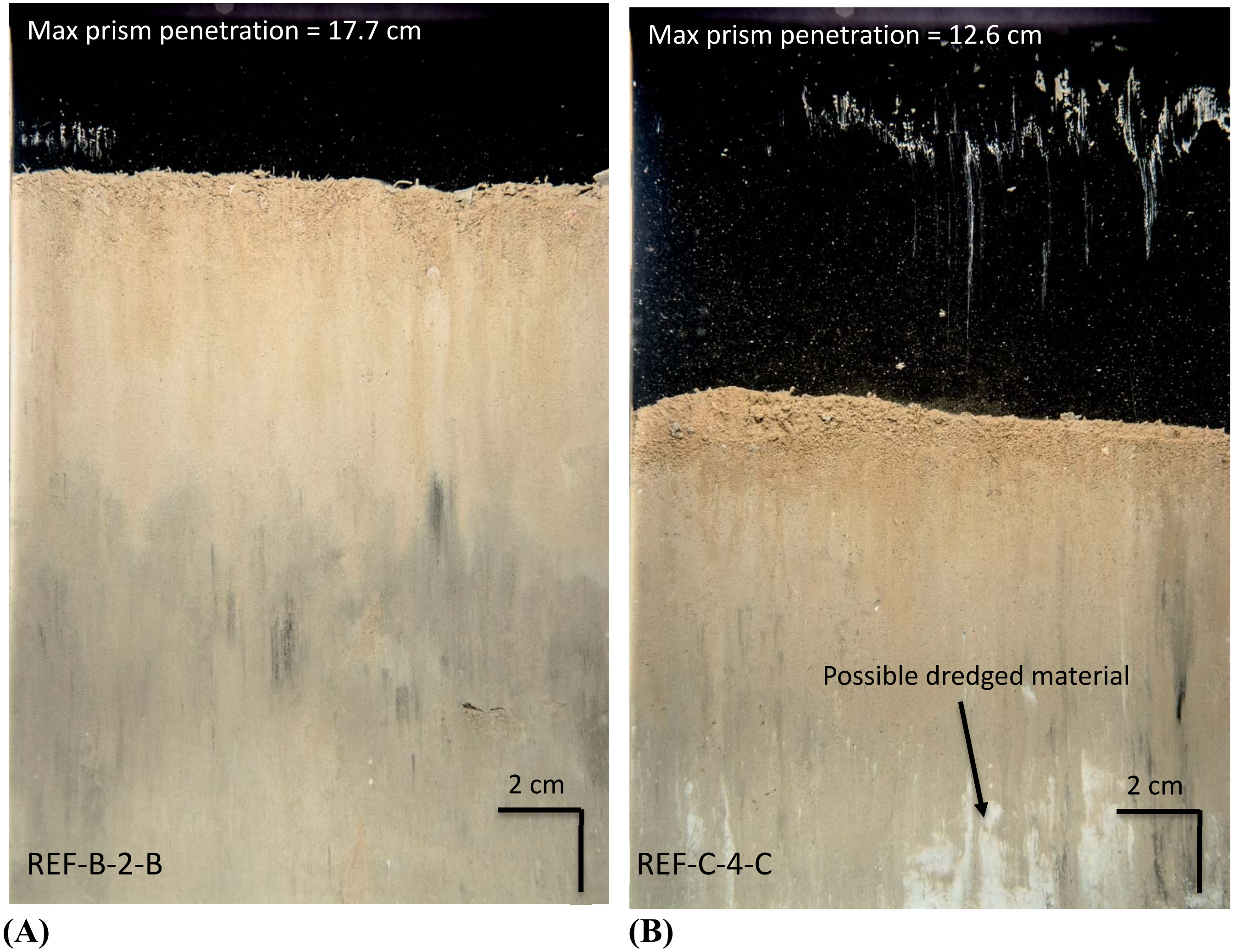

Figure 3-9. Sediment-profile images from (A) Station REF-B-2 and (B) Station REF-C-4 where camera penetration depths were shallower and where there was evidence of possible dredged material at depth

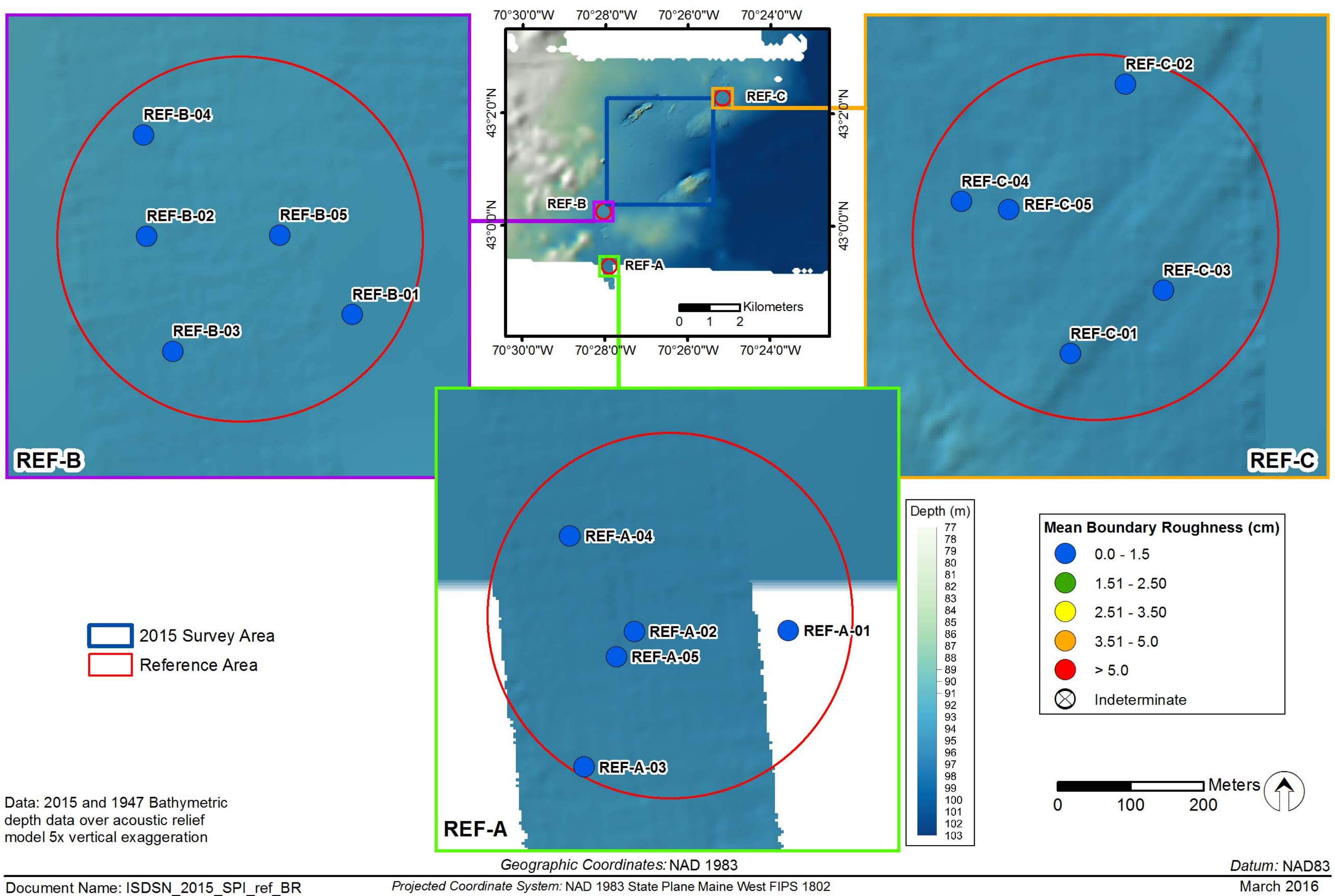

Figure 3-10. Mean station small-scale boundary roughness values (cm) at the ISDSN reference areas

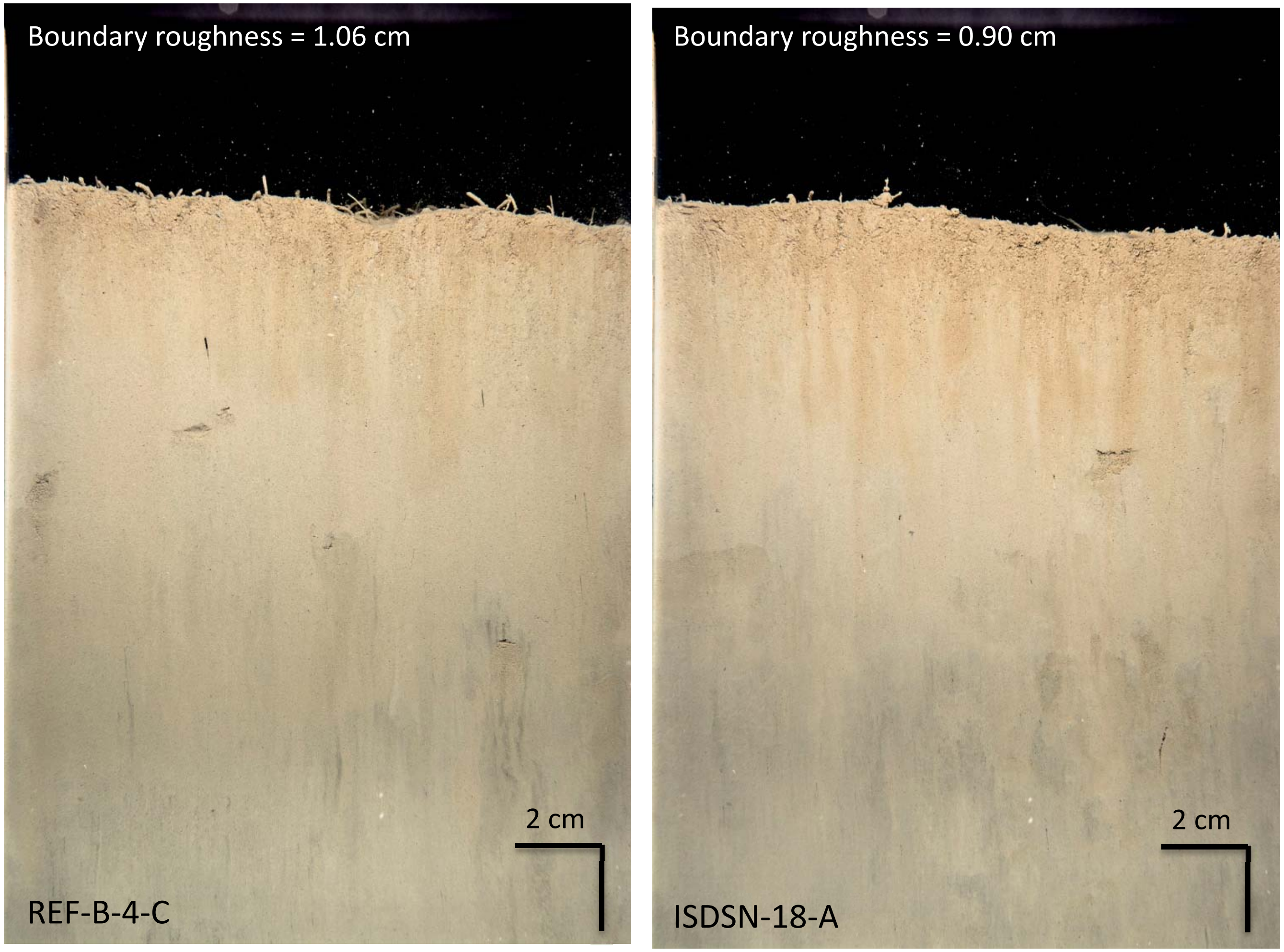

(A) **(B)**

Figure 3-11. Sediment-profile images depicting small-scale boundary roughness created by biological activity of surface and subsurface dwelling infauna at (A) Station REF-B-4 and (B) Station ISDSN-18

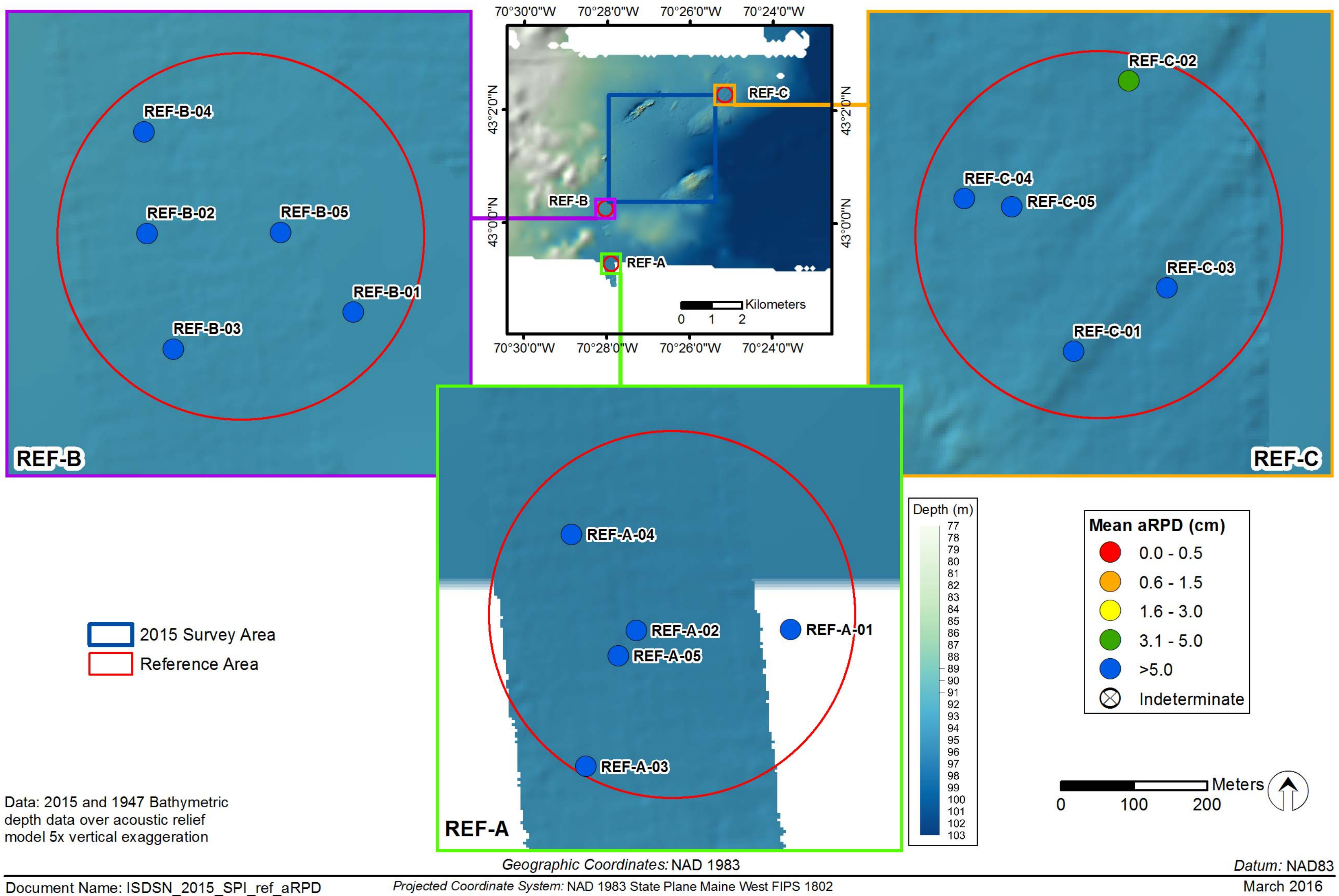

Figure 3-12. Mean station aRPD depths (cm) at the ISDSN reference areas

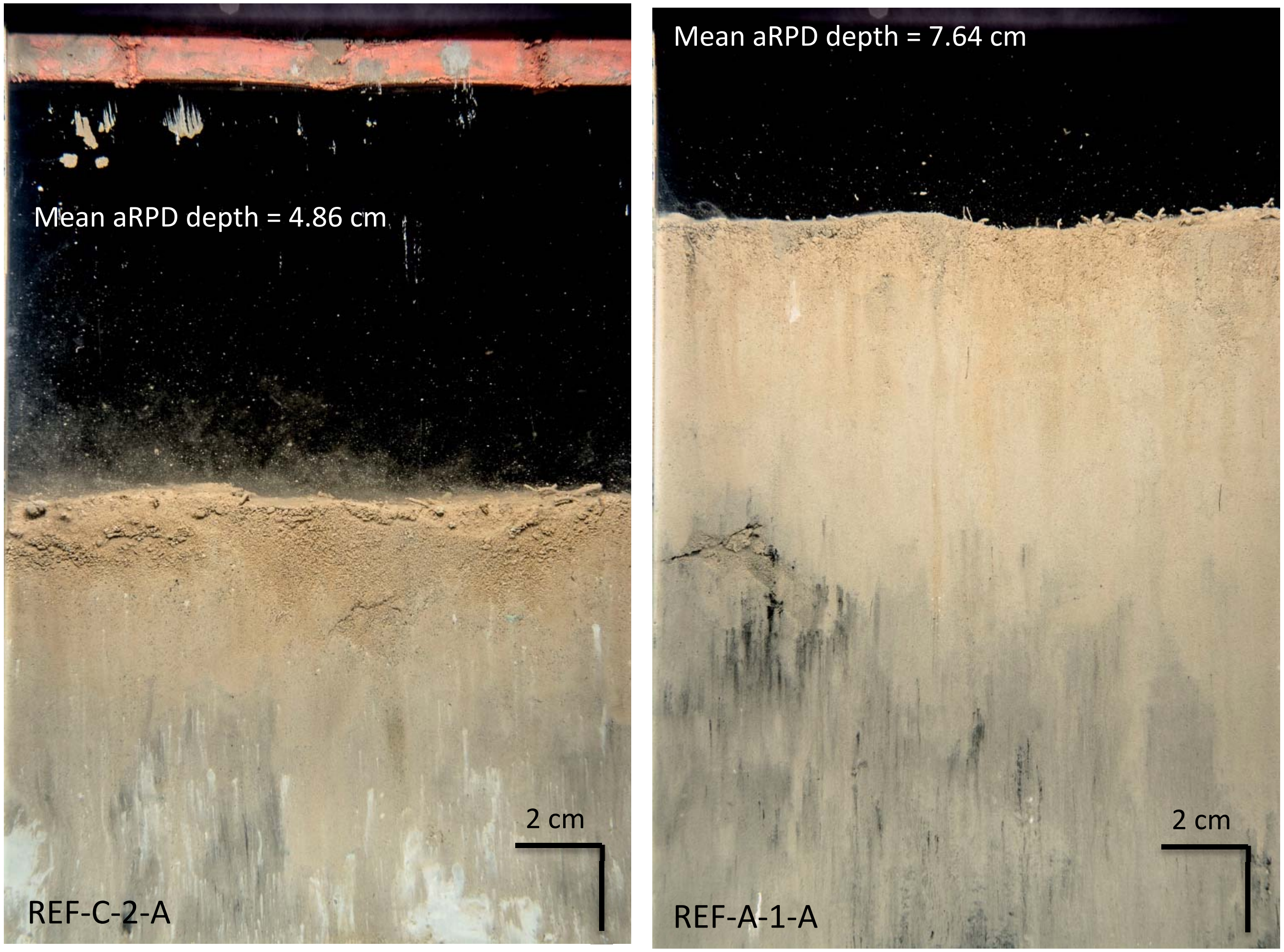

(A) **(B)**

Figure 3-13. Mean aRPD depths (cm) were shallower at (A) Station REF-C-2, compared to the other reference areas, e.g., (B) Station REF-A-1. Note: The sloughing of sediment particles near the surface of (A) is an occasional artifact of the camera action.

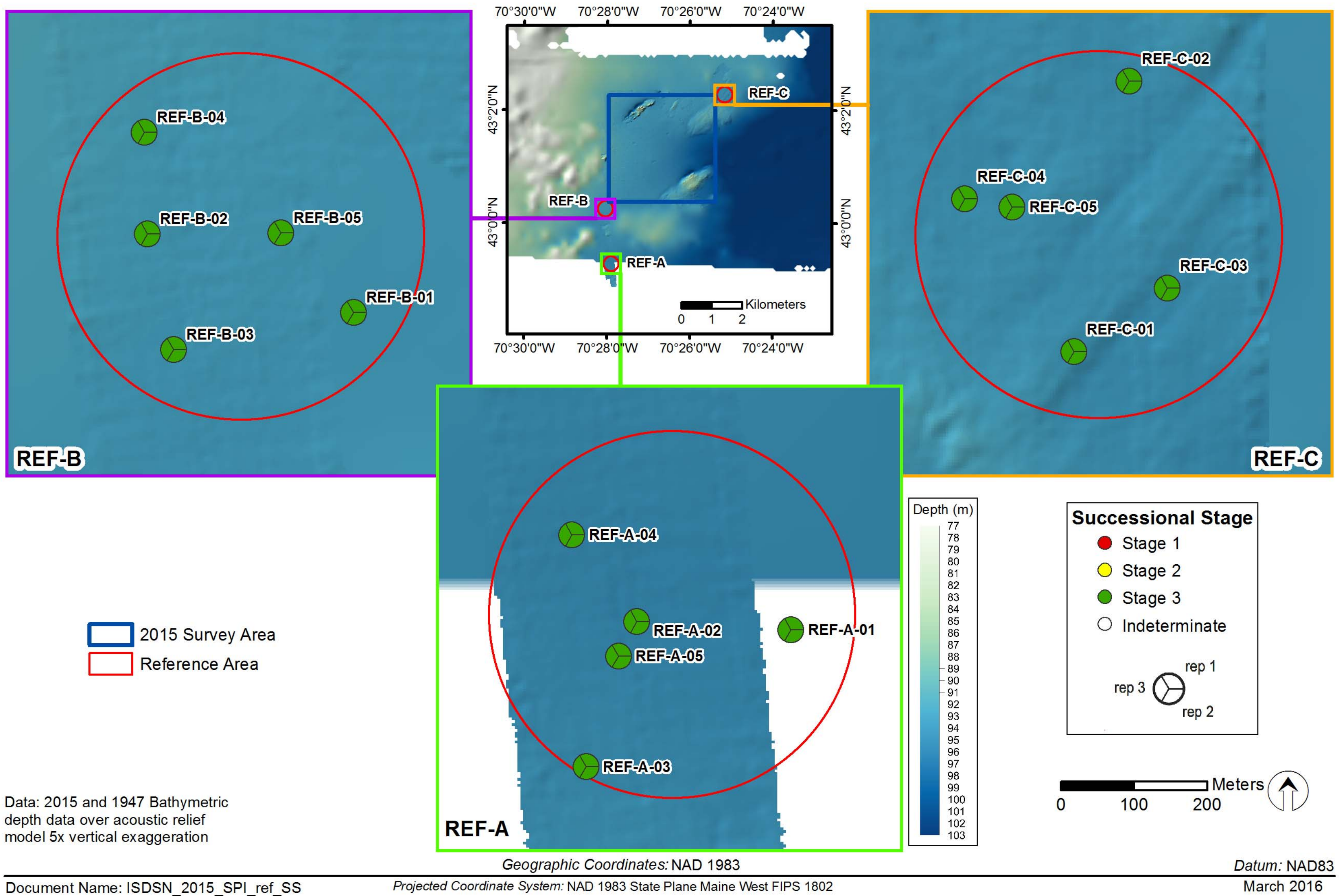

Figure 3-14. Infaunal successional stages found at stations at the ISDSN reference areas

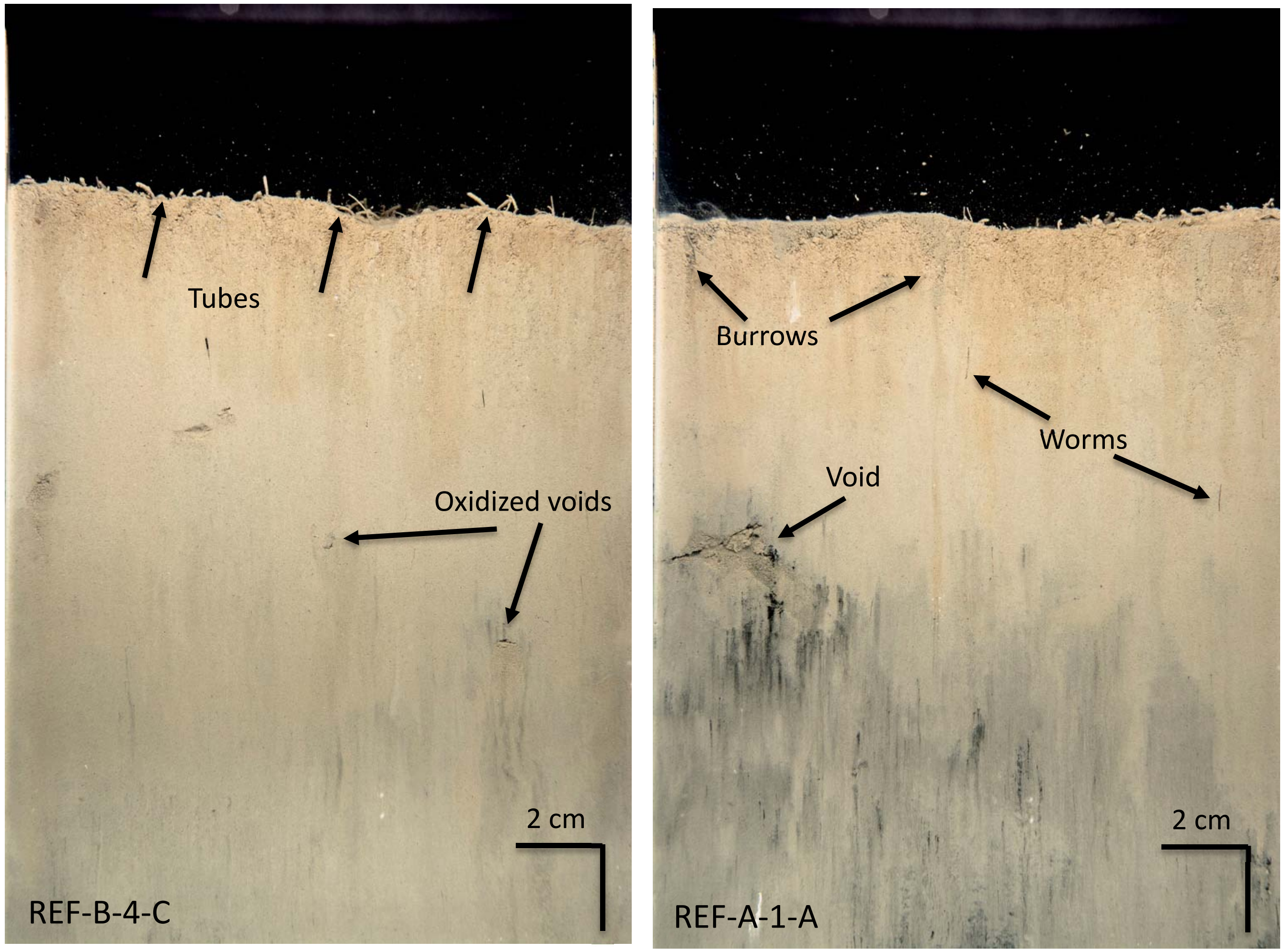

(A) **(B)**

Figure 3-15. Infaunal successional stages found at the ISDSN reference areas: Stage 1 on 3 at (A) Station REF-B-4 with small tubes at surface and oxidized voids at depth; (B) Station REF-A-1 with fecal pellets, small tubes at surface, clear subsurface burrows, polychaetes (worm), and a large void

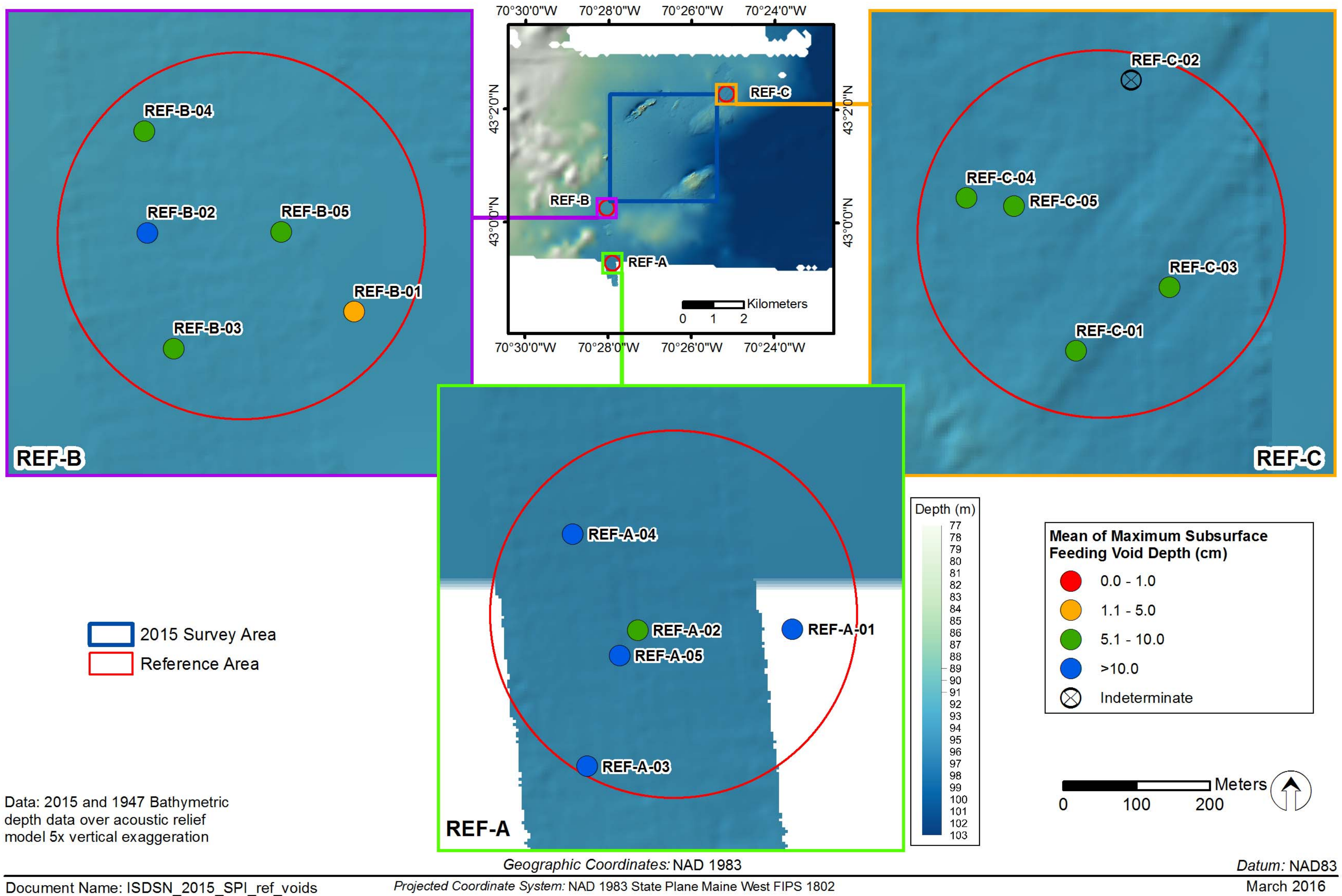

Figure 3-16. Maximum subsurface feeding void depth at ISDSN reference areas

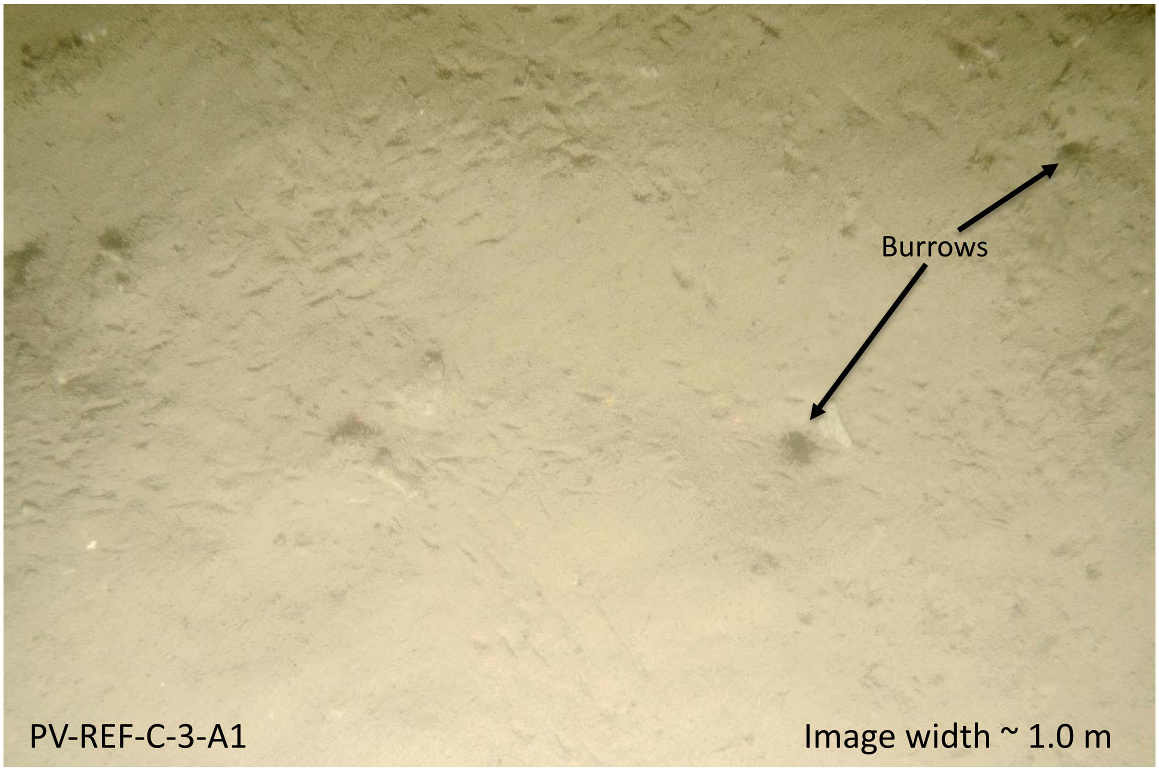

(A)

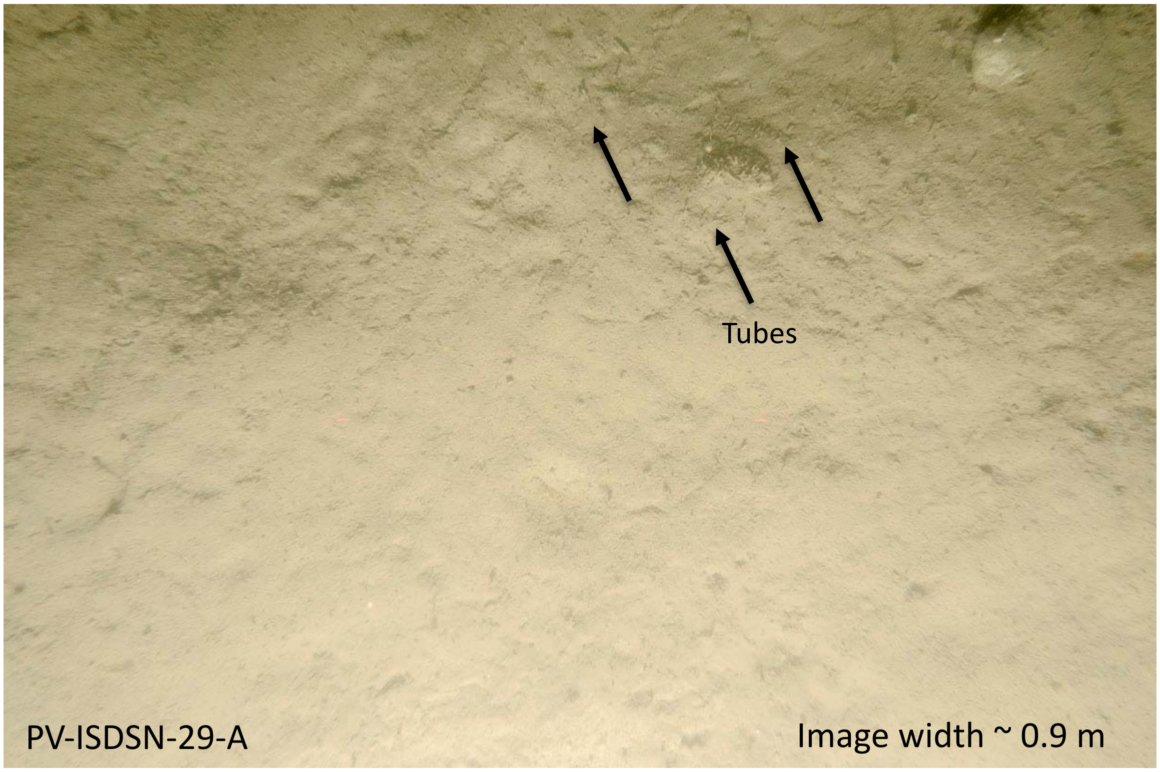

(B)

Figure 3-17. Plan-view images depicting small to medium burrows and small tubes at (A) Station REF-C-3 and (B) ISDSN-29

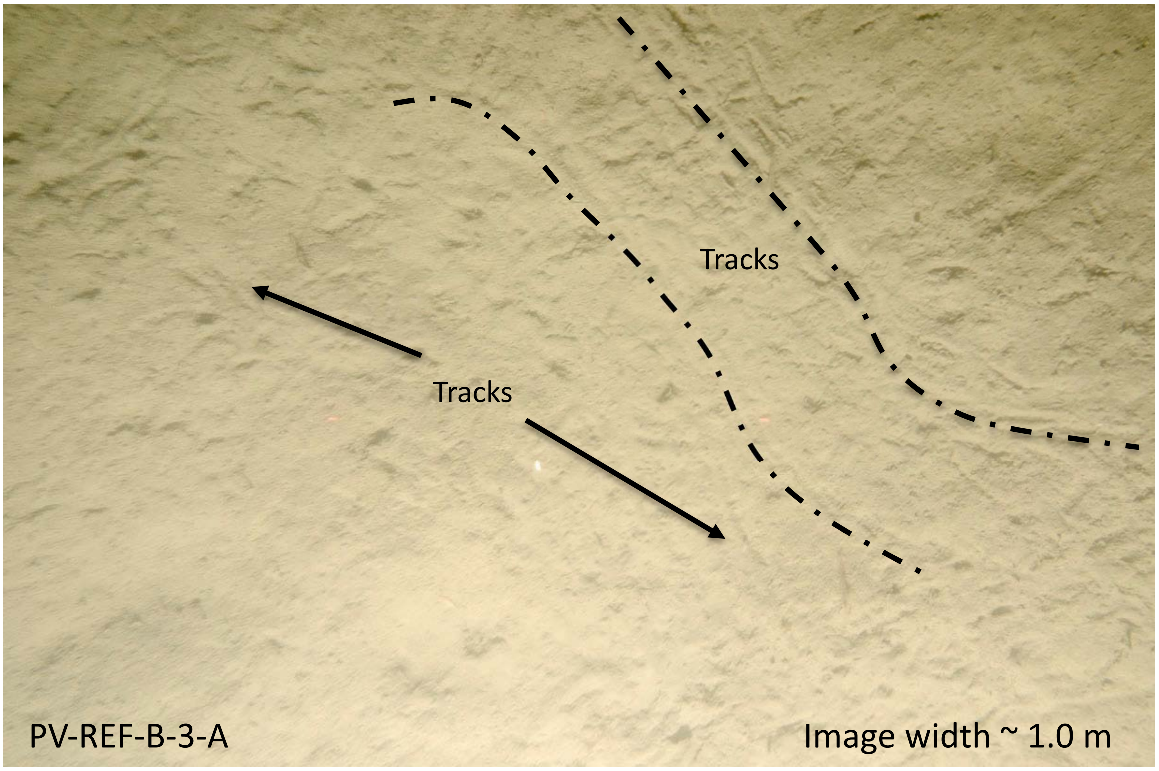

(**A**)

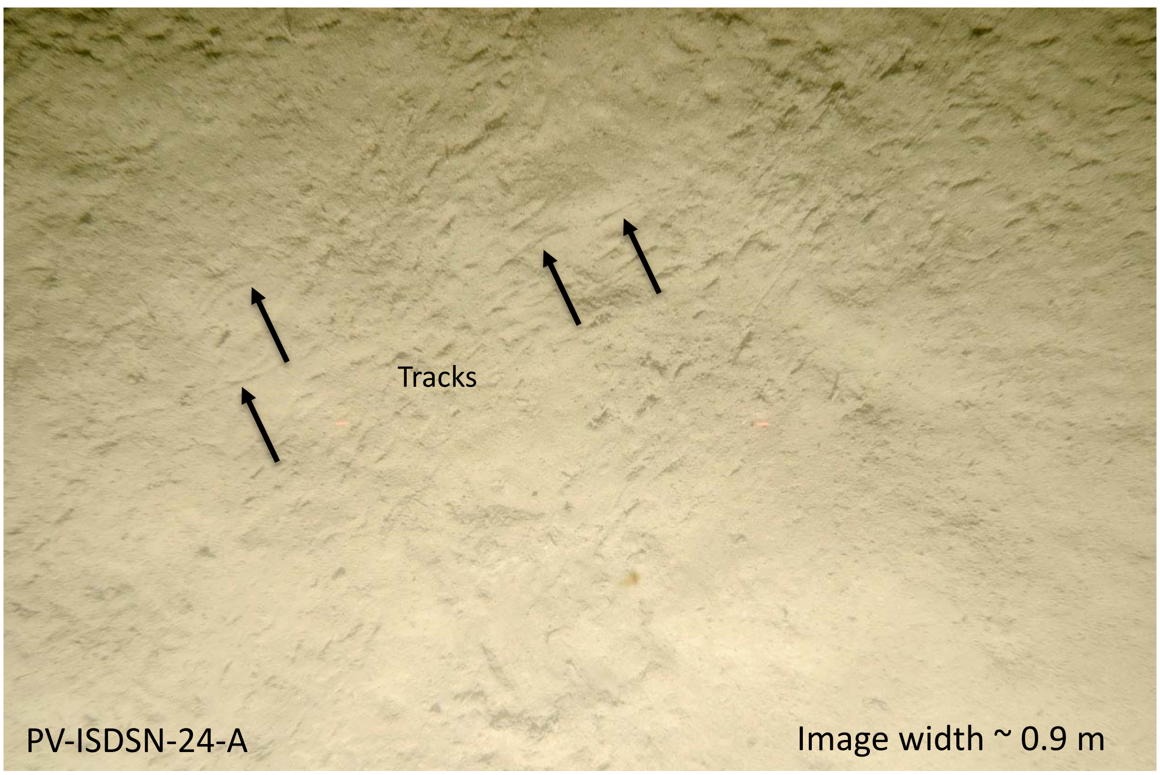

(B)

Figure 3-18. Plan-view images depicting tracks indicative of a mobile epifauna community at (A) Station REF-B-3-A and (B) ISDSN-24-A

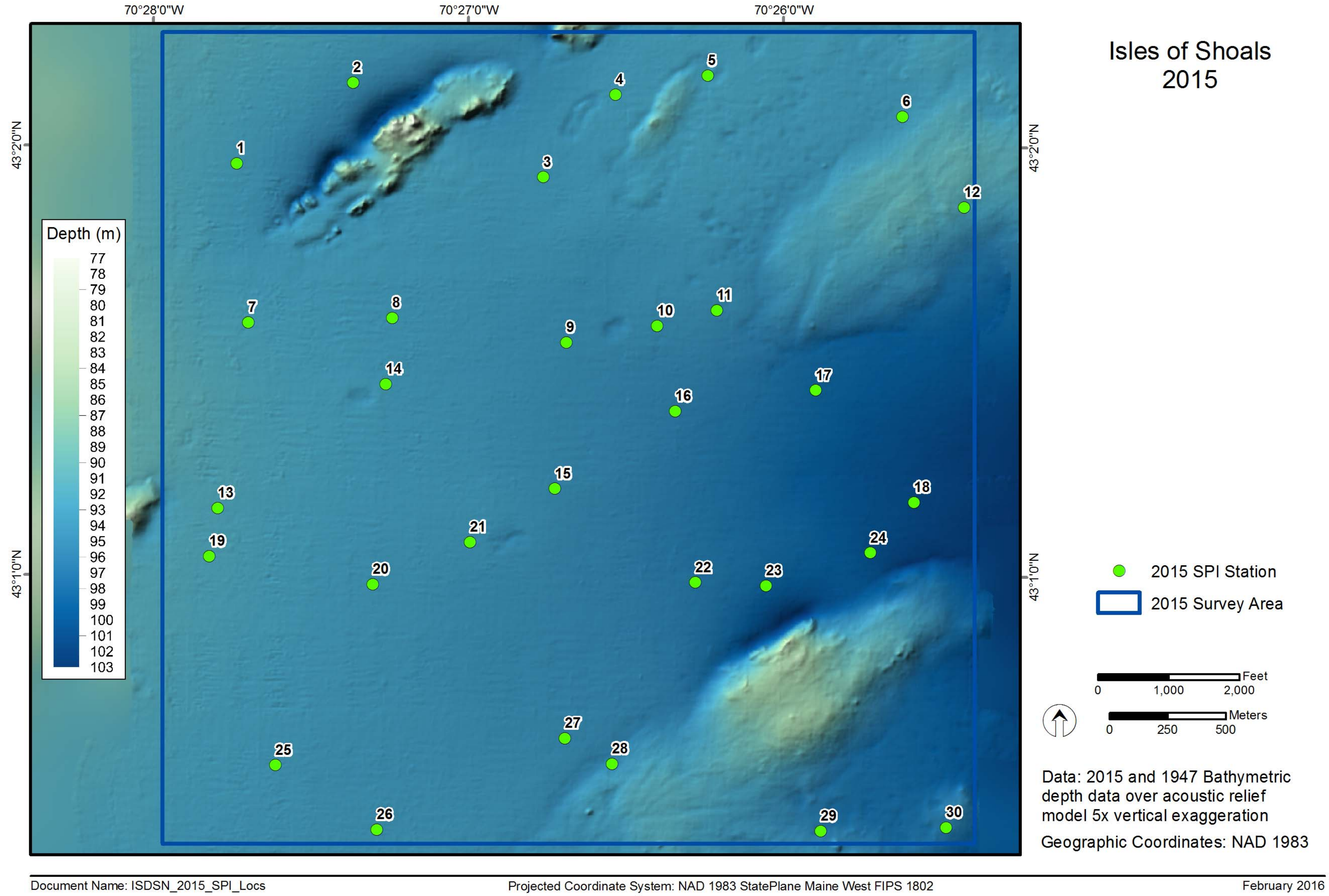

Figure 3-19. ISDSN with SPI/PV stations indicated

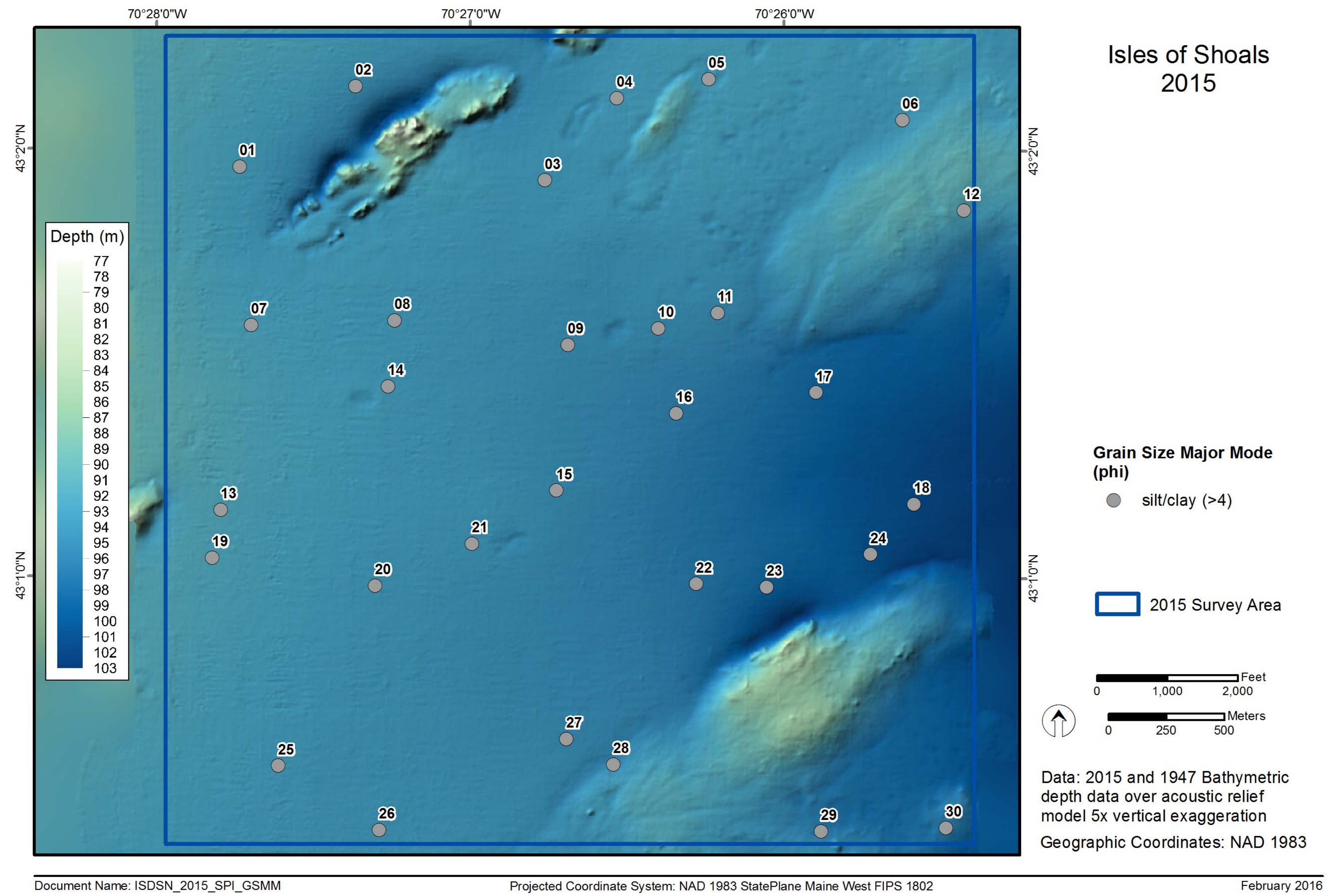

Figure 3-20. Sediment grain size major mode (phi) at ISDSN

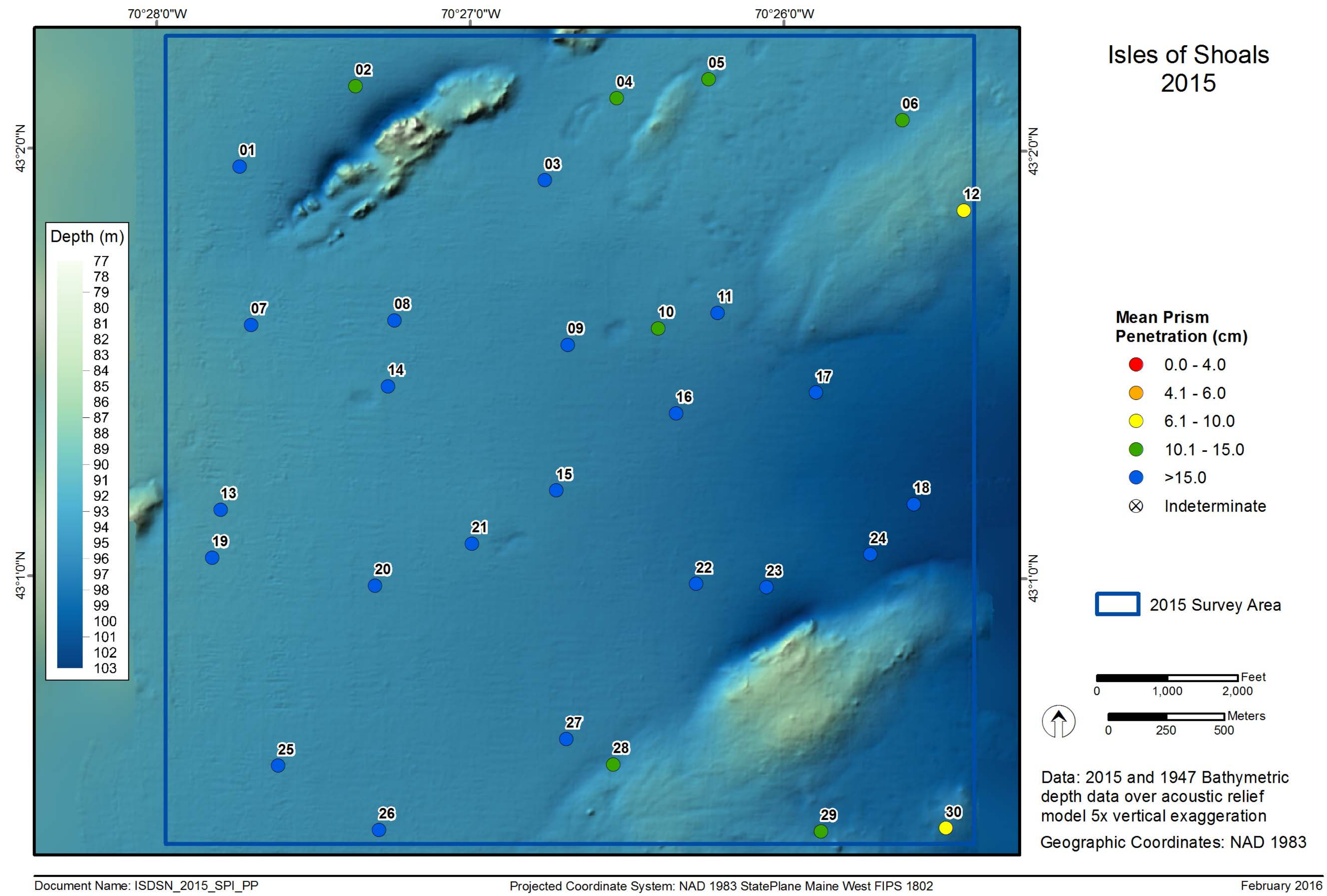

Figure 3-21. Mean station camera prism penetration depth (cm) at ISDSN

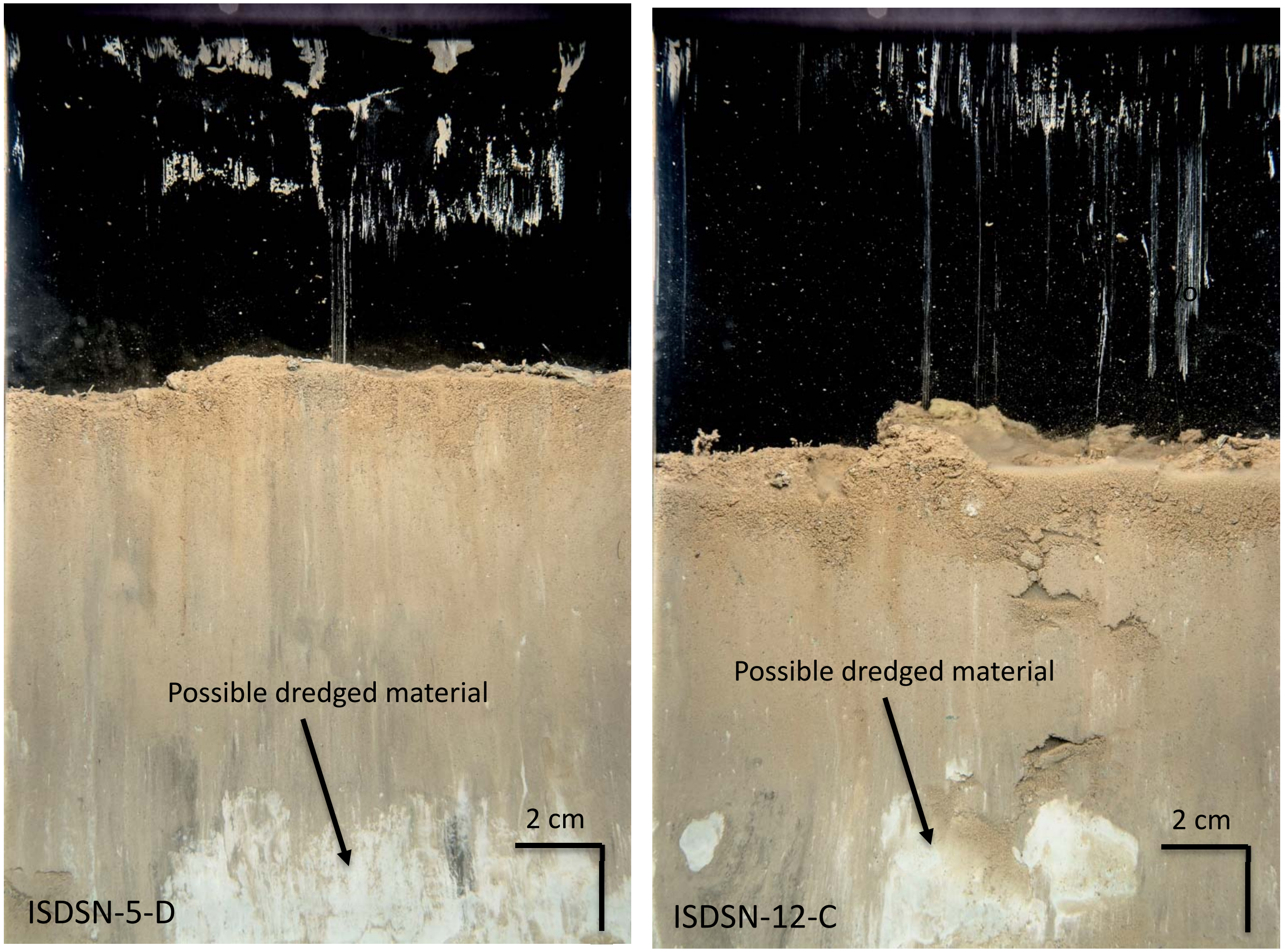

(A) **(B)**

Figure 3-22. Sediment-profile images with evidence of possible dredged material at (A) Station ISDSN-5 and (B) Station ISDSN-12

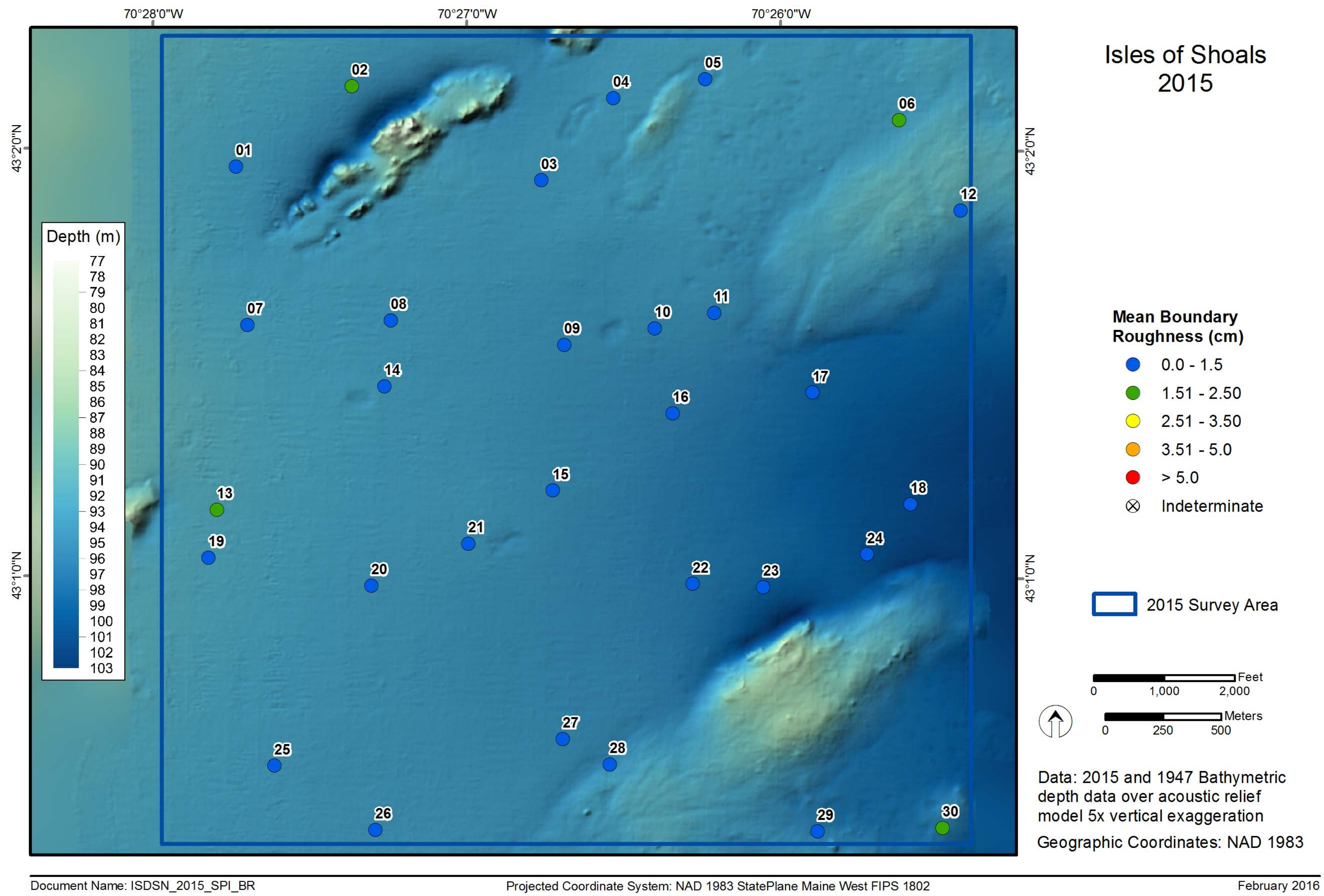

Figure 3-23. Mean station small-scale boundary roughness values (cm) at ISDSN

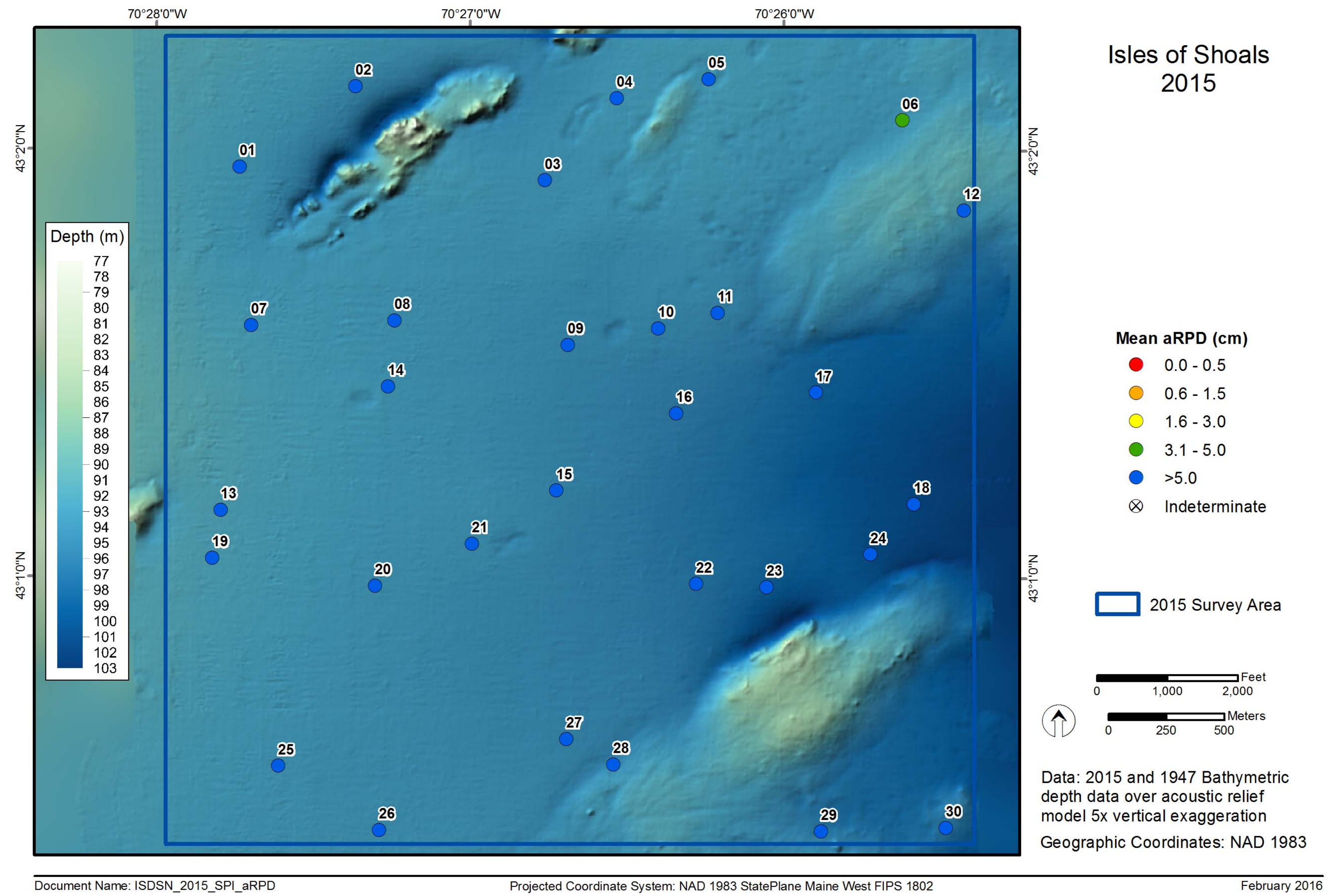

Figure 3-24. Mean station aRPD depth (cm) at ISDSN

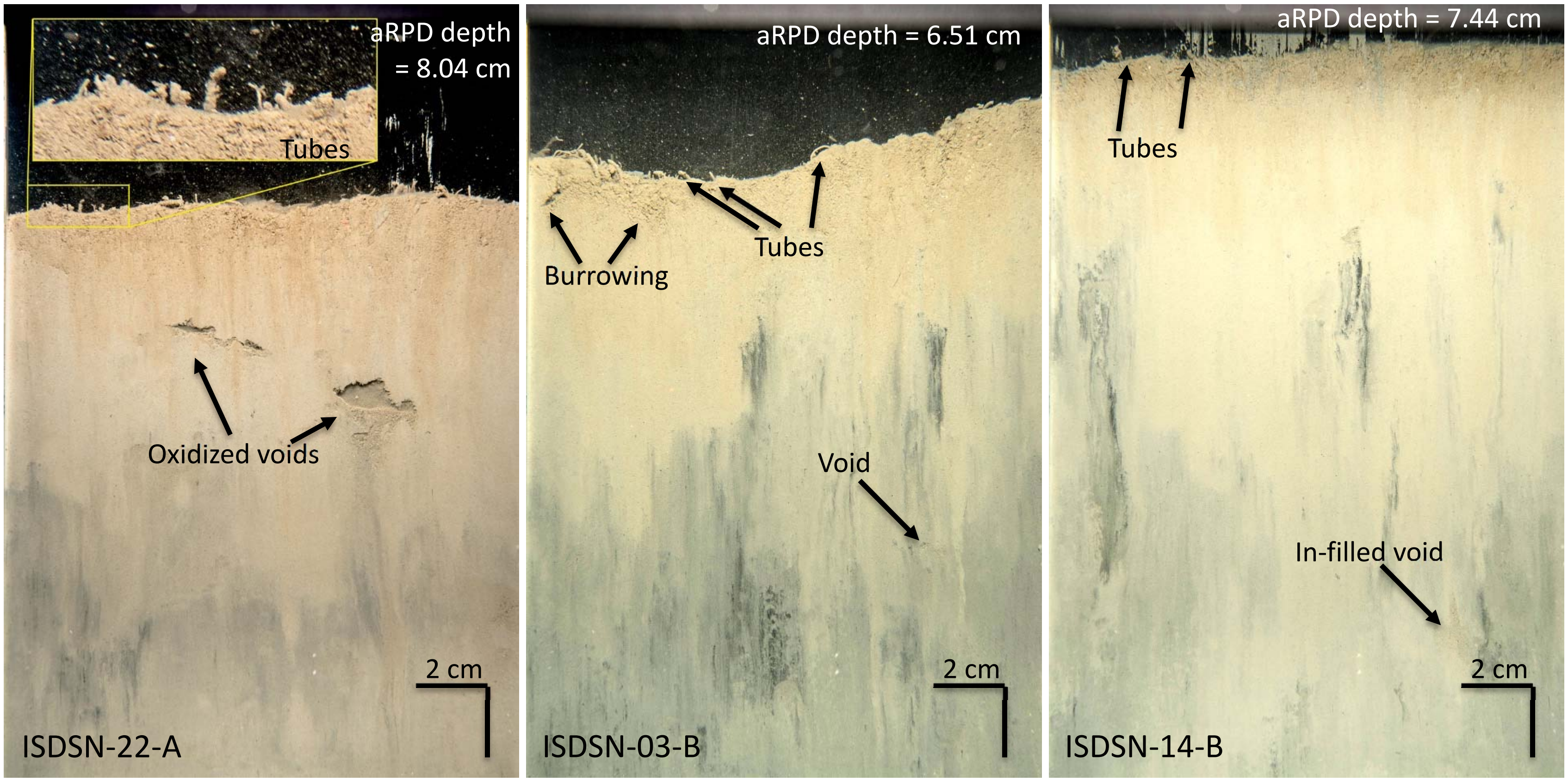

(A) **(B)** **(C)**

Figure 3-25. Mean aRPD depths (cm) and infaunal successional stages found at ISDSN: Stage 1 on 3 at (A) Station ISDSN-22 with small tubes at surface, shallow burrowing, and oxidized voids at depth; (B) Station ISDSN-3 with small tubes at surface, shallow burrowing, and subsurface void; and (C) Station ISDSN-14 with small to medium tubes at surface, shallow burrowing, in-filled voids at depth

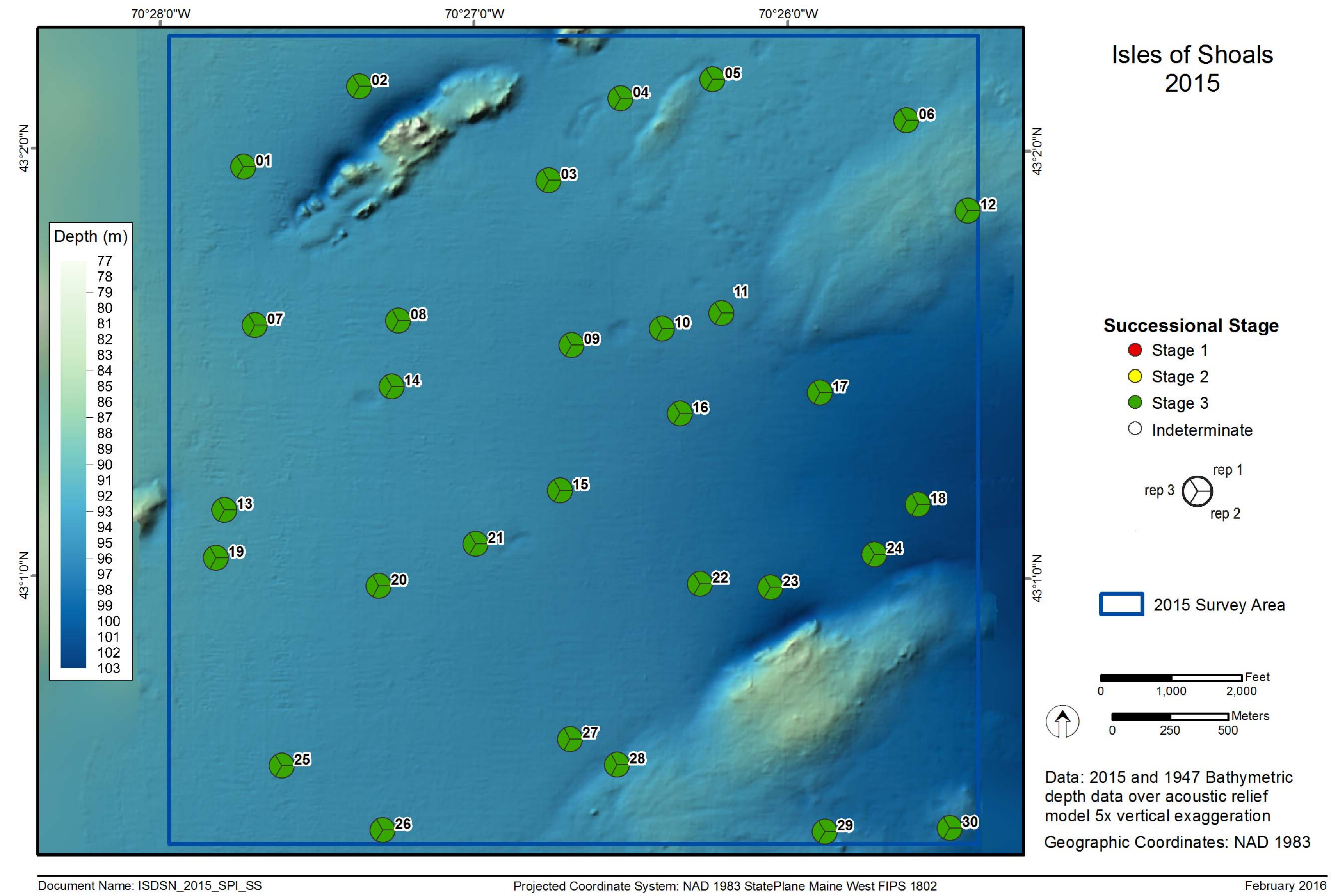

Figure 3-26. Infaunal successional stages found at ISDSN

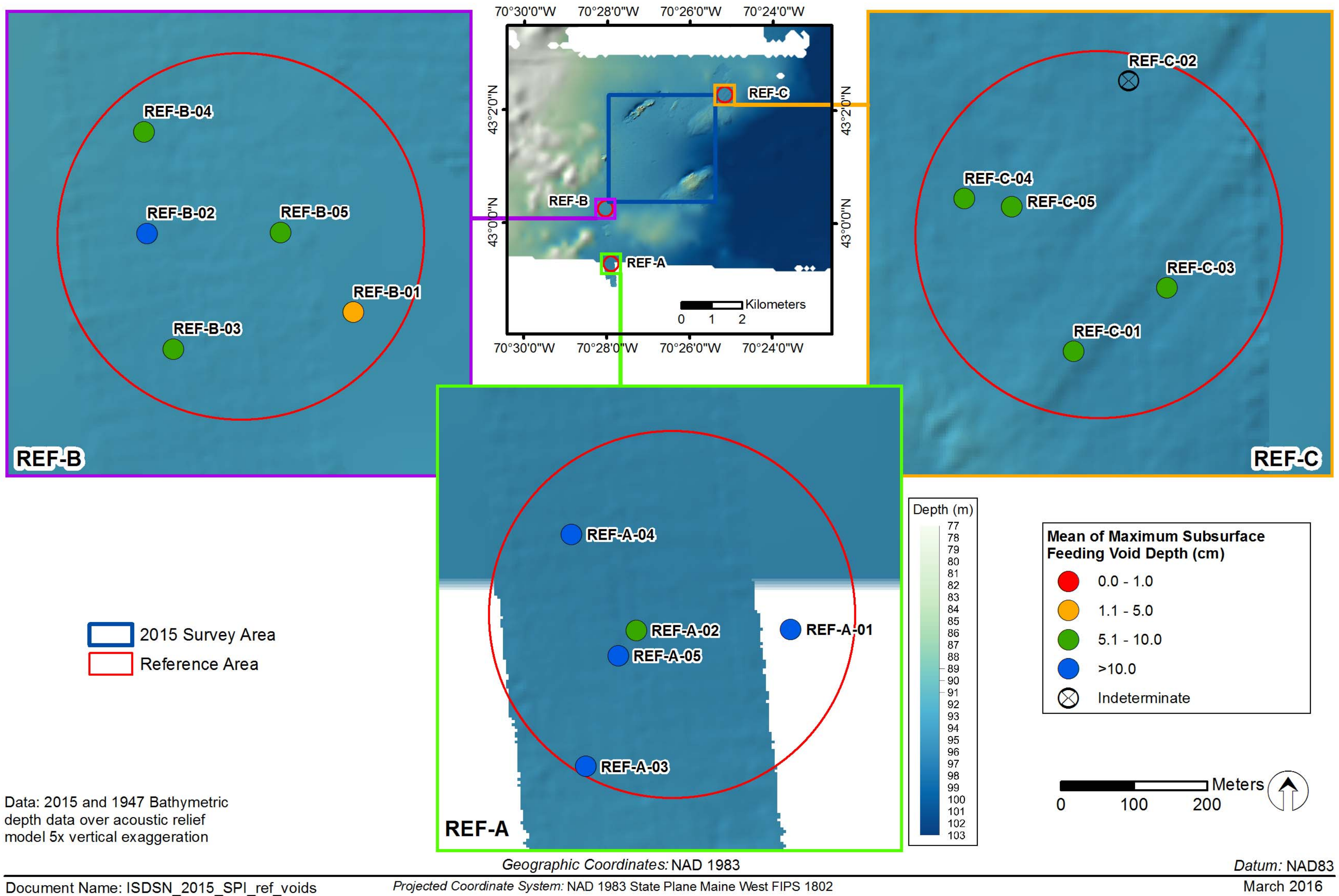

Figure 3-27. Maximum subsurface feeding void depth at ISDSN reference areas

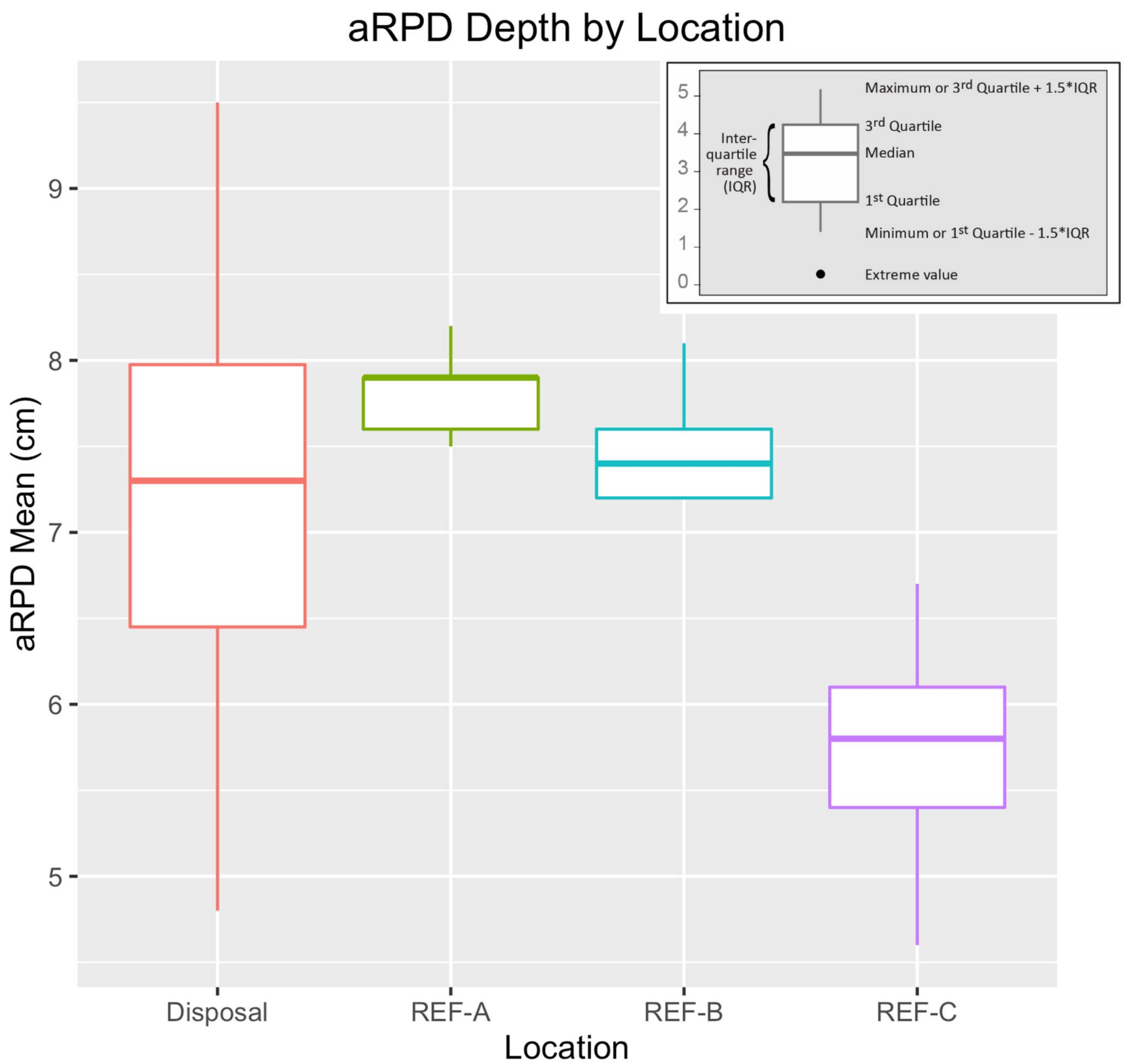

Figure 3-28. Boxplot showing distribution of station mean aRPD depths (cm) for 2015 ISDSN and each of the reference areas

4.0 SUMMARY

The objectives of the 2015 survey at ISDSN were to:

Objective 1: Characterize the seafloor topography and surface features of the potential site and reference areas by completing a multibeam bathymetric survey.

Objective 2: Use SPI and PV to further define the physical characteristics of surface sediment and to assess the benthic status over the proposed site and potential reference areas.

The 2015 survey revealed that ISDSN and the proposed reference areas can generally be characterized as low energy depositional environments dominated by fine-grained soft sediments and robust, mature benthic communities. Acoustic data, camera penetration depth, and grain size determinations indicated the physical nature of the sediments was predominantly soft and fine-grained. The consistently deep aRPD values and Stage 1 on 3 successional stages found in SPI images across the reference areas and the proposed disposal site are characteristic of a healthy, soft-bottom benthic ecosystem. Statistical tests revealed the reference areas and proposed disposal site were statistically equivalent in terms of aRPD depths, a SPI variable that is a reliable indicator of infaunal activity. Further, the ubiquitous presence of epifaunal tracks in PV images signified an active mobile epifaunal community across both the reference areas and at the ISDSN.

Topographic highs in the northwest, northeast, and southeast corners of the survey area, including REF-C, were shallower and harder than sediments in other part of the survey area. However, all SPI stations sampled in these regions had grain size and camera prism penetration depths consistent with soft-bottom habitats. It is important to note that no SPI/PV stations were located on the topographic highs in the northwest and southeast, which appear to be glacial outcrops based on their sharp topographic relief, hard backscatter returns, and textural properties evident in side-scan sonar data.

The results of the 2015 survey point to the possibility that dredged material was previously placed in the vicinity of ISDSN. There was evidence of potential dredged material in SPI images from the northeast and southeast sections of ISDSN and from REF-C. These results should be viewed cautiously as it is possible for the camera to carry cohesive clays, often indicative of dredged materials, from one station to another and create smearing artifacts in images at stations subsequent to where the clay was initially encountered. Acoustic data also revealed an area of small craters in the northeast portion of the survey area, a pattern that is often associated with dredged material placement. The possible presence of dredged material at ISDSN and REF-C should be considered when evaluating the potential designation of ISDSN as a formal disposal site and when finalizing reference areas to be used for future surveys.

The 2015 survey established baseline conditions of seafloor topography as well as physical and biological characteristics of the surface sediment at ISDSN. The results from this survey can be used as a temporal reference point should ISDSN be designated as a formal disposal site and require monitoring as part of the DAMOS Program.

5.0 REFERENCES

Carey, D. A.; Hickey, K.; Germano, J. D.; Read, L. B.; Esten, M. E. 2013. Monitoring Survey at the Massachusetts Bay Disposal Site September/October 2012. DAMOS Contribution No. 195. U.S. Army Corps of Engineers, New England District, Concord, MA, 87 pp.

Fredette, T. J.; French, G. T. 2004. Understanding the physical and environmental consequences of dredged material disposal: history in New England and current perspectives. Mar. Pollut. Bull. 49:93–102.

Germano, J. D. 1999. Ecology, statistics, and the art of misdiagnosis: The need for a paradigm shift. Environmental Reviews 7(4): 167 - 190.

Germano, J. D.; Rhoads, D. C.; Lunz, J. D. 1994. An Integrated, Tiered Approach to Monitoring and Management of Dredged Material Disposal Sites in the New England Regions. DAMOS Contribution No. 87. U.S. Army Corps of Engineers, New England Division, Waltham, MA, 67 pp.

Germano, J. D.; Rhoads, D. C.; Valente, R. M.; Carey, D. A.; Solan, M. 2011. The use of sediment-profile imaging (SPI) for environmental impact assessments and monitoring studies: lessons learned from the past four decades. Oceanogr. Mar. Biol. Ann. Rev. 49:235–285.

McBride, G. B. 1999. Equivalence tests can enhance environmental science and management. Aust. New Zeal. J. Stat. 41(1):19–29.

NOAA. 2015. NOS Hydrographic Surveys Specifications and Deliverables. May 2015.

Rhoads, D. C.; Germano, J. D. 1982. Characterization of organism-sediment relations using sediment profile imaging: An efficient method of remote ecological monitoring of the seafloor (REMOTS System). Mar. Ecol. Prog. Ser. 8:115–128.

Rhoads, D. C.; Germano, J. D. 1986. Interpreting long-term changes in benthic community structure: A new protocol. Hydrobiologia 142:291–308.

Satterthwaite, F. E. 1946. “An Approximate Distribution of Estimates of Variance Components”, Biometrics Bulletin, Vol. 2, No. 6, pp. 110-114.

Schuirmann, D. J. 1987. A comparison of the two one-sided tests procedure and the power approach for assessing the equivalence of average bioavailability. J. Pharmacokinet. Biopharm. 15:657–680.

USACE. 2013. Engineering and Design Hydrographic Surveying. EM1110-2-1003.

University of New Hampshire, Center for Coastal and Ocean Mapping/Joint Hydrographic Center. 2015. Seafloor bathymetry with hillshade for Western Gulf of Maine.

Welch, B. L. 1947. The Generalization of 'Student's' Problem when Several Different Population Variances are Involved. Biometrika, Volume 34, Issue 1/2, pp. 28-35

Zar, J. H. 1996. Biostatistical analysis. Third edition. New Jersey: Prentice Hall.

6.0 DATA TRANSMITTAL

Data transmittal to support this data report will be provided as a separate deliverable for inclusion in a Technical Support Notebook. The data submittal will include:

- Scope of Work
- Raw and processed acoustic survey data
- Report figures and associated files, including an ArcGIS geo-database
- Survey field logs
- Raw and adjusted SPI/PV images (raw NEF images have been converted to JPEG files for ease of use in report and general use by client; image size approximately 1200 x 1800 pixels).
- Report figures and associated files, including an ArcGIS geo-database
- Popup: interactive SPI data map
- Electronic copies of all final report products

APPENDIX A

TABLE OF COMMON CONVERSIONS

Metric Unit Conversion to English Unit		**English Unit Conversion to Metric Unit**	
1 meter 1 m	3.2808 ft	1 foot 1 ft	0.3048 m
1 square meter 1 m^2	10.7639 ft^2	1 square foot 1 ft^2	0.0929 m^2
1 kilometer 1 km	0.6214 mi	1 mile 1 mi	1.6093 km
1 cubic meter 1 m^3	1.3080 yd^3	1 cubic yard 1 yd^3	0.7646 m^3
1 centimeter 1 cm	0.3937 in	1 inch 1 in	2.54 cm

APPENDIX B

ISDSN ACTUAL SPI/PV REPLICATE LOCATIONS

September 2015

ISDSN September 2015 SPI/PV Replicate Locations					
Replicate	**Latitude (N)**	**Longitude (W)**	**Replicate**	**Latitude (N)**	**Longitude (W)**
ISDSN-01-A	43° 1.959'	70° 27.735'	ISDSN-08-A	43° 1.600'	70° 27.239'
ISDSN-01-B	43° 1.959'	70° 27.735'	ISDSN-08-B	43° 1.600'	70° 27.238'
ISDSN-01-C	43° 1.958'	70° 27.734'	ISDSN-08-C	43° 1.600'	70° 27.237'
ISDSN-01-D	43° 1.957'	70° 27.732'	ISDSN-08-D	43° 1.600'	70° 27.237'
ISDSN-02-A	43° 2.147'	70° 27.366'	ISDSN-09-A	43° 1.544'	70° 26.686'
ISDSN-02-B	43° 2.144'	70° 27.364'	ISDSN-09-B	43° 1.544'	70° 26.685'
ISDSN-02-C	43° 2.146'	70° 27.366'	ISDSN-09-C	43° 1.543'	70° 26.686'
ISDSN-02-D	43° 2.148'	70° 27.365'	ISDSN-09-D	43° 1.542'	70° 26.682'
ISDSN-03-A	43° 1.929'	70° 26.760'	ISDSN-10-A	43° 1.583'	70° 26.398'
ISDSN-03-B	43° 1.932'	70° 26.764'	ISDSN-10-B	43° 1.584'	70° 26.399'
ISDSN-03-C	43° 1.931'	70° 26.765'	ISDSN-10-C	43° 1.583'	70° 26.400'
ISDSN-03-D	43° 1.932'	70° 26.762'	ISDSN-10-D	43° 1.585'	70° 26.403'
ISDSN-04-A	43° 2.121'	70° 26.533'	ISDSN-11-A	43° 1.619'	70° 26.209'
ISDSN-04-B	43° 2.120'	70° 26.532'	ISDSN-11-B	43° 1.618'	70° 26.205'
ISDSN-04-C	43° 2.122'	70° 26.534'	ISDSN-11-C	43° 1.617'	70° 26.212'
ISDSN-04-D	43° 2.120'	70° 26.535'	ISDSN-11-D	43° 1.623'	70° 26.212'
ISDSN-05-A	43° 2.166'	70° 26.240'	ISDSN-12-A	43° 1.862'	70° 25.424'
ISDSN-05-B	43° 2.167'	70° 26.243'	ISDSN-12-B	43° 1.859'	70° 25.424'
ISDSN-05-C	43° 2.167'	70° 26.241'	ISDSN-12-C	43° 1.863'	70° 25.424'
ISDSN-05-D	43° 2.167'	70° 26.241'	ISDSN-12-D	43° 1.861'	70° 25.425'
ISDSN-06-A	43° 2.072'	70° 25.621'	ISDSN-13-A	43° 1.155'	70° 27.790'
ISDSN-06-B	43° 2.076'	70° 25.617'	ISDSN-13-B	43° 1.155'	70° 27.790'
ISDSN-06-C	43° 2.075'	70° 25.618'	ISDSN-13-C	43° 1.154'	70° 27.791'
ISDSN-06-D	43° 2.072'	70° 25.620'	ISDSN-13-D	43° 1.153'	70° 27.791'
ISDSN-07-A	43° 1.588'	70° 27.695'	ISDSN-14-A	43° 1.445'	70° 27.259'
ISDSN-07-B	43° 1.590'	70° 27.697'	ISDSN-14-B	43° 1.444'	70° 27.258'
ISDSN-07-C	43° 1.589'	70° 27.694'	ISDSN-14-C	43° 1.444'	70° 27.258'
ISDSN-07-D	43° 1.590'	70° 27.692'	ISDSN-14-D	43° 1.442'	70° 27.258'

Notes:
1) Coordinate system NAD83
2) This table reflects all attempts to collect SPI/PV replicates at each target station. The three replicates with the best quality images were used for analysis.

ISDSN September 2015 SPI/PV Replicate Locations

Replicate	Latitude (N)	Longitude (W)	Replicate	Latitude (N)	Longitude (W)
ISDSN-15-A	43° 1.203'	70° 26.720'	ISDSN-22-A	43° 0.986'	70° 26.274'
ISDSN-15-B	43° 1.206'	70° 26.719'	ISDSN-22-B	43° 0.986'	70° 26.278'
ISDSN-15-C	43° 1.205'	70° 26.718'	ISDSN-22-C	43° 0.987'	70° 26.279'
ISDSN-15-D	43° 1.203'	70° 26.716'	ISDSN-22-D	43° 0.987'	70° 26.277'
ISDSN-16-A	43° 1.385'	70° 26.340'	ISDSN-23-A	43° 0.979'	70° 26.050'
ISDSN-16-B	43° 1.384'	70° 26.339'	ISDSN-23-B	43° 0.973'	70° 26.048'
ISDSN-16-C	43° 1.384'	70° 26.340'	ISDSN-23-C	43° 0.977'	70° 26.052'
ISDSN-16-D	43° 1.384'	70° 26.340'	ISDSN-23-D	43° 0.980'	70° 26.048'
ISDSN-17-A	43° 1.434'	70° 25.894'	ISDSN-24-A	43° 1.056'	70° 25.718'
ISDSN-17-B	43° 1.437'	70° 25.898'	ISDSN-24-B	43° 1.057'	70° 25.719'
ISDSN-17-C	43° 1.434'	70° 25.899'	ISDSN-24-C	43° 1.056'	70° 25.718'
ISDSN-17-D	43° 1.432'	70° 25.898'	ISDSN-24-D	43° 1.054'	70° 25.718'
ISDSN-18-A	43° 1.174'	70° 25.580'	ISDSN-25-A	43° 0.557'	70° 27.605'
ISDSN-18-B	43° 1.173'	70° 25.579'	ISDSN-25-B	43° 0.559'	70° 27.608'
ISDSN-18-C	43° 1.175'	70° 25.580'	ISDSN-25-C	43° 0.560'	70° 27.609'
ISDSN-18-D	43° 1.172'	70° 25.579'	ISDSN-25-D	43° 0.560'	70° 27.607'
ISDSN-19-A	43° 1.043'	70° 27.816'	ISDSN-26-A	43° 0.408'	70° 27.283'
ISDSN-19-B	43° 1.044'	70° 27.817'	ISDSN-26-B	43° 0.408'	70° 27.281'
ISDSN-19-C	43° 1.043'	70° 27.817'	ISDSN-26-C	43° 0.406'	70° 27.282'
ISDSN-19-D	43° 1.042'	70° 27.816'	ISDSN-26-D	43° 0.408'	70° 27.280'
ISDSN-20-A	43° 0.980'	70° 27.297'	ISDSN-27-A	43° 0.623'	70° 26.686'
ISDSN-20-B	43° 0.980'	70° 27.297'	ISDSN-27-B	43° 0.625'	70° 26.696'
ISDSN-20-C	43° 0.981'	70° 27.295'	ISDSN-27-C	43° 0.625'	70° 26.690'
ISDSN-20-D	43° 0.980'	70° 27.295'	ISDSN-27-D	43° 0.625'	70° 26.693'
ISDSN-21-A	43° 1.079'	70° 26.989'	ISDSN-28-A	43° 0.563'	70° 26.536'
ISDSN-21-B	43° 1.077'	70° 26.987'	ISDSN-28-B	43° 0.562'	70° 26.535'
ISDSN-21-C	43° 1.079'	70° 26.988'	ISDSN-28-C	43° 0.564'	70° 26.538'
ISDSN-21-D	43° 1.077'	70° 26.986'	ISDSN-28-D	43° 0.565'	70° 26.536'

Notes:
1) Coordinate system NAD83
2) This table reflects all attempts to collect SPI/PV replicates at each target station. The three replicates with the best quality images were used for analysis.

ISDSN September 2015 SPI/PV Replicate Locations					
Replicate	**Latitude (N)**	**Longitude (W)**	**Replicate**	**Latitude (N)**	**Longitude (W)**
ISDSN-29-A	43° 0.408'	70° 25.874'	REF-B-01-A	43° 0.201'	70° 27.926'
ISDSN-29-B	43° 0.408'	70° 25.871'	REF-B-01-B	43° 0.204'	70° 27.925'
ISDSN-29-C	43° 0.409'	70° 25.872'	REF-B-01-C	43° 0.203'	70° 27.924'
ISDSN-29-D	43° 0.410'	70° 25.875'	REF-B-01-D	43° 0.205'	70° 27.925'
ISDSN-30-A	43° 0.417'	70° 25.475'	REF-B-02-A	43° 0.259'	70° 28.133'
ISDSN-30-B	43° 0.417'	70° 25.476'	REF-B-02-B	43° 0.261'	70° 28.133'
ISDSN-30-C	43° 0.417'	70° 25.473'	REF-B-02-C	43° 0.260'	70° 28.131'
ISDSN-30-D	43° 0.417'	70° 25.475'	REF-B-02-D	43° 0.259'	70° 28.134'
REF-A-01-A	43° -0.729'	70° 27.776'	REF-B-03-A	43° 0.174'	70° 28.106'
REF-A-01-B	43° -0.731'	70° 27.780'	REF-B-03-B	43° 0.172'	70° 28.108'
REF-A-01-C	43° -0.731'	70° 27.776'	REF-B-03-C	43° 0.173'	70° 28.109'
REF-A-01-D	43° -0.730'	70° 27.776'	REF-B-03-D	43° 0.172'	70° 28.107'
REF-A-02-A	43° -0.730'	70° 27.931'	REF-B-04-A	43° 0.334'	70° 28.135'
REF-A-02-B	43° -0.725'	70° 27.931'	REF-B-04-B	43° 0.334'	70° 28.136'
REF-A-02-C	43° -0.727'	70° 27.931'	REF-B-04-C	43° 0.333'	70° 28.139'
REF-A-02-D	43° -0.730'	70° 27.931'	REF-B-04-D	43° 0.333'	70° 28.135'
REF-A-03-A	43° -0.831'	70° 27.981'	REF-B-05-A	43° 0.260'	70° 27.999'
REF-A-03-B	43° -0.834'	70° 27.975'	REF-B-05-B	43° 0.257'	70° 27.994'
REF-A-03-C	43° -0.832'	70° 27.977'	REF-B-05-C	43° 0.256'	70° 27.995'
REF-A-03-D	43° -0.831'	70° 27.979'	REF-B-05-D	43° 0.256'	70° 27.993'
REF-A-04-A	43° -0.660'	70° 27.996'	REF-C-01-A	43° 2.194'	70° 25.190'
REF-A-04-B	43° -0.662'	70° 27.996'	REF-C-01-B	43° 2.197'	70° 25.196'
REF-A-04-C	43° -0.659'	70° 27.996'	REF-C-01-C	43° 2.195'	70° 25.194'
REF-A-04-D	43° -0.660'	70° 27.995'	REF-C-01-D	43° 2.195'	70° 25.193'
REF-A-05-A	43° -0.749'	70° 27.949'	REF-C-02-A	43° 2.393'	70° 25.136'
REF-A-05-B	43° -0.752'	70° 27.942'	REF-C-02-B	43° 2.395'	70° 25.136'
REF-A-05-C	43° -0.752'	70° 27.948'	REF-C-02-C	43° 2.394'	70° 25.138'
REF-A-05-D	43° -0.748'	70° 27.945'	REF-C-02-D	43° 2.396'	70° 25.141'

Notes:
1) Coordinate system NAD83
2) This table reflects all attempts to collect SPI/PV replicates at each target station. The three replicates with the best quality images were used for analysis.

ISDSN September 2015 SPI/PV Replicate Locations					
Replicate	**Latitude (N)**	**Longitude (W)**	**Replicate**	**Latitude (N)**	**Longitude (W)**
REF-C-03-A	43° 2.241'	70° 25.097'			
REF-C-03-B	43° 2.246'	70° 25.096'			
REF-C-03-C	43° 2.243'	70° 25.099'			
REF-C-03-D	43° 2.244'	70° 25.099'			
REF-C-04-A	43° 2.306'	70° 25.300'			
REF-C-04-B	43° 2.306'	70° 25.301'			
REF-C-04-C	43° 2.307'	70° 25.303'			
REF-C-04-D	43° 2.305'	70° 25.303'			
REF-C-05-A	43° 2.301'	70° 25.253'			
REF-C-05-B	43° 2.299'	70° 25.255'			
REF-C-05-C	43° 2.301'	70° 25.255'			
REF-C-05-D	43° 2.300'	70° 25.257'			

Notes: 1) Coordinate system NAD83
2) This table reflects all attempts to collect SPI/PV replicates at each target station. The three replicates with the best quality images were used for analysis.

APPENDIX C

SEDIMENT-PROFILE AND PLAN-VIEW IMAGE ANALYSIS RESULTS FOR ISDSN SURVEY, SEPTEMBER 2015

Location	Station	Replicate	Date	Time	Depth (ft)	Stop Collar Setting (in)	# of Weights (per side)	Grain Size Major Mode (phi)	Grain Size Minimum (phi)	Grain Size Maximum (phi)	Grain Size Range	Penetration Area (sq cm)	Penetration Mean (cm)	Penetration Minimum (cm)	Penetration Maximum (cm)	Boundary Roughness (cm)	Boundary Roughness Type	aRPD > Pen	aRPD Area (sq cm)	Mean aRPD (cm)
Site	1	A	09/27/15	7:28:10	310	12.5	1	>4	>4	2	>4 to 2	250.4	17.3	17.0	17.9	0.9	Biological	FALSE	80.6	5.6
Site	1	B	09/27/15	7:28:59	310	12.5	1	>4	>4	2	>4 to 2	242.2	16.7	16.3	17.0	0.7	Biological	FALSE	92.1	6.4
Site	1	C	09/27/15	7:29:53	310	12.5	1	>4	>4	2	>4 to 2	261.4	18.0	17.5	18.3	0.8	Biological	FALSE	135.9	9.4
Site	2	A	09/27/15	17:08:59	308	12.5	1	>4	>4	2	>4 to 2	209.2	14.4	12.6	15.0	2.4	Biological	FALSE	104.3	7.2
Site	2	B	09/27/15	17:09:44	308	12.5	1	>4	>4	2	>4 to 2	229.0	15.8	15.3	16.0	0.7	Biological	FALSE	92.1	6.4
Site	2	D	09/27/15	17:11:09	308	12.5	1	>4	>4	2	>4 to 2	173.2	11.9	10.7	13.1	2.4	Physical	FALSE	75.0	5.2
Site	3	A	09/27/15	10:31:27	319	12.5	1	>4	>4	2	>4 to 2	246.9	17.0	16.7	17.3	0.6	Biological	FALSE	114.7	7.9
Site	3	B	09/27/15	10:32:39	319	12.5	1	>4	>4	2	>4 to 2	228.3	15.7	15.5	15.9	0.5	Biological	FALSE	94.4	6.5
Site	3	D	09/27/15	10:34:11	319	12.5	1	>4	>4	2	>4 to 2	215.5	14.9	14.5	15.0	0.6	Biological	FALSE	112.2	7.7
Site	4	A	09/27/15	10:44:18	316	12.5	1	>4	>4	2	>4 to 2	223.8	15.4	15.3	15.6	0.2	Biological	FALSE	74.2	5.1
Site	4	C	09/27/15	10:45:52	316	12.5	1	>4	>4	2	>4 to 2	189.9	13.1	12.6	13.6	0.9	Biological	FALSE	86.9	6.0
Site	4	D	09/27/15	10:46:35	316	12.5	1	>4	>4	2	>4 to 2	204.4	14.1	13.6	14.7	1.0	Biological	FALSE	87.8	6.1

Location	Station	Replicate	Date	Time	Depth (ft)	Stop Collar Setting (in)	# of Weights (per side)	Grain Size Major Mode (phi)	Grain Size Minimum (phi)	Grain Size Maximum (phi)	Grain Size Range	Penetration Area (sq cm)	Penetration Mean (cm)	Penetration Minimum (cm)	Penetration Maximum (cm)	Boundary Roughness (cm)	Boundary Roughness Type	aRPD > Pen	aRPD Area (sq cm)	Mean aRPD (cm)
Site	5	A	09/27/15	10:55:54	315	12.5	1	>4	>4	2	>4 to 2	171.6	11.8	10.6	12.3	1.7	Biological	FALSE	88.6	6.1
Site	5	B	09/27/15	10:56:43	315	12.5	1	>4	>4	2	>4 to 2	201.2	13.9	13.4	14.4	1.0	Biological	FALSE	95.5	6.6
Site	5	D	09/27/15	10:58:26	315	12.5	1	>4	>4	2	>4 to 2	190.6	13.1	12.5	13.6	1.1	Biological	FALSE	88.4	6.1
Site	6	A	09/27/15	11:09:44	317	12.5	1	>4	>4	2	>4 to 2	191.9	13.2	11.5	14.7	3.2	Biological	FALSE	82.3	5.7
Site	6	B	09/27/15	11:10:30	317	12.5	1	>4	>4	2	>4 to 2	169.1	11.7	10.0	12.6	2.7	Biological	FALSE	77.2	5.3
Site	6	D	09/27/15	11:12:04	317	12.5	1	>4	>4	2	>4 to 2	155.2	10.7	10.2	11.5	1.4	Biological	FALSE	47.7	3.3
Site	7	A	09/27/15	7:52:41	310	12.5	1	>4	>4	2	>4 to 2	249.8	17.2	16.7	17.7	1.0	Biological	FALSE	98.7	6.8
Site	7	B	09/27/15	7:53:26	310	12.5	1	>4	>4	2	>4 to 2	234.4	16.2	15.5	16.6	1.1	Biological	FALSE	78.7	5.4
Site	7	C	09/27/15	7:54:08	310	12.5	1	>4	>4	2	>4 to 2	208.3	14.4	14.0	14.8	0.8	Biological	FALSE	101.3	7.0
Site	8	A	09/27/15	8:04:46	312	12.5	1	>4	>4	2	>4 to 2	272.5	18.8	18.5	19.1	0.6	Biological	FALSE	107.5	7.4
Site	8	B	09/27/15	8:05:28	312	12.5	1	>4	>4	2	>4 to 2	233.3	16.1	15.7	16.9	1.3	Biological	FALSE	108.7	7.5
Site	8	C	09/27/15	8:06:17	312	12.5	1	>4	>4	2	>4 to 2	259.3	17.9	17.1	18.2	1.1	Biological	FALSE	129.7	8.9

Location	Station	Replicate	Date	Time	Depth (ft)	Stop Collar Setting (in)	# of Weights (per side)	Grain Size Major Mode (phi)	Grain Size Minimum (phi)	Grain Size Maximum (phi)	Grain Size Range	Penetration Area (sq cm)	Penetration Mean (cm)	Penetration Minimum (cm)	Penetration Maximum (cm)	Boundary Roughness (cm)	Boundary Roughness Type	aRPD > Pen	aRPD Area (sq cm)	Mean aRPD (cm)
Site	9	A	09/27/15	9:37:28	322	12.5	1	>4	>4	2	>4 to 2	249.5	17.2	16.7	17.5	0.8	Biological	FALSE	105.2	7.2
Site	9	C	09/27/15	9:38:57	322	12.5	1	>4	>4	2	>4 to 2	239.2	16.5	16.2	16.7	0.5	Biological	FALSE	94.9	6.5
Site	9	D	09/27/15	9:39:51	322	12.5	1	>4	>4	2	>4 to 2	242.0	16.7	16.3	16.9	0.6	Biological	FALSE	96.4	6.6
Site	10	A	09/27/15	10:08:47	322	12.5	1	>4	>4	2	>4 to 2	218.6	15.1	14.5	15.8	1.3	Biological	FALSE	99.5	6.9
Site	10	B	09/27/15	10:09:30	322	12.5	1	>4	>4	2	>4 to 2	239.7	16.5	16.1	17.0	0.8	Biological	FALSE	92.2	6.4
Site	10	C	09/27/15	10:10:18	322	12.5	1	>4	>4	2	>4 to 2	189.2	13.0	12.8	13.2	0.4	Biological	FALSE	93.5	6.4
Site	11	A	09/27/15	10:15:29	322	12.5	1	>4	>4	2	>4 to 2	234.5	16.2	14.5	16.9	2.3	Biological	FALSE	76.2	5.3
Site	11	B	09/27/15	10:16:20	322	12.5	1	>4	>4	2	>4 to 2	217.0	15.0	14.5	15.5	1.0	Biological	FALSE	73.2	5.0
Site	11	D	09/27/15	10:18:13	322	12.5	1	>4	>4	2	>4 to 2	259.6	17.9	17.6	18.2	0.7	Biological	FALSE	116.8	8.1
Site	12	A	09/27/15	12:42:29	312	12.5	1	>4	>4	2	>4 to 2	102.0	7.0	6.6	7.5	0.9	Biological	TRUE	102.0	7.0
Site	12	B	09/27/15	12:43:15	312	12.5	1	>4	>4	2	>4 to 2	143.9	9.9	9.6	10.4	0.8	Biological	FALSE	117.0	8.1
Site	12	C	09/27/15	12:44:14	312	12.5	1	>4	>4	2	>4 to 2	163.4	11.3	10.9	11.9	1.0	Biological	FALSE	91.0	6.3
Site	13	A	09/27/15	8:29:09	308	12.5	1	>4	>4	2	>4 to 2	211.1	14.6	12.9	16.2	3.4	Physical	FALSE	103.0	7.1

Location	Station	Replicate	Date	Time	Depth (ft)	Stop Collar Setting (in)	# of Weights (per side)	Grain Size Major Mode (phi)	Grain Size Minimum (phi)	Grain Size Maximum (phi)	Grain Size Range	Penetration Area (sq cm)	Penetration Mean (cm)	Penetration Minimum (cm)	Penetration Maximum (cm)	Boundary Roughness (cm)	Boundary Roughness Type	aRPD > Pen	aRPD Area (sq cm)	Mean aRPD (cm)
Site	13	B	09/27/15	8:29:52	308	12.5	1	>4	>4	2	>4 to 2	229.7	15.8	15.4	16.2	0.8	Biological	FALSE	95.1	6.6
Site	13	C	09/27/15	8:30:39	308	12.5	1	>4	>4	2	>4 to 2	226.7	15.6	15.5	15.9	0.4	Biological	FALSE	124.1	8.6
Site	14	A	09/27/15	8:16:05	312	12.5	1	>4	>4	2	>4 to 2	192.0	13.2	11.6	14.5	2.9	Biological	FALSE	105.1	7.2
Site	14	B	09/27/15	8:16:46	312	12.5	1	>4	>4	2	>4 to 2	209.8	14.5	13.8	14.8	0.9	Biological	FALSE	107.9	7.4
Site	14	C	09/27/15	8:17:27	312	12.5	1	>4	>4	2	>4 to 2	265.2	18.3	18.1	18.5	0.4	Biological	FALSE	105.4	7.3
Site	15	A	09/27/15	9:12:09	320	12.5	1	>4	>4	2	>4 to 2	245.9	17.0	16.5	17.3	0.8	Biological	FALSE	130.3	9.0
Site	15	B	09/27/15	9:12:53	320	12.5	1	>4	>4	2	>4 to 2	219.5	15.1	13.9	16.0	2.1	Biological	FALSE	114.5	7.9
Site	15	C	09/27/15	9:13:38	320	12.5	1	>4	>4	2	>4 to 2	254.0	17.5	17.1	17.8	0.7	Biological	FALSE	103.9	7.2
Site	16	A	09/27/15	9:25:14	325	12.5	1	>4	>4	2	>4 to 2	248.9	17.2	16.5	17.5	1.0	Biological	FALSE	171.9	11.9
Site	16	C	09/27/15	9:26:52	325	12.5	1	>4	>4	2	>4 to 2	215.1	14.8	14.0	16.2	2.2	Biological	FALSE	130.3	9.0
Site	16	D	09/27/15	9:27:41	325	12.5	1	>4	>4	2	>4 to 2	228.6	15.8	15.4	16.0	0.6	Biological	FALSE	110.8	7.6
Site	17	A	09/27/15	12:57:07	332	12.5	1	>4	>4	2	>4 to 2	228.4	15.7	14.8	16.5	1.7	Biological	FALSE	115.5	8.0
Site	17	B	09/27/15	12:58:13	332	12.5	1	>4	>4	2	>4 to 2	247.7	17.1	16.9	17.2	0.3	Biological	FALSE	124.5	8.6
Site	17	C	09/27/15	12:59:02	332	12.5	1	>4	>4	2	>4 to 2	267.1	18.4	17.7	19.0	1.3	Biological	FALSE	143.4	9.9
Site	18	A	09/27/15	13:11:18	340	12.5	1	>4	>4	2	>4 to 2	245.1	16.9	16.4	17.3	0.9	Biological	FALSE	119.0	8.2

Location	Station	Replicate	Date	Time	Depth (ft)	Stop Collar Setting (in)	# of Weights (per side)	Grain Size Major Mode (phi)	Grain Size Minimum (phi)	Grain Size Maximum (phi)	Grain Size Range	Penetration Area (sq cm)	Penetration Mean (cm)	Penetration Minimum (cm)	Penetration Maximum (cm)	Boundary Roughness (cm)	Boundary Roughness Type	aRPD > Pen	aRPD Area (sq cm)	Mean aRPD (cm)
Site	18	B	09/27/15	13:12:11	340	12.5	1	>4	>4	2	>4 to 2	277.6	19.1	18.6	19.5	0.9	Biological	FALSE	115.2	7.9
Site	18	D	09/27/15	13:13:56	340	12.5	1	>4	>4	2	>4 to 2	258.0	17.8	17.6	18.3	0.8	Biological	FALSE	114.8	7.9
Site	19	A	09/27/15	8:35:26	310	12.5	1	>4	>4	2	>4 to 2	256.6	17.7	17.3	18.1	0.7	Biological	FALSE	154.9	10.7
Site	19	B	09/27/15	8:36:16	310	12.5	1	>4	>4	2	>4 to 2	278.7	19.2	19.0	19.6	0.6	Biological	FALSE	130.7	9.0
Site	19	D	09/27/15	8:37:47	310	12.5	1	>4	>4	2	>4 to 2	276.9	19.1	18.8	19.7	0.9	Biological	FALSE	107.9	7.4
Site	20	A	09/27/15	8:47:38	315	12.5	1	>4	>4	2	>4 to 2	224.3	15.5	14.8	16.2	1.3	Biological	FALSE	117.6	8.1
Site	20	B	09/27/15	8:48:29	315	12.5	1	>4	>4	2	>4 to 2	227.8	15.7	14.7	16.5	1.8	Biological	FALSE	117.3	8.1
Site	20	C	09/27/15	8:49:16	315	12.5	1	>4	>4	2	>4 to 2	248.5	17.1	16.6	17.4	0.8	Biological	FALSE	117.7	8.1
Site	21	A	09/27/15	9:00:33	317	12.5	1	>4	>4	2	>4 to 2	224.2	15.5	14.8	15.9	1.1	Biological	FALSE	106.7	7.4
Site	21	B	09/27/15	9:01:13	317	12.5	1	>4	>4	2	>4 to 2	248.4	17.1	15.8	18.0	2.2	Biological	FALSE	125.9	8.7
Site	21	D	09/27/15	9:02:43	317	12.5	1	>4	>4	2	>4 to 2	242.6	16.7	16.2	17.0	0.8	Biological	FALSE	108.7	7.5
Site	22	A	09/27/15	13:44:28	325	12.5	1	>4	>4	2	>4 to 2	233.1	16.1	15.7	16.5	0.8	Biological	FALSE	116.6	8.0
Site	22	B	09/27/15	13:45:17	325	12.5	1	>4	>4	2	>4 to 2	260.1	17.9	17.5	18.3	0.7	Biological	FALSE	121.9	8.4
Site	22	C	09/27/15	13:46:20	325	12.5	1	>4	>4	2	>4 to 2	255.4	17.6	17.3	18.1	0.7	Biological	FALSE	117.3	8.1

Location	Station	Replicate	Date	Time	Depth (ft)	Stop Collar Setting (in)	# of Weights (per side)	Grain Size Major Mode (phi)	Grain Size Minimum (phi)	Grain Size Maximum (phi)	Grain Size Range	Penetration Area (sq cm)	Penetration Mean (cm)	Penetration Minimum (cm)	Penetration Maximum (cm)	Boundary Roughness (cm)	Boundary Roughness Type	aRPD > Pen	aRPD Area (sq cm)	Mean aRPD (cm)
Site	23	A	09/27/15	13:36:47	331	12.5	1	>4	>4	2	>4 to 2	228.5	15.7	14.8	16.4	1.6	Biological	FALSE	108.6	7.5
Site	23	C	09/27/15	13:38:34	331	12.5	1	>4	>4	2	>4 to 2	256.5	17.7	17.0	18.2	1.2	Biological	FALSE	133.1	9.2
Site	23	D	09/27/15	13:39:35	331	12.5	1	>4	>4	2	>4 to 2	227.9	15.7	15.2	16.1	1.0	Biological	FALSE	96.8	6.7
Site	24	A	09/27/15	13:23:19	326	12.5	1	>4	>4	2	>4 to 2	218.4	15.1	14.5	15.8	1.3	Biological	FALSE	114.5	7.9
Site	24	B	09/27/15	13:24:32	326	12.5	1	>4	>4	2	>4 to 2	213.8	14.7	14.5	14.9	0.5	Biological	FALSE	86.6	6.0
Site	24	C	09/27/15	13:25:19	326	12.5	1	>4	>4	2	>4 to 2	241.4	16.6	16.3	17.0	0.7	Biological	FALSE	116.4	8.0
Site	25	A	09/27/15	15:01:18	308	12.5	1	>4	>4	2	>4 to 2	181.6	12.5	12.2	12.8	0.6	Biological	FALSE	109.8	7.6
Site	25	B	09/27/15	15:02:15	308	12.5	1	>4	>4	2	>4 to 2	230.5	15.9	15.5	16.3	0.8	Biological	FALSE	100.7	6.9
Site	25	C	09/27/15	15:03:03	308	12.5	1	>4	>4	2	>4 to 2	259.0	17.9	17.4	18.1	0.7	Biological	FALSE	102.5	7.1
Site	26	A	09/27/15	14:52:28	311	12.5	1	>4	>4	2	>4 to 2	239.3	16.5	16.2	16.9	0.7	Biological	FALSE	125.2	8.6
Site	26	C	09/27/15	14:54:18	311	12.5	1	>4	>4	2	>4 to 2	230.4	15.9	15.4	16.1	0.7	Biological	FALSE	138.0	9.5
Site	26	D	09/27/15	14:55:05	311	12.5	1	>4	>4	2	>4 to 2	222.3	15.3	14.8	15.9	1.1	Biological	FALSE	127.2	8.8
Site	27	A	09/27/15	14:37:46	315	12.5	1	>4	>4	2	>4 to 2	241.3	16.6	16.1	16.8	0.7	Biological	FALSE	119.2	8.2
Site	27	B	09/27/15	14:38:51	315	12.5	1	>4	>4	2	>4 to 2	227.7	15.7	15.2	16.0	0.8	Biological	FALSE	92.8	6.4
Site	27	C	09/27/15	14:39:35	315	12.5	1	>4	>4	2	>4 to 2	233.1	16.1	15.8	16.3	0.5	Biological	FALSE	110.2	7.6

Location	Station	Replicate	Date	Time	Depth (ft)	Stop Collar Setting (in)	# of Weights (per side)	Grain Size Major Mode (phi)	Grain Size Minimum (phi)	Grain Size Maximum (phi)	Grain Size Range	Penetration Area (sq cm)	Penetration Mean (cm)	Penetration Minimum (cm)	Penetration Maximum (cm)	Boundary Roughness (cm)	Boundary Roughness Type	aRPD > Pen	aRPD Area (sq cm)	Mean aRPD (cm)
Site	28	A	09/27/15	14:31:22	314	12.5	1	>4	>4	2	>4 to 2	157.5	10.9	9.8	11.8	2.0	Biological	FALSE	86.3	5.9
Site	28	B	09/27/15	14:32:08	314	12.5	1	>4	>4	2	>4 to 2	185.6	12.8	12.3	13.2	0.9	Biological	FALSE	100.0	6.9
Site	28	C	09/27/15	14:32:57	314	12.5	1	>4	>4	2	>4 to 2	138.6	9.6	9.3	9.7	0.4	Biological	FALSE	88.1	6.1
Site	29	A	09/27/15	14:16:32	322	12.5	1	>4	>4	2	>4 to 2	201.8	13.9	13.2	14.4	1.2	Biological	FALSE	133.0	9.2
Site	29	B	09/27/15	14:17:19	322	12.5	1	>4	>4	2	>4 to 2	168.1	11.6	11.3	11.9	0.6	Biological	FALSE	101.0	7.0
Site	29	C	09/27/15	14:18:18	322	12.5	1	>4	>4	2	>4 to 2	179.0	12.3	11.7	13.1	1.4	Biological	FALSE	81.7	5.6
Site	30	B	09/27/15	14:04:15	322	12.5	1	>4	>4	2	>4 to 2	148.6	10.2	9.5	10.7	1.2	Biological	FALSE	100.0	6.9
Site	30	C	09/27/15	14:05:12	322	12.5	1	>4	>4	2	>4 to 2	143.6	9.9	9.3	10.3	1.0	Biological	FALSE	84.8	5.8
Site	30	D	09/27/15	14:06:07	322	12.5	1	>4	>4	2	>4 to 2	112.3	7.7	6.4	8.8	2.4	Physical	FALSE	76.7	5.3
REF-A	1	A	09/27/15	16:23:17	314	12.5	1	>4	>4	2	>4 to 2	243.8	16.8	16.6	17.0	0.4	Biological	FALSE	110.8	7.6
REF-A	1	B	09/27/15	16:24:09	314	12.5	1	>4	>4	2	>4 to 2	231.8	16.0	15.2	16.9	1.7	Biological	FALSE	96.8	6.7
REF-A	1	C	09/27/15	16:25:09	314	12.5	1	>4	>4	2	>4 to 2	230.0	15.9	15.4	16.2	0.8	Biological	FALSE	149.4	10.3
REF-A	2	A	09/27/15	16:11:34	315	12.5	1	>4	>4	2	>4 to 2	267.5	18.4	17.9	18.7	0.9	Biological	FALSE	100.6	6.9

Location	Station	Replicate	Date	Time	Depth (ft)	Stop Collar Setting (in)	# of Weights (per side)	Grain Size Major Mode (phi)	Grain Size Minimum (phi)	Grain Size Maximum (phi)	Grain Size Range	Penetration Area (sq cm)	Penetration Mean (cm)	Penetration Minimum (cm)	Penetration Maximum (cm)	Boundary Roughness (cm)	Boundary Roughness Type	aRPD > Pen	aRPD Area (sq cm)	Mean aRPD (cm)
REF-A	2	B	09/27/15	16:12:27	315	12.5	1	>4	>4	2	>4 to 2	254.3	17.5	16.9	18.3	1.4	Biological	FALSE	137.4	9.5
REF-A	2	C	09/27/15	16:13:17	315	12.5	1	>4	>4	2	>4 to 2	212.9	14.7	14.4	15.0	0.7	Biological	FALSE	104.8	7.2
REF-A	3	A	09/27/15	16:31:31	310	12.5	1	>4	>4	2	>4 to 2	251.1	17.3	17.0	17.6	0.7	Biological	FALSE	122.6	8.4
REF-A	3	B	09/27/15	16:32:48	310	12.5	1	>4	>4	2	>4 to 2	215.0	14.8	14.2	16.0	1.7	Biological	FALSE	103.0	7.1
REF-A	3	C	09/27/15	16:33:38	310	12.5	1	>4	>4	2	>4 to 2	224.5	15.5	14.3	16.2	1.9	Biological	FALSE	105.6	7.3
REF-A	4	A	09/27/15	16:02:40	311	12.5	1	>4	>4	2	>4 to 2	244.1	16.8	16.3	17.1	0.8	Biological	FALSE	137.9	9.5
REF-A	4	C	09/27/15	16:04:16	311	12.5	1	>4	>4	2	>4 to 2	217.4	15.0	15.4	18.0	2.6	Biological	FALSE	107.1	7.4
REF-A	4	D	09/27/15	16:05:06	311	12.5	1	>4	>4	2	>4 to 2	213.5	14.7	14.4	15.3	0.9	Biological	FALSE	100.1	6.9
REF-A	5	A	09/27/15	16:16:41	312	12.5	1	>4	>4	2	>4 to 2	252.3	17.4	16.6	17.9	1.2	Biological	FALSE	140.2	9.7
REF-A	5	B	09/27/15	16:17:34	312	12.5	1	>4	>4	2	>4 to 2	248.3	17.1	16.6	17.9	1.3	Biological	FALSE	88.1	6.1
REF-A	5	D	09/27/15	16:19:26	312	12.5	1	>4	>4	2	>4 to 2	235.0	16.2	15.8	17.2	1.4	Biological	FALSE	98.1	6.8
REF-B	1	A	09/27/15	15:36:35	304	12.5	1	>4	>4	2	>4 to 2	218.1	15.0	13.8	15.8	2.0	Biological	FALSE	113.5	7.8
REF-B	1	B	09/27/15	15:37:23	304	12.5	1	>4	>4	2	>4 to 2	233.1	16.1	15.8	16.4	0.6	Biological	FALSE	118.9	8.2
REF-B	1	C	09/27/15	15:38:10	304	12.5	1	>4	>4	2	>4 to 2	232.1	16.0	15.4	16.4	1.0	Biological	FALSE	120.3	8.3

Location	Station	Replicate	Date	Time	Depth (ft)	Stop Collar Setting (in)	# of Weights (per side)	Grain Size Major Mode (phi)	Grain Size Minimum (phi)	Grain Size Maximum (phi)	Grain Size Range	Penetration Area (sq cm)	Penetration Mean (cm)	Penetration Minimum (cm)	Penetration Maximum (cm)	Boundary Roughness (cm)	Boundary Roughness Type	aRPD > Pen	aRPD Area (sq cm)	Mean aRPD (cm)
REF-B	2	A	09/27/15	15:21:55	306	12.5	1	>4	>4	2	>4 to 2	221.5	15.3	15.0	15.6	0.6	Biological	FALSE	119.1	8.2
REF-B	2	B	09/27/15	15:23:12	306	12.5	1	>4	>4	2	>4 to 2	253.4	17.5	17.1	17.7	0.7	Biological	FALSE	108.4	7.5
REF-B	2	C	09/27/15	15:24:14	306	12.5	1	>4	>4	2	>4 to 2	185.5	12.8	11.9	13.8	1.9	Biological	FALSE	103.9	7.2
REF-B	3	A	09/27/15	15:44:16	305	12.5	1	>4	>4	2	>4 to 2	243.2	16.8	16.1	17.2	1.1	Biological	FALSE	103.7	7.1
REF-B	3	B	09/27/15	15:45:10	305	12.5	1	>4	>4	2	>4 to 2	216.0	14.9	14.4	15.3	0.9	Biological	FALSE	103.7	7.1
REF-B	3	C	09/27/15	15:46:00	305	12.5	1	>4	>4	2	>4 to 2	264.6	18.2	17.8	18.6	0.8	Biological	FALSE	112.8	7.8
REF-B	4	B	09/27/15	15:16:27	310	12.5	1	>4	>4	2	>4 to 2	201.1	13.9	13.7	14.1	0.3	Biological	FALSE	97.3	6.7
REF-B	4	C	09/27/15	15:17:19	310	12.5	1	>4	>4	2	>4 to 2	248.3	17.1	16.6	17.6	1.1	Biological	FALSE	119.8	8.3
REF-B	4	D	09/27/15	15:18:05	310	12.5	1	>4	>4	2	>4 to 2	223.6	15.4	14.6	16.4	1.8	Biological	FALSE	97.4	6.7
REF-B	5	A	09/27/15	15:29:06	306	12.5	1	>4	>4	2	>4 to 2	262.6	18.1	16.8	18.9	2.1	Biological	FALSE	111.7	7.7
REF-B	5	B	09/27/15	15:30:13	306	12.5	1	>4	>4	2	>4 to 2	237.6	16.4	16.2	16.7	0.5	Biological	FALSE	101.2	7.0
REF-B	5	C	09/27/15	15:31:07	306	12.5	1	>4	>4	2	>4 to 2	196.7	13.6	12.6	14.3	1.6	Biological	FALSE	101.1	7.0
REF-C	1	A	09/27/15	11:23:16	318	12.5	1	>4	>4	2	>4 to 2	172.6	11.9	11.5	12.3	0.7	Biological	FALSE	96.2	6.6
REF-C	1	B	09/27/15	11:24:00	318	12.5	1	>4	>4	2	>4 to 2	151.4	10.4	9.6	11.3	1.7	Physical	FALSE	82.3	5.7

Location	Station	Replicate	Date	Time	Depth (ft)	Stop Collar Setting (in)	# of Weights (per side)	Grain Size Major Mode (phi)	Grain Size Minimum (phi)	Grain Size Maximum (phi)	Grain Size Range	Penetration Area (sq cm)	Penetration Mean (cm)	Penetration Minimum (cm)	Penetration Maximum (cm)	Boundary Roughness (cm)	Boundary Roughness Type	aRPD > Pen	aRPD Area (sq cm)	Mean aRPD (cm)
REF-C	1	C	09/27/15	11:24:49	318	12.5	1	>4	>4	2	>4 to 2	132.1	9.1	8.3	9.5	1.2	Biological	FALSE	85.1	5.9
REF-C	2	A	09/27/15	11:39:53	318	12.5	1	>4	>4	2	>4 to 2	85.1	5.9	9.8	10.4	0.6	Biological	FALSE	70.6	4.9
REF-C	2	B	09/27/15	11:40:46	318	12.5	1	>4	>4	2	>4 to 2	148.1	10.2	10.0	10.4	0.5	Biological	FALSE	63.5	4.4
REF-C	2	C	09/27/15	11:41:38	318	12.5	1	>4	>4	2	>4 to 2	156.1	10.8	9.6	11.5	1.9	Biological	FALSE	64.7	4.5
REF-C	3	A	09/27/15	11:30:04	320	12.5	1	>4	>4	2	>4 to 2	155.3	10.7	9.6	11.3	1.7	Biological	FALSE	91.6	6.3
REF-C	3	B	09/27/15	11:31:12	320	12.5	1	>4	>4	2	>4 to 2	166.5	11.5	11.3	11.7	0.4	Biological	FALSE	91.8	6.3
REF-C	3	D	09/27/15	11:33:09	320	12.5	1	>4	>4	2	>4 to 2	147.2	10.1	9.8	10.5	0.7	Biological	FALSE	67.2	4.6
REF-C	4	A	09/27/15	11:56:13	318	12.5	1	>4	>4	2	>4 to 2	178.2	12.3	11.3	12.9	1.7	Biological	FALSE	76.1	5.2
REF-C	4	B	09/27/15	11:57:17	318	12.5	1	>4	>4	2	>4 to 2	170.0	11.7	11.3	12.0	0.7	Biological	FALSE	65.4	4.5
REF-C	4	C	09/27/15	11:58:12	318	12.5	1	>4	>4	2	>4 to 2	173.6	12.0	11.3	12.6	1.3	Biological	FALSE	93.8	6.5
REF-C	5	A	09/27/15	11:49:01	318	12.5	1	>4	>4	2	>4 to 2	175.9	12.1	11.7	12.8	1.1	Biological	FALSE	94.5	6.5
REF-C	5	B	09/27/15	11:49:52	318	12.5	1	>4	>4	2	>4 to 2	185.3	12.8	12.3	13.0	0.7	Biological	FALSE	101.8	7.0
REF-C	5	C	09/27/15	11:50:47	318	12.5	1	>4	>4	2	>4 to 2	171.7	11.8	10.7	12.6	1.9	Biological	FALSE	97.1	6.7

Location	Station	Replicate	Dredged Material	Dredged Material Comments	Mud Clast Number	Mud Clast State	Methane?	Low DO?	Sediment Oxygen Demand	Beggiatoa Present?	Beggiatoa Type/Extent SPI	# of Feeding Voids	Void Minimum Depth (cm)	Void Maximum Depth (cm)	Void Average Depth (cm)	Successional Stage
Site	1	A	No		0	-	No	No	Low	No	-	2	2.7	9.0	5.9	1 on 3
Site	1	B	No		0	-	No	No	Low	No	-	1	4.1	6.3	5.2	1 on 3
Site	1	C	No		0	-	No	No	Low	No	-	3	3.2	11.3	7.2	1 on 3
Site	2	A	No		0	-	No	No	Low	No	-	1	5.2	6.2	5.7	1 on 3
Site	2	B	No		0	-	No	No	Low	No	-	1	6.3	8.0	7.1	1 on 3
Site	2	D	No		10	Ox	No	No	Low	No	-	0				1 on 3
Site	3	A	No		5	Mix	No	No	Low	No	-	1	10.9	12.3	11.6	1 on 3
Site	3	B	No		0	-	No	No	Low	No	-	1	6.2	7.5	6.9	1 on 3
Site	3	D	No		0	-	No	No	Low	No	-	1	6.4	7.4	6.9	1 on 3
Site	4	A	No		0	-	No	No	Low	No	-	3	4.8	8.7	6.8	1 on 3
Site	4	C	No		10	Mix	No	No	Low	No	-	0				1 on 3
Site	4	D	No		0	-	No	No	Low	No	-	1	3.7	4.8	4.3	1 on 3

Location	Station	Replicate	Dredged Material	Dredged Material Comments	Mud Clast Number	Mud Clast State	Methane?	Low DO?	Sediment Oxygen Demand	Beggiatoa Present?	Beggiatoa Type/Extent SPI	# of Feeding Voids	Void Minimum Depth (cm)	Void Maximum Depth (cm)	Void Average Depth (cm)	Successional Stage
Site	5	A	Possible	Dark gray sediment streaked with white clay.	0	-	No	No	Low	No	-	0				1 on 3
Site	5	B	Possible	Dark gray sediment streaked with white clay.	1	Reduced	No	No	Low	No	-	0				1 on 3
Site	5	D	Possible	White fines at depth.	0	-	No	No	Low	No	-	1	10.9	12.4	11.6	1 on 3
Site	6	A	Possible	Mottled gray and white clay beneath ambient sediment.	0	-	No	No	Low	No	-	2	2.8	6.8	4.8	1 on 3
Site	6	B	Possible	Mottled gray and white clay beneath ambient sediment.	1	Red	No	No	Low	No	-	3	4.2	8.7	6.5	1 on 3
Site	6	D	Possible	Mottled gray and white clay beneath ambient sediment.	6	Mix	No	No	Low	No	-	7	1.6	10.4	6.0	1 on 3
Site	7	A	No		0	-	No	No	Low	No	-	1	6.0	7.1	6.5	1 on 3
Site	7	B	No		0	-	No	No	Low	No	-	3	3.6	14.6	9.1	1 on 3
Site	7	C	No		0	-	No	No	Low	No	-	1	6.5	7.3	6.9	1 on 3
Site	8	A	No		0	-	No	No	Low	No	-	6	4.5	16.4	10.5	1 on 3
Site	8	B	No		0	-	No	No	Low	No	-	1	14.3	15.4	14.8	1 on 3
Site	8	C	No		0	-	No	No	Low	No	-	0				1 on 3

Location	Station	Replicate	Dredged Material	Dredged Material Comments	Mud Clast Number	Mud Clast State	Methane?	Low DO?	Sediment Oxygen Demand	Beggiatoa Present?	Beggiatoa Type/Extent SPI	# of Feeding Voids	Void Minimum Depth (cm)	Void Maximum Depth (cm)	Void Average Depth (cm)	Successional Stage
Site	9	A	No		0	-	No	No	Low	No	-	1	7.5	8.4	8.0	1 on 3
Site	9	C	No		0	-	No	No	Low	No	-	1	9.1	11.8	10.4	1 on 3
Site	9	D	No		0	-	No	No	Low	No	-	4	8.4	14.1	11.2	1 on 3
Site	10	A	No		0	-	No	No	Low	No	-	0				1 on 3
Site	10	B	No		0	-	No	No	Low	No	-	0				1 on 3
Site	10	C	No		0	-	No	No	Low	No	-	0				1 on 3
Site	11	A	No		0	-	No	No	Low	No	-	1	12.5	12.8	12.6	1 on 3
Site	11	B	No		0	-	No	No	Low	No	-	0				1 on 3
Site	11	D	No		0	-	No	No	Low	No	-	1	5.0	5.5	5.3	1 on 3
Site	12	A	Possible	Small white and green clay deposits in SWI.	0	-	No	No	Low	No	-	0				1 on 3
Site	12	B	Possible	Small white and green clay deposits in SWI.	2	Mix	No	No	Low	No	-	0				1 on 3
Site	12	C	Possible	Clay inclusions at depth.	5	Mix	No	No	Low	No	-	2	2.4	9.2	5.8	1 on 3
Site	13	A	No		0	-	No	No	Low	No	-	1	6.8	7.1	7.0	1 on 3

Location	Station	Replicate	Dredged Material	Dredged Material Comments	Mud Clast Number	Mud Clast State	Methane?	Low DO?	Sediment Oxygen Demand	Beggiatoa Present?	Beggiatoa Type/Extent SPI	# of Feeding Voids	Void Minimum Depth (cm)	Void Maximum Depth (cm)	Void Average Depth (cm)	Successional Stage
Site	13	B	No		2	Red	No	No	Low	No	-	5	4.3	8.8	6.5	1 on 3
Site	13	C	No		0	-	No	No	Low	No	-	1	2.3	2.9	2.6	1 on 3
Site	14	A	No		0	-	No	No	Low	No	-	3	4.4	13.6	9.0	1 on 3
Site	14	B	No		0	-	No	No	Low	No	-	1	4.2	5.4	4.8	1 on 3
Site	14	C	No		0	-	No	No	Low	No	-	0				1 on 3
Site	15	A	No		0	-	No	No	Low	No	-	0				1 on 3
Site	15	B	No		2	Red	No	No	Low	No	-	2	3.7	7.4	5.5	1 on 3
Site	15	C	No		0	-	No	No	Low	No	-	2	10.3	17.2	13.7	1 on 3
Site	16	A	No		0	-	No	No	Low	No	-	1	3.7	4.7	4.2	1 on 3
Site	16	C	No		0	-	No	No	Low	No	-	0				1 on 3
Site	16	D	No		0	-	No	No	Low	No	-	1	9.9	10.5	10.2	1 on 3
Site	17	A	No		2	Red	No	No	Low	No	-	2	5.1	9.9	7.5	1 on 3
Site	17	B	No		0	-	No	No	Low	No	-	2	15.9	17.2	16.6	1 on 3
Site	17	C	No		1	Red	No	No	Low	No	-	2	6.3	14.9	10.6	1 on 3
Site	18	A	No		0	-	No	No	Low	No	-	1	4.9	5.6	5.3	1 on 3

Location	Station	Replicate	Dredged Material	Dredged Material Comments	Mud Clast Number	Mud Clast State	Methane?	Low DO?	Sediment Oxygen Demand	Beggiatoa Present?	Beggiatoa Type/Extent SPI	# of Feeding Voids	Void Minimum Depth (cm)	Void Maximum Depth (cm)	Void Average Depth (cm)	Successional Stage
Site	18	B	No		0	-	No	No	Low	No	-	0				1 on 3
Site	18	D	No		0	-	No	No	Low	No	-	6	8.5	17.6	13.0	1 on 3
Site	19	A	No		0	-	No	No	Low	No	-	1	4.4	6.6	5.5	1 on 3
Site	19	B	No		0	-	No	No	Low	No	-	4	2.3	15.5	8.9	1 on 3
Site	19	D	No		0	-	No	No	Low	No	-	2	6.4	18.5	12.4	1 on 3
Site	20	A	No		0	-	No	No	Low	No	-	0				1 on 3
Site	20	B	No		0	-	No	No	Low	No	-	1	9.9	10.3	10.1	1 on 3
Site	20	C	No		4	Mix	No	No	Low	No	-	3	3.4	13.3	8.4	1 on 3
Site	21	A	No		0	-	No	No	Low	No	-	1	2.4	3.4	2.9	1 on 3
Site	21	B	No		0	-	No	No	Low	No	-	1	8.8	11.5	10.1	1 on 3
Site	21	D	No		0	-	No	No	Low	No	-	0				1 on 3
Site	22	A	No		0	-	No	No	Low	No	-	3	3.2	7.9	5.5	1 on 3
Site	22	B	No		0	-	No	No	Low	No	-	3	1.9	8.0	4.9	1 on 3
Site	22	C	No		0	-	No	No	Low	No	-	1	4.5	6.7	5.6	3

Location	Station	Replicate	Dredged Material	Dredged Material Comments	Mud Clast Number	Mud Clast State	Methane?	Low DO?	Sediment Oxygen Demand	Beggiatoa Present?	Beggiatoa Type/Extent SPI	# of Feeding Voids	Void Minimum Depth (cm)	Void Maximum Depth (cm)	Void Average Depth (cm)	Successional Stage
Site	23	A	No		0	-	No	No	Low	No	-	0				1 on 3
Site	23	C	No		0	-	No	No	Low	No	-	1	3.0	11.2	7.1	1 on 3
Site	23	D	No		0	-	No	No	Low	No	-	1	12.6	14.7	13.6	1 on 3
Site	24	A	No		0	-	No	No	Low	No	-	1	4.4	8.6	6.5	1 on 3
Site	24	B	No		0	-	No	No	Low	No	-	1	8.7	9.1	8.9	1 on 3
Site	24	C	No		0	-	No	No	Low	No	-	6	4.0	15.4	9.7	1 on 3
Site	25	A	No		0	-	No	No	Low	No	-	3	2.7	10.5	6.6	1 on 3
Site	25	B	No		0	-	No	No	Low	No	-	3	5.1	10.3	7.7	1 on 3
Site	25	C	No		0	-	No	No	Low	No	-	4	3.0	12.5	7.7	1 on 3
Site	26	A	No		0	-	No	No	Low	No	-	1	6.3	7.2	6.8	1 on 3
Site	26	C	No		0	-	No	No	Low	No	-	2	9.1	10.4	9.8	1 on 3
Site	26	D	No		0	-	No	No	Low	No	-	2	5.4	13.0	9.2	1 on 3
Site	27	A	No		0	-	No	No	Low	No	-	0				1 on 3
Site	27	B	No		0	-	No	No	Low	No	-	0				1 on 3
Site	27	C	No		0	-	No	No	Low	No	-	0				1 on 3

Location	Station	Replicate	Dredged Material	Dredged Material Comments	Mud Clast Number	Mud Clast State	Methane?	Low DO?	Sediment Oxygen Demand	Beggiatoa Present?	Beggiatoa Type/Extent SPI	# of Feeding Voids	Void Minimum Depth (cm)	Void Maximum Depth (cm)	Void Average Depth (cm)	Successional Stage
Site	28	A	Possible	Dark mottled sediment under aRPD.	0	-	No	No	Low	No	-	2	5.0	6.2	5.6	1 on 3
Site	28	B	Possible	Dark mottled sediment under aRPD.	0	-	No	No	Low	No	-	0				1 on 3
Site	28	C	Possible	Dark mottled sediment under aRPD.	3	Mix	No	No	Low	No	-	2	4.8	7.2	6.0	1 on 3
Site	29	A	Possible	Dark mottled sediment under aRPD.	0	-	No	No	Low	No	-	4	4.5	11.6	8.1	1 on 3
Site	29	B	Possible	White sediment is irregularly distributed in lower layers of sediment.	0	-	No	No	Low	No	-	2	4.5	8.2	6.3	1 on 3
Site	29	C	Possible	White sediment is irregularly distributed in lower layers of sediment.	0	-	No	No	Low	No	-	1	4.3	5.2	4.7	1 on 3
Site	30	B	Possible	Dark gray and white mottled sediment to pen maximum.	4	Red	No	No	Low	No	-	1	5.7	5.7	5.7	1 on 3
Site	30	C	Possible	Dark gray and white mottled sediment to pen maximum.	3	Red	No	No	Low	No	-	0				1 on 3
Site	30	D	Possible	Dark gray and white mottled sediment to pen maximum.	10	Mix	No	No	Low	No	-	0				1 on 3
REF-A	1	A	No		0	-	No	No	Low	No	-	1	6.9	8.6	7.8	1 on 3
REF-A	1	B	No		0	-	No	No	Low	No	-	2	10.3	15.3	12.8	1 on 3
REF-A	1	C	No		0	-	No	No	Low	No	-	1	5.7	6.7	6.2	1 on 3
REF-A	2	A	No		0	-	No	No	Low	No	-	0				1 on 3

Location	Station	Replicate	Dredged Material	Dredged Material Comments	Mud Clast Number	Mud Clast State	Methane?	Low DO?	Sediment Oxygen Demand	Beggiatoa Present?	Beggiatoa Type/Extent SPI	# of Feeding Voids	Void Minimum Depth (cm)	Void Maximum Depth (cm)	Void Average Depth (cm)	Successional Stage
REF-A	2	B	No		0	-	No	No	Low	No	-	3	4.6	7.1	5.9	1 on 3
REF-A	2	C	No		0	-	No	No	Low	No	-	1	9.3	9.4	9.4	1 on 3
REF-A	3	A	No		0	-	No	No	Low	No	-	4	5.0	17.1	11.1	1 on 3
REF-A	3	B	No		0	-	No	No	Low	No	-	2	3.3	8.4	5.9	1 on 3
REF-A	3	C	No		0	-	No	No	Low	No	-	5	4.2	10.3	7.2	1 on 3
REF-A	4	A	No		0	-	No	No	Low	No	-	2	1.8	8.1	4.9	1 on 3
REF-A	4	C	No		0	-	No	No	Low	No	-	3	3.2	13.0	8.1	1 on 3
REF-A	4	D	No		0	-	No	No	Low	No	-	2	1.9	14.9	8.4	1 on 3
REF-A	5	A	No		0	-	No	No	Low	No	-	0				1 on 3
REF-A	5	B	No		0	-	No	No	Low	No	-	3	6.7	11.9	9.3	1 on 3
REF-A	5	D	No		0	-	No	No	Low	No	-	3	2.4	11.9	7.1	1 on 3
REF-B	1	A	No		0	-	No	No	Low	No	-	0				1 on 3
REF-B	1	B	No		0	-	No	No	Low	No	-	1	2.1	2.5	2.3	1 on 3
REF-B	1	C	No		0	-	No	No	Low	No	-	0				1 on 3

Location	Station	Replicate	Dredged Material	Dredged Material Comments	Mud Clast Number	Mud Clast State	Methane?	Low DO?	Sediment Oxygen Demand	Beggiatoa Present?	Beggiatoa Type/Extent SPI	# of Feeding Voids	Void Minimum Depth (cm)	Void Maximum Depth (cm)	Void Average Depth (cm)	Successional Stage
REF-B	2	A	No		0	-	No	No	Low	No	-	2	5.1	6.8	6.0	1 on 3
REF-B	2	B	No		0	-	No	No	Low	No	-	1	12.3	12.6	12.5	1 on 3
REF-B	2	C	No		0	-	No	No	Low	No	-	2	5.7	11.3	8.5	1 on 3
REF-B	3	A	No		0	-	No	No	Low	No	-	3	3.7	6.0	4.8	1 on 3
REF-B	3	B	No		0	-	No	No	Low	No	-	2	5.9	12.8	9.3	1 on 3
REF-B	3	C	No		0	-	No	No	Low	No	-	0				1 on 3
REF-B	4	B	No		0	-	No	No	Low	No	-	1	11.1	11.7	11.4	1 on 3
REF-B	4	C	No		0	-	No	No	Low	No	-	4	4.8	10.4	7.6	1 on 3
REF-B	4	D	No		0	-	No	No	Low	No	-	1	3.1	4.2	3.6	1 on 3
REF-B	5	A	No		0	-	No	No	Low	No	-	1	3.0	3.7	3.4	1 on 3
REF-B	5	B	No		0	-	No	No	Low	No	-	5	2.3	14.3	8.3	1 on 3
REF-B	5	C	No		0	-	No	No	Low	No	-	0				1 on 3
REF-C	1	A	Possible	Large inclusions of white clay near penetration maximum.	0	-	No	No	Low	No	-	4	5.5	11.2	8.3	1 on 3
REF-C	1	B	Possible	White clay near penetration maximum.	0	-	No	No	Low	No	-	0				1 on 3

Location	Station	Replicate	Dredged Material	Dredged Material Comments	Mud Clast Number	Mud Clast State	Methane?	Low DO?	Sediment Oxygen Demand	Beggiatoa Present?	Beggiatoa Type/Extent SPI	# of Feeding Voids	Void Minimum Depth (cm)	Void Maximum Depth (cm)	Void Average Depth (cm)	Successional Stage
REF-C	1	C	Possible	White clay near penetration maximum.	0	-	No	No	Low	No	-	1	3.3	3.9	3.6	1 on 3
REF-C	2	A	Possible	Mottled white clay near penetration maximum.	0	-	No	No	Low	No	-	0				1 on 3
REF-C	2	B	Possible	Mottled white clay near penetration maximum.	0	-	No	No	Low	No	-	0				1 on 3
REF-C	2	C	Possible	Mottled white clay near penetration maximum.	0	-	No	No	Low	No	-	0				1 on 3
REF-C	3	A	Possible	Mottled white clay near penetration maximum.	0	-	No	No	Low	No	-	3	3.4	7.3	5.4	1 on 3
REF-C	3	B	Possible	Mottled white clay near penetration maximum.	1	Ox	No	No	Low	No	-	4	3.5	10.2	6.8	1 on 3
REF-C	3	D	Possible	Mottled white clay near penetration maximum.	0	-	No	No	Low	No	-	0				1 on 3
REF-C	4	A	Possible	Very dark black and gray clay.	0	-	No	No	Low	No	-	1	3.3	5.8	4.5	1 on 3
REF-C	4	B	Possible	Very dark black and gray clay.	0	-	No	No	Low	No	-	0				1 on 3
REF-C	4	C	Possible	Mottled white clay near penetration maximum.	0	-	No	No	Low	No	-	0				1 on 3
REF-C	5	A	Possible	Mottled white clay near penetration maximum.	0	-	No	No	Low	No	-	0				1 on 3
REF-C	5	B	Possible	Mottled white clay near penetration maximum.	0	-	No	No	Low	No	-	0				1 on 3
REF-C	5	C	Possible	Very dark black and gray and white clay.	0	-	No	No	Low	No	-	1	4.2	5.2	4.7	1 on 3

Location	Station	Replicate	Comment
Site	1	A	Fine sediment with fluffy pelleted layer at SWI. Reddish tan in upper layer, becoming streaked with gray and black material deeper below SWI. Few tubes visible at SWI. Large void at ~6 cm below SWI. Long burrow opening transected to far right. Small brittle star dragged into sediment. Thin burrow halos abundant in upper 10 cm of sediment column. *Corymorpha* in background
Site	1	B	Fine sediment with fluffy pelleted surface and cohesive reduced material deposited by prism. Pullback from prism causing material to fall between prism sediment interface. Sediment is reddish tan, streaked with pale tan in upper portion of sediment column, transitions to darker streaked material deep in column. Large void at 5 cm below SWI. Burrowing organism transected with crushed shell dragged from position.
Site	1	C	Fine sediment with fluffy pelleted layer at SWI. Reddish tan in upper layer, becoming gray and black material deep in sediment column. Few tubes visible at SWI. Three large voids in sediment column. Very thick aRPD. Infauna visible.
Site	2	A	Fine sediment with fluffy pelleted surface with large transected burrow opening to far right. Pullback from prism causing material to fall between prism sediment interface. Sediment is reddish tan, streaked with pale tan in upper portion of sediment column, transitions to slightly darker material deep in column. Large void at 5 cm below SWI. Small tubes at SWI and dragged into sediment column.
Site	2	B	Fine sediment with fluffy pelleted layer at SWI. Reddish tan in upper layer, becoming slightly less luminous past aRPD. Thin streaks of gray begin at 7 cm below SI. Single small void. Two burrowing textures in upper 6 cm of sediment. Small stage 1 tubes at SWI.
Site	2	D	Fine sediment at SWI with many clasts and rough boundary. SWI was physically disturbed by camera (previous reps). Distinct transition at aRPD from bright tan to pale gray-tan. Abundant burrowing textures in sediment. Small shell crushed at lower right corner. Large tubes at SWI.
Site	3	A	Fine sediment at SWI is heavily pelleted and loose. Small clasts of mixed state and small tubes present. Long red burrows visible extending from SWI. Large void at 12 cm below SWI. Sediment in upper portion of sediment column is bright tan and red hued transitions to pale gray with patches of near black at depth. Infauna abundant.
Site	3	B	Fine sediment at SWI is heavily pelleted and loose. Stage 1 tubes present. Large void in sediment column contains oxidized material Infauna near small black patch near bottom edge of image.
Site	3	D	Fine sediment at SWI is heavily pelleted and loose. Sediment column is mostly pale tan with dark streaks deep in sediment column. Long oxidized halos stemming from SWI. Small streak of white clay near penetration maximum. Stage 1 tubes present. Large infilled void in sediment column.
Site	4	A	Fine sediment at SWI is heavily pelleted and loose. Sediment column is mostly pale tan becoming darker and streaked deep in sediment column. Long oxidized halos stemming from SWI. Stage 1 tubes present. Few large voids in sediment column.
Site	4	C	Fine sediment at SWI is heavily pelleted and loose. Sediment column is mostly pale tan becoming slightly darker and streaked deep in sediment column. Long oxidized halos stemming from SWI. Stage 1 tubes present, large tubes also visible. Small patch of white fines near pen maximum. Burrow opening transected at SWI. Small burrows transected in sediment column.
Site	4	D	Fine sediment at SWI is heavily pelleted and loose. Sediment column is mostly pale tan becoming slightly darker and streaked deep in sediment column. Long oxidized halos stemming from SWI. Stage 1 tubes present. Large oxidized void in sediment column.

Location	Station	Replicate	Comment
Site	5	A	Fine sediment at SWI is heavily pelleted and loose, burrow opening transected at SWI. Sediment column is mostly pale tan transitioning to what appears to be historical DM, slightly darker and streaked deep in sediment column. Long oxidized halos stemming from SWI. Stage 1 tubes present. White fines are streaked throughout sediment column.
Site	5	B	Fine sediment at SWI is heavily pelleted and loose. Sediment column is mostly pale tan transitioning to what appears to be historical DM, slightly darker and streaked deep in sediment column. Long oxidized halos stemming from SWI. Stage 1 tubes present, transected burrows at depth
Site	5	D	Fine sediment at SWI is heavily pelleted and loose. Sediment column is mostly pale tan transitioning to what appears to be historical DM, slightly darker and streaked deep in sediment column with large mass of white fines near penetration maximum. Long oxidized halos stemming from SWI. Stage 1 tubes present. Small network of voids in lower left.
Site	6	A	Fine sediment at SWI is heavily pelleted and loose. Upper layer of sediment column is pale and rusty orange with small inclusions of white fines. Underlying layer is streaked and mottled white and gray with what appears to be historical DM. SWI is slightly disturbed by prism pullback. Tubes visible at SWI. Few large voids in sediment.
Site	6	B	Fine sediment at SWI is heavily pelleted and loose. Upper layer of sediment column is pale and rusty orange with small inclusions of white fines. Underlying layer is streaked and mottled white and gray with what appears to be historical DM. SWI is disturbed by large burrow opening to far left and smaller opening to far right. Few large voids visible in sediment column.
Site	6	D	Fine sediment at SWI is heavily pelleted and loose. Upper layer of sediment column is pale and rusty orange with small inclusions of white fines. Underlying layer is streaked and mottled white and gray with what appears to be historical DM. Large object in far field is encrusted with organisms. Many small clasts near prism. Abundant voids in sediment column.
Site	7	A	Fine sediment with fluffy pelleted layer at SWI. Reddish tan in upper layer, becoming slightly less luminous past aRPD. Single infilled void in upper 7 cm of sediment column. Burrowing evident as oxidized halos stemming from SWI.
Site	7	B	Fine sediment with fluffy pelleted layer at SWI. Reddish tan in upper layer, becoming slightly less luminous past aRPD. Several small voids are infilled. Polychaete visible in sediment. Camera artifacts deposited at SWI. Burrowing evident as oxidized halos stemming from SWI.
Site	7	C	Fine sediment with fluffy pelleted layer at SWI. Reddish tan in upper layer, becoming slightly less luminous past aRPD. Single small void. Burrowing evident as oxidized halos stemming from SWI.
Site	8	A	Fine sediment with fluffy pelleted layer at SWI. Reddish tan in upper layer, becoming slightly less luminous past aRPD. Burrowing evident as oxidized halos stemming from SWI. Cluster of small voids in sediment column. Burrowing evident as oxidized halos stemming from SWI.
Site	8	B	Fine sediment with fluffy pelleted layer at SWI. Reddish tan in upper layer, becoming slightly less luminous past aRPD. Burrowing evident as oxidized halos stemming from SWI. Small void deep in sediment column. Small tubes at SWI, dragged into sediment column. Large red polychaete visible.
Site	8	C	Fine sediment with fluffy pelleted layer at SWI. Reddish tan in upper layer transitions to a streaked and mottled pale tan sediment. Burrowing evident as oxidized halos stemming from SWI. Evidence of subsurface burrowing. Small tubes at SWI, dragged into sediment column.

Location	Station	Replicate	Comment
Site	9	A	Fine sediment with fluffy pelleted layer at SWI. Reddish tan in upper layer transitions to a streaked and mottled pale tan sediment. Burrowing evident as oxidized halos stemming from SWI. Void to far right. Polychaete visible in sediment. Sediment is especially mottled and dark surrounding void.
Site	9	C	Fine sediment with fluffy pelleted layer at SWI. Reddish tan in upper layer transitions to slightly duller gray-tan sediment. Burrowing evident as oxidized halos stemming from SWI. Large, deep void in sediment column. Additional burrowing textures near penetration maximum. Material deposited on SWI by prism. Few tubes dragged into sediment column.
Site	9	D	Fine sediment with fluffy pelleted layer at SWI. Reddish tan in upper layer transitions to slightly duller gray-tan sediment. Burrowing evident as oxidized halos stemming from SWI. Several large infilled voids in sediment. Infaunal appendages visible throughout sediment column.
Site	10	A	Fine sediment with fluffy pelleted layer at SWI. Reddish tan in upper layer transitions to slightly duller gray-tan sediment. Burrowing evident as oxidized halos stemming from SWI. Burrowing textures visible deep in sediment column. Small patch of darker sediment near center of image, ~5 cm below SWI. Tubes visible at SWI.
Site	10	B	Fine sediment with fluffy pelleted layer at SWI. Reddish tan in upper layer transitions to slightly duller gray-tan sediment. Burrowing evident as oxidized halos stemming from SWI. Burrowing textures visible deep in sediment column. Small tubes at SWI. Reduced sediment at SWI deposited by prism faceplate.
Site	10	C	Fine sediment with fluffy pelleted layer at SWI. Reddish tan in upper layer transitions to slightly duller gray-tan sediment. Burrowing evident as oxidized halos stemming from SWI. Very small red sea star dragged into sediment.. Small tubes at SWI. Reduced sediment at SWI deposited by prism faceplate.
Site	11	A	Fine sediment with fluffy pelleted layer at SWI. Reddish tan in upper layer transitions to slightly duller, streaky, gray-tan sediment. Burrowing evident as oxidized halos stemming from SWI. Abundant tubes at SWI.
Site	11	B	Fine sediment with fluffy pelleted layer at SWI. Reddish tan in upper layer transitions to slightly duller, streaky, gray-tan sediment. Burrowing evident as oxidized halos stemming from SWI. Abundant burrowing textures in sediment column. SWI dips to far left where burrow was transected.
Site	11	D	Fine sediment with fluffy pelleted layer at SWI. Reddish tan in upper layer transitions to slightly duller, streaky, gray-tan sediment. Burrowing evident as oxidized halos stemming from SWI. Abundant burrowing textures in sediment column. Single small void at 5 cm below SWI. Reduced material at SWI deposited by prism.
Site	12	A	Reddish tan fine sediment with large burrow in center of SWI. Many tubes at SWI. Traces of white and green clay in sediment column suggest historical DM. Shallow penetration. aRPD > Pen.
Site	12	B	Reddish tan fine sediment with large burrow in center of SWI. Many tubes at SWI. Traces of white and green clay in sediment column suggest historical DM. Shallow penetration. Large clast at SWI. Large red worm at depth to far right.
Site	12	C	Reddish tan fine sediment with large burrow in center of SWI. Many tubes at SWI. Traces of white and green clay in sediment column and mass of white clay in lower half of image suggest historical DM. Shallow penetration.
Site	13	A	Fine sediment with fluffy pelleted layer at SWI. Reddish tan in upper layer transitions to slightly duller, gray tan sediment. Burrow structures evident in textural changes throughout sediment column. SPI camera appears to have contact on slight slope.

Location	Station	Replicate	Comment
Site	13	B	Fine sediment with loose layer at SWI. Reddish tan in upper layer transitions to slightly duller, gray tan sediment. Burrow structures evident in textural changes throughout sediment column. Small tubes at surface. Cluster of small voids in sediment column.
Site	13	C	Fine sediment with loose layer at SWI. Reddish tan in upper layer transitions to slightly duller, gray tan sediment. Burrow structures evident in textural changes throughout sediment column. Few tubes visible at SWI. Large void 2 cm below SWI, transected burrows at depth.
Site	14	A	Fine sediment with loose layer at SWI. Reddish tan in upper layer transitions to slightly duller, gray tan sediment. Burrow structures evident in textural changes throughout sediment column. Small tubes at SWI. SWI depresses to left, ridge is visible in far field.
Site	14	B	Fine sediment with loose layer at SWI. Reddish tan in upper layer transitions to slightly duller, gray tan sediment. Burrow structures evident in textural changes throughout sediment column. Small tubes at SWI. Infilled voids and burrows visible throughout sediment column.
Site	14	C	Fine sediment with loose layer at SWI. Reddish tan in upper layer transitions to slightly duller, gray tan sediment. Burrow structures evident in textural changes throughout sediment column. Small tubes at SWI. Infilled voids and burrows visible throughout sediment column.
Site	15	A	Fine sediment with loose layer at SWI. Reddish tan in upper layer transitions to slightly duller, gray tan sediment. Burrow structures evident in textural changes throughout sediment column. Small tubes at SWI.
Site	15	B	Fine sediment with loose layer at SWI. Reddish tan in upper layer transitions to slightly duller, gray tan sediment. Burrow structures evident in textural changes throughout sediment column. Large tubes at SWI Large burrow to right side of SWI terminating in two voids.
Site	15	C	Fine sediment with loose layer at SWI. Reddish tan in upper layer transitions to slightly duller, gray tan sediment. Burrow structures evident in textural changes throughout sediment column. Small tubes at SWI. Large burrow in lower left corner of image. Infilled burrow in right side of sediment column.
Site	16	A	Silt-clay to penetration. Orange-tan in upper layer with mottled gray sed to penetration maximum. Small tubes recolonizing SWI. Sediment column has been extensively reworked, very thick aRPD. Infilled void just under SWI. Prism pullback has caused slight slumping under SWI.
Site	16	C	Silt-clay to penetration. Orange-tan in upper layer with mottled gray sed to penetration maximum. Small tubes recolonizing SWI. Sediment column has been extensively reworked, very thick aRPD. Mud clasts artifacts from wiper blade on SWI; transected burrows at depth
Site	16	D	Silt-clay to penetration. Orange-tan in upper layer with mottled gray sed to penetration maximum. Small tubes dragged into sediment.. Sediment column has been extensively reworked, very thick aRPD. Small void along left edge. Burrow visible at right edge.
Site	17	A	Silt-clay to penetration. Orange-tan in upper layer with mottled gray sed to penetration maximum. Small tubes at SWI. Sediment column has been extensively reworked. Two partially infilled voids along left edge of image. Large polychaete near penetration maximum.
Site	17	B	Silt-clay to penetration. Orange-tan in upper layer with mottled gray sed to penetration maximum. Small tubes at SWI. Sediment column has been extensively reworked. Large void cut off by bottom of image. Mud clast artifact on SWI deposited by prism.
Site	17	C	Silt-clay to penetration. Orange-tan in upper layer with mottled gray sed to penetration maximum. Small tubes at SWI. Sediment column is mottled and streaked at depth. Dark gray material present in lower few cm of column. Camera deposited mud clast artifacts at SWI.
Site	18	A	Silt-clay to penetration. Orange-tan in upper layer with slightly gray material at depth. aRPD is very thick, extensive reworking is apparent. Stage 1 tubes have recolonized and pelletized SWI. Infilled voids, partially infilled void, and infaunal bodies visible in sediment column.

Location	Station	Replicate	Comment
Site	18	B	Silt-clay to penetration. Orange-tan in upper layer with mottled gray sed with white and black streaks to penetration maximum. Small tubes at SWI. Sediment column is mottled and streaked at depth. Long burrow visible in center of image with infilled reduced void. Camera deposited mud clast artifacts at SWI. Prism pullback causing slumping of upper few cm.
Site	18	D	Silt-clay to penetration. Orange-tan in upper layer with mottled gray sed to penetration maximum. Small tubes at SWI. Sediment column is mottled and streaked at depth. Many open and infilled relic voids in sediment column. Prism pullback creating slumping in upper few centimeters.
Site	19	A	Silt-clay to penetration. Orange-tan in upper layer with mottled gray sed to penetration maximum. Small tubes at SWI. Sediment column is mottled and streaked at depth. Infilled void to center right. Material is much darker and streaked in lower portion of image.
Site	19	B	Silt-clay to penetration. Orange-tan in upper layer with mottled gray sed to penetration maximum. Small tubes at SWI. Sediment column is mottled and streaked at depth, black patch near penetration maximum. Several small void networks have been transected.
Site	19	D	Silt-clay to penetration. Orange-tan in upper layer with mottled gray sed to penetration maximum. Small tubes at SWI. Sediment column is light colored to penetration maximum, with streaks of gray under aRPD. Two large voids.
Site	20	A	Silt-clay to penetration. Orange-tan in upper layer with slightly gray material at depth. aRPD is very thick, extensive reworking is apparent. Stage 1 tubes have recolonized and pelletized SWI. Few infilled voids and burrow structures visible in sediment column.
Site	20	B	Silt-clay to penetration. Orange-tan in upper layer with gray material at depth. Small tubes at SWI. Sediment column is extensively reworked. Polychaetes and small voids visible in sediment column.
Site	20	C	Silt-clay to penetration. Orange-tan in upper layer with gray material at depth. Small tubes at SWI. Sediment column is extensively reworked. Many small infilled void structures. Three open voids. Cluster of clasts of mixed redox state at SWI.
Site	21	A	Silt-clay to penetration. Orange-tan in upper layer with mottled dark gray sed to penetration maximum. Small tubes at SWI. Sediment column is extensively reworked. Pelleted depression at SWI is vertical transport from void and burrow below.
Site	21	B	Silt-clay to penetration. Sediment is mottled from SWI to pen maximum. Large void to right edge of image. SWI is mounded in center. Camera artifacts at SWI. Few small tubes.
Site	21	D	Silt-clay to penetration. Orange-tan in upper layer with mottled dark gray sed to near penetration maximum. Many tubes recolonizing SWI, few quite large. Mud clast artifacts from prism at SWI. Slight pullback slumping at SWI.
Site	22	A	Silt-clay to penetration. Orange-tan in upper layer with mottled gray material at depth. Small tubes at SWI. Sediment column is extensively reworked. Two large voids, single infilled void. Small red brittle star dragged into sediment.
Site	22	B	Silt-clay to penetration. Orange-tan in upper layer with slightly gray material at depth. aRPD is very thick, extensive reworking is apparent. Stage 1 tubes have recolonized and pelletized SWI. Reduced mud clasts artifacts have fallen from prism. Very large void just under SWI.
Site	22	C	Silt-clay to penetration. Orange-tan in upper layer with slightly gray material at depth. aRPD is very thick, extensive reworking is apparent. Polychaetes visible in sediment column. Very large infilled void near SWI. Several reduced mud clast artifacts have fallen from wiper blade.

Location	Station	Replicate	Comment
Site	23	A	Silt-clay to penetration. Orange-tan in upper layer with slightly mottled sed to penetration maximum. Small tubes at SWI. Sediment column is extensively reworked. Polychaete visible along left edge. Gastropod at SWI.
Site	23	C	Silt-clay to penetration. Orange-tan in upper layer. aRPD is very thick, extensive reworking is apparent. Stage 1 tubes have recolonized and pelletized SWI. Large burrow opening transected at SWI, ejecting reduced material. Large void network below opening. Black material to far left edge.
Site	23	D	Silt-clay to penetration. Orange-tan in upper layer. aRPD is very thick, extensive reworking is apparent. Stage 1 tubes have recolonized and pelletized SWI. Burrow opening transected at SWI. Void near penetration max, directly below opening.
Site	24	A	Silt-clay to penetration. Orange-tan in upper layer with slightly gray material at depth. aRPD is very thick, extensive reworking is apparent. Abundant tubes at heavily pelleted SWI.. Large void is mostly infilled.
Site	24	B	Silt-clay to penetration. Very mottled tan, orange, and gray sediment, streaking downward. Few tubes at SWI. Large mud clast artifacts deposited by prism. Small polychaete visible. Small void to far right.
Site	24	C	Silt-clay to penetration. Very mottled tan, orange, and gray sediment, streaking downward. Few tubes at SWI. Large mud clast artifacts deposited by prism. Many small voids in sediment column. Burrow opening at SWI. Prism pullback slumping in first few cm of sediment column.
Site	25	A	Silt-clay to penetration. Orange-tan in upper layer with slightly gray material to penetration maximum. Several voids in sediment column. Reworking of sediment is obvious. SWI is colonized by small tubes and heavily pelleted.
Site	25	B	Silt-clay to penetration. Orange-tan in upper layer with slightly gray material to penetration maximum. Several small voids in sediment column. Light mottling in center of image. Few small tubes at SWI.
Site	25	C	Silt-clay to penetration. Orange-tan in upper layer with slightly gray material to penetration maximum. Several small voids in sediment column. Small tubes at SWI. Prism pullback causing slumping in upper few cm of sediment column.
Site	26	A	Silt-clay to penetration. Orange-tan in upper layer with slightly gray material at depth. aRPD is very thick, extensive reworking is apparent. Abundant tubes at heavily pelleted SWI. Small void to left edge. Burrowing textures abundant.
Site	26	C	Silt-clay to penetration. Orange-tan in upper layer with some reduced organics at depth. Mud clast artifacts from prism at SWI. Black deposit deep in sediment column. Abundant burrow textures.
Site	26	D	Silt-clay to penetration. Orange-tan in upper layer with some reduced organics at depth. Mud clast artifacts from prism at SWI. Black deposit deep in sediment column. Burrow and mound transected at surface, terminating in large void in center of image.
Site	27	A	Silt-clay to penetration. Orange-tan in upper layer with slightly gray sed to penetration maximum. SWI is heavily pelleted. Small tubes present. Small polychaete visible in sediment column. Deep burrow halo transected extends from SWI to pen maximum. Black sediment near penetration maximum.
Site	27	B	Silt-clay to penetration. Orange-tan in upper layer with slightly gray sed to penetration maximum. SWI is heavily pelleted. Small tubes present. Small polychaete visible in sediment column. Deep aRPD.
Site	27	C	Silt-clay to penetration. Orange-tan in upper layer with slightly gray sed to penetration maximum. SWI is heavily pelleted. Small tubes present. Few polychaetes visible in sediment column.

Location	Station	Replicate	Comment
Site	28	A	Silt-clay to penetration. Orange-tan in upper layer with what appears to be dark gray and white historical DM to penetration maximum. SWI is heavily pelleted. Small tubes present. Small voids in sediment column, polychaetes visible.
Site	28	B	Silt-clay to penetration. Orange-tan in upper layer with what appears to be dark gray and white historical DM to penetration maximum. SWI is heavily pelleted. Small tubes present. Large areas of burrowing textures at aRPD. Small organisms visible in sediment column. Reduced mud clast artifacts from camera deposited at SWI. Transected burrows at depth
Site	28	C	Silt-clay to penetration. Orange-tan in upper layer with what appears to be dark gray and white historical DM to penetration maximum. SWI is heavily pelleted. Small tubes present. Few small voids and burrow textures in sediment. Sediment column is heavily streaked. Few small clasts at SWI.
Site	29	A	Silt-clay to penetration. Orange-tan in upper layer with what appears to be dark gray and white historical DM to penetration maximum. SWI is heavily pelleted. Small tubes present. Few small voids and burrow textures in sediment. Pullback slumping at SWI. Long oxic halo transected.
Site	29	B	Silt-clay to penetration. Orange-tan sediment becomes slightly less saturated at aRPD. White clay inclusions abundant in lower portion of sediment column. SWI is heavily pelleted. Small tubes present. Large burrow opening transected, terminating in pair of large voids. Reduced mud clast artifacts deposited by prism at SWI.
Site	29	C	Silt-clay to penetration. Orange-tan sediment becomes slightly less saturated at aRPD. White clay inclusions abundant in lower portion of sediment column. SWI is heavily pelleted. Small tubes present. Single void near transected burrow at SWI. Mud clast artifacts at SWI deposited by prism.
Site	30	B	Silt-clay to penetration. Orange-tan in upper layer with what appears to be slightly gray and white mottled historical DM to penetration maximum. SWI is heavily pelleted. Small tubes present. Void to far left edge of image. Polychaetes visible.
Site	30	C	Silt-clay to penetration. Orange-tan in upper layer with what appears to be slightly gray and white mottled historical DM to penetration maximum. SWI is heavily pelleted. Small tubes present. Clasts at SWI from camera wiper blade.
Site	30	D	Silt clay to penetration. SWI is disturbed. Clasts of different redox states at SWI. Abundant tubes. What appears to be historical DM to penetration. Shallow penetration.
REF-A	1	A	Silt-clay to penetration. Orange-tan in upper layer with slightly gray sed to penetration maximum. SWI is heavily pelleted. Small tubes present. Few polychaetes visible in sediment column. Long burrow halo to penetration max.
REF-A	1	B	Silt-clay to penetration. Orange-tan in upper layer with slightly gray sed to penetration maximum. SWI is heavily pelleted. Small tubes present. Very small voids near pen maximum.
REF-A	1	C	Silt-clay to penetration. Orange-tan in upper layer with slightly gray sed to penetration maximum. SWI is heavily pelleted. Small tubes present. Small void under transected burrowing opening.
REF-A	2	A	Silt-clay to penetration. Orange-tan in upper layer with slightly mottled gray and white sed to penetration maximum. SWI is heavily pelleted. Small tubes present. Burrow halos and infilled voids suggest reworking.

Location	Station	Replicate	Comment
REF-A	2	B	Silt-clay to penetration. Orange-tan in upper layer with slightly gray sediment underneath. SWI is heavily pelleted. Small tubes present. Small voids below SWI.
REF-A	2	C	Silt-clay to penetration. Orange-tan in upper layer with mottled black and tan sed to pen maximum. SWI is heavily pelleted. Few small tubes at SWI and dragged into sediment. Very small void to left side of image.
REF-A	3	A	Silt-clay to penetration. Orange-tan in upper layer with mottled dark gray and tan sed to pen maximum. SWI is heavily pelleted. Few small tubes at SWI. Large network of voids in sediment column.
REF-A	3	B	Silt-clay to penetration. Orange-tan in upper layer with mottled dark gray and tan sed to pen maximum. SWI is heavily pelleted. Small tubes at SWI. Large void 3 cm below SWI. Abundant burrow textures throughout sediment column.
REF-A	3	C	Silt-clay to penetration. Orange-tan in upper layer with mottled light gray to pen maximum. SWI is heavily pelleted. Small tubes at SWI. Network of large voids in sediment column,
REF-A	4	A	Silt-clay to penetration. Orange-tan in upper layer with mottled light gray to pen maximum. SWI is heavily pelleted. Small tubes at SWI. Large void and polychaete in sediment column.
REF-A	4	C	Silt-clay to penetration. Orange-tan in upper layer with mottled light gray to pen maximum. SWI is heavily pelleted. Small tubes at SWI. Several voids in sediment column. Reduced mud clast artifacts deposited by prism at SWI.
REF-A	4	D	Silt-clay to penetration. Orange-tan in upper layer with mottled light gray to pen maximum. SWI is heavily pelleted. Small tubes at SWI. Large transected burrow in lower left corner .
REF-A	5	A	Silt-clay to penetration. Orange-tan in upper layer with mottled light gray to pen maximum. SWI is heavily pelleted. Small tubes at SWI. Large infilled burrows transected near penetration depth.
REF-A	5	B	Silt-clay to penetration. Orange-tan in upper layer with mottled light gray to pen maximum. SWI is heavily pelleted. Small tubes at SWI. Three partially infilled burrows in sediment column. Large gray mud clast artifacts deposited by prism at SWI.
REF-A	5	D	Silt-clay to penetration. Orange-tan in upper layer with patches of reduced sediment at depth. SWI is heavily pelleted. Small tubes at SWI. Three partially infilled burrows in sediment column. Small gray mud clast artifacts deposited by prism at SWI.
REF-B	1	A	Silt-clay to penetration. Orange-tan transitions to pale gray at depth. SWI is heavily pelleted. Small tubes at SWI. Burrowing evident in textures throughout sediment column.
REF-B	1	B	Silt-clay to penetration. Orange-tan transitions to pale gray at depth. SWI is heavily pelleted. Few small tubes at SWI. Large mud clast artifacts deposited by prism. Reworking is evident by deep aRPD and small voids.
REF-B	1	C	Silt-clay to penetration. Orange-tan transitions to mottled gray at depth. SWI is heavily pelleted. Large mud clast artifacts deposited by prism. Reworking is evident by deep aRPD and burrowing textures.

Location	Station	Replicate	Comment
REF-B	2	A	Silt-clay to penetration. Orange-tan transitions to mottled gray and black sed at depth. SWI is heavily pelleted. Small tubes at SWI. :Large void in sediment column. Infauna visible near penetration maximum.
REF-B	2	B	Silt-clay to penetration. Orange-tan transitions to mottled gray with few black streaks at depth. SWI is heavily pelleted. Small tubes at SWI. Small void. Long burrow halo extends in patches to penetration maximum.
REF-B	2	C	Silt-clay to penetration. Orange-tan transitions to mottled gray compact clay sed to penetration. SWI is heavily pelleted. Small tubes at SWI. Long burrow terminating in two voids.
REF-B	3	A	Silt-clay to penetration. Orange-tan transitions to mottled gray with few black streaks at depth. SWI is heavily pelleted. Small tubes at SWI. Few small voids in upper portion of sediment column.
REF-B	3	B	Silt-clay to penetration. Orange-tan transitions to mottled gray and black sed at depth. SWI is heavily pelleted. Small tubes at SWI. Mostly infilled oxidized voids visible in sediment column. Infaunal body in sediment. Streaking and oxidized halos suggest extensive reworking.
REF-B	3	C	Silt-clay to penetration. Orange-tan transitions to mottled gray and black sed at depth. SWI is heavily pelleted. Small tubes at SWI. Mostly infilled oxidized voids visible in sediment column. Infaunal body in sediment. Long burrow halos in sediment. Mud clasts artifacts deposited at SWI by prism.
REF-B	4	B	Silt-clay to penetration. Orange-tan transitions to pale gray at depth. SWI is heavily pelleted. Few very small tubes at SWI. Void near penetration maximum.
REF-B	4	C	Silt-clay to penetration. Orange-tan transitions to pale gray at depth. SWI is heavily pelleted. Dense assemblage of small tubes at SWI. Several small oxidized voids in sediment column. Very slight color change under aRPD.
REF-B	4	D	Silt-clay to penetration. Orange-tan transitions to mottled gray with few black streaks at depth. SWI is heavily pelleted. Small tubes at SWI. Small mud clast artifacts deposited by prism at SWI. Oxidized void in upper 3 cm of sediment. Large oxidized burrow texture near penetration maximum.
REF-B	5	A	Silt-clay to penetration. Orange-tan transitions to mottled gray sed with few black streaks at depth. SWI is heavily pelleted. Small tubes at SWI. Small near SWI.
REF-B	5	B	Silt-clay to penetration. Orange-tan transitions to pale gray at depth with slight mottling. SWI is heavily pelleted. Small tubes at SWI. Sediment column has been extensively reworked. Abundant a small voids and burrows visible.
REF-B	5	C	Silt-clay to penetration. Orange-tan transitions to pale gray at depth with slight mottling. SWI is heavily pelleted. Abundant small tubes at SWI. Small black inclusions in sediment column. Long oxidized halos extending from SWI.
REF-C	1	A	Silt-clay to penetration. Orange-tan transitions to what appears to be white clay DM near penetration maximum. Transition at aRPD is very slight. Infilled burrows and voids throughout sediment. Large anemone visible at SWI. SWI is heavily pelletized with few small tubes.
REF-C	1	B	Silt-clay to penetration. Orange-tan transitions to what appears to be mottled white clay DM near penetration maximum. Transition at aRPD is very slight. Infilled burrows and voids throughout sediment. Firm object in midfield may be contributing to boundary roughness. Tubes at SWI.

Location	Station	Replicate	Comment
REF-C	1	C	Silt-clay to penetration. Dark orange-tan transitions to what appears to be mottled white clay DM near penetration maximum. Transition at aRPD is very slight. Mall void at right edge of image. Few tubes at SWI. Mud clast artifacts deposited at SWI by prism.
REF-C	2	A	Silt-clay to penetration. Dark orange-tan transitions to what appears to be very mottled white clay DM near penetration maximum. Few tube sat SWI/ Small reduced mud clast artifacts at Swig, deposited by prism. Infilled burrow opening three cm below SWI.
REF-C	2	B	Silt-clay to penetration. Dark orange-tan transitions to what appears to be very mottled white clay DM near penetration maximum. Few tube sat SWI/ Small reduced mud clast artifacts at SWI, deposited by prism. Infilled burrow Along far left edge of image as well as below white clay to mid right. Small infauna visible to far right.
REF-C	2	C	Silt-clay to penetration. Dark orange-tan transitions to what appears to be very mottled white clay DM near penetration maximum. Few tube sat SWI/ Small reduced mud clast artifacts at SWI, deposited by prism. Large burrow opening transected at SWI.
REF-C	3	A	Silt-clay to penetration. Dark orange-tan transitions to what appears to be very mottled white clay DM near penetration maximum. Tubes at SWI. SWI is heavily pelleted. Several large voids in sediment column. Burrow transected to far left. Shell dragdown near center of image causing circular feature in sediment.
REF-C	3	B	Silt-clay to penetration. Orange-tan transitions to what appears to be very mottled white and dark gray DM near penetration maximum. Tubes at SWI. SWI is heavily pelleted. Small voids and transected burrows in sediment column. Reduced sediment at depth. Polychaete near pen maximum.
REF-C	3	D	Silt-clay to penetration. Orange-tan transitions to what appears to be very mottled white and dark gray DM near penetration maximum. Tubes at SWI. SWI is heavily pelleted. Transected burrows at depth; PV image at this station shows large burrow openings. Mud clast artifacts deposited at SWI by prism.
REF-C	4	A	Silt-clay to penetration. Orange-tan transitions to what appears to be very mottled black and dark gray DM near penetration maximum. Tubes at SWI. SWI is heavily pelleted. Large void to far right of image. Polychaete visible near image center.
REF-C	4	B	Silt-clay to penetration. Orange-tan transitions to what appears to be very mottled black and dark gray DM near penetration maximum. Tubes at SWI. SWI is heavily pelleted. Long oxidized halos extending from SWI. Possible burrow transected near penetration maximum.
REF-C	4	C	Silt-clay to penetration. Orange-tan transitions to what appears to be very mottled white historical DM near penetration maximum. Tubes at SWI. SWI is heavily pelleted. Long oxidized halos extending from SWI, transected burrows at depth.
REF-C	5	A	Silt-clay to penetration. Orange-tan transitions to what appears to be very mottled white historical DM near penetration maximum. Tubes at SWI. SWI is heavily pelleted. Large polychaete visible in sediment column. Pullback fro prism causing slumping between sediment and prism interface.
REF-C	5	B	Silt-clay to penetration. Orange-tan transitions to what appears to be very mottled white historical DM near penetration maximum. Small organism transected. Large animal in far field (crab).
REF-C	5	C	Silt-clay to penetration. Orange-tan transitions to what appears to be very mottled white and gray historical DM near penetration maximum. Small void with surrounding burrow halo extending to penetration maximum.

Location	Station	Replicate	Date	Time	Image Width (cm)	Image Height (cm)	Field of View imaged (m^2)	Sediment Type	Surface Ox	Debris	Bedforms	Tubes	Burrows	Tracks	Epifauna	Flora	Number of Fish
Site	1	A	09/27/15	7:27:57	88.9	59.3	0.5	Silt/Clay	Ox	None	None	Present	Sparse	None	None	None	0
Site	1	C	09/27/15	7:29:39	79.1	52.8	0.4	Silt/Clay	Ox	None	None	Present	Sparse	None	None	None	0
Site	1	D	09/27/15	7:30:29	85.3	56.9	0.5	Silt/Clay	Ox	None	None	Present	Present	None	Shrimp	None	0
Site	2	A	09/27/15	17:08:46	89.2	59.5	0.5	Silt/Clay	Ox	None	None	Present	Present	Abundant	Shrimp	None	0
Site	3	A	09/27/15	10:31:15	85.9	57.3	0.5	Silt/Clay	Ox	None	None	Present	Present	Sparse	Shrimp	None	0
Site	3	C	09/27/15	10:33:08	88.2	58.8	0.5	Silt/Clay	Ox	None	None	Present	Present	Present	IND	None	IND
Site	4	A	09/27/15	10:44:05	96.4	64.2	0.6	Silt/Clay	Ox	None	None	Sparse	Present	Present	Shrimp	None	0
Site	5	A	09/27/15	10:55:42	91.0	60.6	0.6	Silt/Clay	Ox	None	None	Present	Present	Present	None	None	0
Site	6	A	09/27/15	11:09:29	95.5	63.6	0.6	Silt/Clay	Ox	Shell fragments and small clasts	None	Present	Present	Sparse	Shrimp	None	0
Site	7	A	09/27/15	7:52:29	89.1	59.4	0.5	Silt/Clay	Ox	None	None	Present	Present	Present	None	None	0
Site	7	D	09/27/15	7:54:42	89.0	59.4	0.5	Silt/Clay	Ox	None	None	Abundant	Present	Present	Gastropod; Shrimp	None	0
Site	8	A	09/27/15	8:04:34	91.6	61.1	0.6	Silt/Clay	Ox	None	None	Present	Abundant	Present	Shrimp	None	0
Site	8	C	09/27/15	8:06:04	83.4	55.6	0.5	Silt/Clay	Ox	None	None	Present	Abundant	Abundant	None	None	0

Location	Station	Replicate	Date	Time	Image Width (cm)	Image Height (cm)	Field of View imaged (m²)	Sediment Type	Surface Ox	Debris	Bedforms	Tubes	Burrows	Tracks	Epifauna	Flora	Number of Fish
Site	9	A	09/27/15	9:37:16	84.4	56.3	0.5	Silt/Clay	Ox	None	None	Present	Abundant	Abundant	None	None	0
Site	10	A	09/27/15	10:08:34	91.5	61.0	0.6	Silt/Clay	Ox	None	None	Present	Abundant	Present	Shrimp	None	0
Site	10	B	09/27/15	10:09:18	IND	IND	IND	Silt/Clay	Ox	None	None	Present	Sparse	Sparse	Shrimp	None	0
Site	11	A	09/27/15	10:15:16	103.4	68.9	0.7	Silt/Clay	Ox	None	None	Present	Present	Sparse	None	None	0
Site	11	B	09/27/15	10:16:05	95.5	63.6	0.6	Silt/Clay	Ox	None	None	Sparse	Present	Sparse	None	None	0
Site	11	D	09/27/15	10:18:00	98.5	65.7	0.6	Silt/Clay	Ox	None	None	Sparse	Present	Sparse	Shrimp	None	0
Site	12	A	09/27/15	12:42:18	91.0	60.6	0.6	Silt/Clay	Ox	Small shell fragments	None	Present	Sparse	Sparse	Shrimp	None	0
Site	12	B	09/27/15	12:43:02	IND	IND	IND	Silt/Clay	Ox	IND	IND	IND	IND	IND	IND	IND	0
Site	12	D	09/27/15	12:44:49	IND	IND	IND	Silt/Clay	Ox	Shell fragments	None	IND	Sparse	IND	IND	IND	0
Site	13	A	09/27/15	8:28:56	86.7	57.8	0.5	Silt/Clay	Ox	None	None	Present	Present	Dense	None	None	0
Site	13	C	09/27/15	8:30:27	95.4	63.6	0.6	Silt/Clay	Ox	Small mud clasts	None	Sparse	Present	Abundant	Shrimp	None	0
Site	13	D	09/27/15	8:31:16	93.7	62.5	0.6	Silt/Clay	Ox	Small to large mud clasts	None	Sparse	Sparse	None	None	None	0
Site	14	A	09/27/15	8:15:51	94.8	63.2	0.6	Silt/Clay	Ox	None	None	Sparse	Present	Present	Shrimp	None	0

Location	Station	Replicate	Date	Time	Image Width (cm)	Image Height (cm)	Field of View imaged (m²)	Sediment Type	Surface Ox	Debris	Bedforms	Tubes	Burrows	Tracks	Epifauna	Flora	Number of Fish
Site	15	A	09/27/15	9:11:57	84.8	56.5	0.5	Silt/Clay	Ox	None	None	Present	Sparse	Present	Shrimp	None	1
Site	15	D	09/27/15	9:14:09	87.8	58.6	0.5	Silt/Clay	Ox	None	None	Present	Present	Abundant	Shrimp	None	0
Site	16	A	09/27/15	9:25:02	87.2	58.1	0.5	Silt/Clay	Ox	None	None	Present	Present	Abundant	None	None	0
Site	17	A	09/27/15	12:56:54	90.6	60.4	0.5	Silt/Clay	Ox	None	None	Present	Present	Abundant	Crab	None	0
Site	17	B	09/27/15	12:57:57	85.9	57.3	0.5	Silt/Clay	Ox	None	None	Sparse	Present	Abundant	None	None	0
Site	18	A	09/27/15	13:11:06	83.6	55.8	0.5	Silt/Clay	Ox	None	None	Present	Present	Abundant	Shrimp	None	0
Site	18	B	09/27/15	13:11:57	81.5	54.3	0.4	Silt/Clay	Ox	None	None	Present	Sparse	Abundant	None	None	0
Site	19	A	09/27/15	8:35:14	92.5	61.6	0.6	Silt/Clay	Ox	None	None	Sparse	Sparse	Abundant	None	None	0
Site	19	B	09/27/15	8:36:04	94.6	63.1	0.6	Silt/Clay	Ox	None	None	Present	Present	Abundant	None	None	0
Site	19	D	09/27/15	8:37:34	92.9	61.9	0.6	Silt/Clay	Ox	None	None	Present	Present	Present	None	None	0
Site	20	A	09/27/15	8:47:25	88.9	59.3	0.5	Silt/Clay	Ox	None	None	Present	Present	Present	Shrimp	None	0
Site	21	A	09/27/15	9:00:18	98.2	65.5	0.6	Silt/Clay	Ox	None	None	Present	Present	Abundant	Shrimp	None	0
Site	22	A	09/27/15	13:44:15	97.3	64.8	0.6	Silt/Clay	Ox	None	None	Present	Present	Abundant	None	None	0
Site	22	C	09/27/15	13:46:08	86.1	57.4	0.5	Silt/Clay	Ox	None	None	Present	Present	Abundant	None	None	0
Site	23	A	09/27/15	13:36:34	89.6	59.7	0.5	Silt/Clay	Ox	None	None	Present	Present	Abundant	Shrimp	None	0

Location	Station	Replicate	Date	Time	Image Width (cm)	Image Height (cm)	Field of View imaged (m^2)	Sediment Type	Surface Ox	Debris	Bedforms	Tubes	Burrows	Tracks	Epifauna	Flora	Number of Fish
Site	23	B	09/27/15	13:37:24	90.0	60.0	0.5	Silt/Clay	Ox	None	None	Present	Present	Present	Shrimp	None	0
Site	23	C	09/27/15	13:38:21	97.7	65.1	0.6	Silt/Clay	Ox	None	None	Present	Present	Present	Shrimp	None	0
Site	24	A	09/27/15	13:23:07	86.7	57.8	0.5	Silt/Clay	Ox	None	None	Sparse	Present	Present	Shrimp	None	0
Site	24	B	09/27/15	13:24:17	86.4	57.6	0.5	Silt/Clay	Ox	None	None	Present	Sparse	None	Shrimp	None	0
Site	24	C	09/27/15	13:25:05	86.9	57.9	0.5	Silt/Clay	Ox	None	None	Sparse	Sparse	Present	None	None	0
Site	25	A	09/27/15	15:01:05	90.2	60.1	0.5	Silt/Clay	Ox	None	None	Present	Present	Abundant	None	None	0
Site	26	A	09/27/15	14:52:14	89.1	59.4	0.5	Silt/Clay	Ox	None	None	Sparse	Present	Present	Shrimp	Algae	0
Site	26	B	09/27/15	14:53:17	98.4	65.6	0.6	Silt/Clay	Ox	None	None	Abundant	Present	Present	None	None	0
Site	26	C	09/27/15	14:54:05	96.6	64.4	0.6	Silt/Clay	Ox	None	None	Sparse	Sparse	Sparse	None	None	0
Site	27	A	09/27/15	14:37:33	103.9	69.2	0.7	Silt/Clay	Ox	None	None	Present	Present	Present	Shrimp	None	0
Site	27	B	09/27/15	14:38:39	92.5	61.7	0.6	Silt/Clay	Ox	None	None	Present	Sparse	Present	Shrimp	Algae	0
Site	27	C	09/27/15	14:39:23	93.8	62.5	0.6	Silt/Clay	Ox	None	None	Present	Present	Present	Shrimp	None	0
Site	28	A	09/27/15	14:31:10	98.0	65.3	0.6	Silt/Clay	Ox	None	None	Present	Present	Abundant	None	None	0
Site	29	A	09/27/15	14:16:20	87.2	58.1	0.5	Silt/Clay	Ox	Large mud clast	None	Present	Present	Present	None	None	0

Location	Station	Replicate	Date	Time	Image Width (cm)	Image Height (cm)	Field of View imaged (m^2)	Sediment Type	Surface Ox	Debris	Bedforms	Tubes	Burrows	Tracks	Epifauna	Flora	Number of Fish
Site	30	A	09/27/15	14:03:05	85.4	57.0	0.5	Silt/Clay	Ox	None	None	Sparse	Sparse	Present	Anemone	None	0
REF-A	1	A	09/27/15	16:23:05	96.3	64.2	0.6	Silt/Clay	Ox	None	None	Present	Sparse	Abundant	None	None	0
REF-A	1	B	09/27/15	16:23:57	93.0	62.0	0.6	Silt/Clay	Ox	None	None	Present	Sparse	Abundant	Shrimp	None	0
REF-A	1	C	09/27/15	16:24:57	90.2	60.2	0.5	Silt/Clay	Ox	None	None	Abundant	Sparse	Sparse	Shrimp	None	0
REF-A	2	A	09/27/15	16:11:20	92.9	61.9	0.6	Silt/Clay	Ox	None	None	Present	Present	Present	Shrimp	None	0
REF-A	2	B	09/27/15	16:12:15	90.2	60.2	0.5	Silt/Clay	Ox	None	None	Present	Present	Present	Shrimp	None	0
REF-A	3	A	09/27/15	16:31:18	96.7	64.4	0.6	Silt/Clay	Ox	None	None	Present	Present	Present	Shrimp	None	0
REF-A	3	B	09/27/15	16:32:36	85.4	56.9	0.5	Silt/Clay	Ox	None	None	Present	Abundant	Present	None	None	0
REF-A	3	C	09/27/15	16:33:26	87.4	58.3	0.5	Silt/Clay	Ox	None	None	Present	Present	Present	None	None	0
REF-A	4	A	09/27/15	16:02:28	91.7	61.1	0.6	Silt/Clay	Ox	None	None	Present	Sparse	Present	None	None	0
REF-A	5	A	09/27/15	16:16:27	94.2	62.8	0.6	Silt/Clay	Ox	None	None	Present	Present	Sparse	None	None	0
REF-B	1	A	09/27/15	15:36:22	100.1	66.7	0.7	Silt/Clay	Ox	None	None	Present	Present	Abundant	Shrimp	None	0
REF-B	1	B	09/27/15	15:37:09	94.1	62.7	0.6	Silt/Clay	Ox	None	None	Present	Sparse	Abundant	None	None	0

Location	Station	Replicate	Date	Time	Image Width (cm)	Image Height (cm)	Field of View imaged (m^2)	Sediment Type	Surface Ox	Debris	Bedforms	Tubes	Burrows	Tracks	Epifauna	Flora	Number of Fish
REF-B	1	C	09/27/15	15:37:58	92.1	61.4	0.6	Silt/Clay	Ox	None	None	Present	Present	Abundant	None	None	0
REF-B	2	A	09/27/15	15:21:42	83.9	55.9	0.5	Silt/Clay	Ox	None	None	Abundant	Present	Abundant	Shrimp	None	0
REF-B	2	B	09/27/15	15:23:00	91.8	61.2	0.6	Silt/Clay	Ox	None	None	Abundant	Present	Abundant	Shrimp	None	0
REF-B	2	D	09/27/15	15:24:47	88.2	58.8	0.5	Silt/Clay	Ox	None	None	Present	Sparse	Present	Shrimp	None	0
REF-B	3	A	09/27/15	15:44:04	84.6	56.4	0.5	Silt/Clay	Ox	None	None	Sparse	Abundant	Abundant	Shrimp	None	0
REF-B	3	B	09/27/15	15:44:57	80.8	53.9	0.4	Silt/Clay	Ox	None	None	Present	Present	Abundant	Shrimp	None	0
REF-B	3	C	09/27/15	15:45:48	92.4	61.6	0.6	Silt/Clay	Ox	None	None	Present	Present	Present	Shrimp	None	0
REF-B	4	A	09/27/15	15:15:30	88.3	58.9	0.5	Silt/Clay	Ox	None	None	Present	Present	Abundant	None	None	0
REF-B	4	C	09/27/15	15:17:08	92.3	61.5	0.6	Silt/Clay	Ox	None	None	Present	Present	Abundant	None	None	0
REF-B	5	A	09/27/15	15:28:55	98.0	65.3	0.6	Silt/Clay	Ox	None	None	Present	Present	Abundant	Shrimp	None	0
REF-B	5	B	09/27/15	15:30:00	100.5	67.0	0.7	Silt/Clay	Ox	None	None	Abundant	Sparse	Abundant	Shrimp	None	0
REF-B	5	C	09/27/15	15:30:55	90.3	60.2	0.5	Silt/Clay	Ox	None	None	Abundant	Present	Abundant	Shrimp	None	0
REF-C	1	A	09/27/15	11:23:02	95.1	63.4	0.6	Silt/Clay	Ox	None	None	Sparse	Present	Present	Anemone	None	0

Location	Station	Replicate	Date	Time	Image Width (cm)	Image Height (cm)	Field of View imaged (m^2)	Sediment Type	Surface Ox	Debris	Bedforms	Tubes	Burrows	Tracks	Epifauna	Flora	Number of Fish
REF-C	1	B	09/27/15	11:23:47	90.6	60.4	0.5	Silt/Clay	Ox	Small mud clasts	None	Sparse	Sparse	Sparse	None	None	0
REF-C	2	A	09/27/15	11:39:41	85.7	57.1	0.5	Silt/Clay	Ox	Small mud clasts	None	Sparse	Present	Sparse	Shrimp	None	0
REF-C	2	D	09/27/15	11:42:38	IND	IND	IND	Silt/Clay	Ox	IND	IND	IND	IND	IND	Anemone	IND	IND
REF-C	3	A	09/27/15	11:29:48	96.4	64.2	0.6	Silt/Clay	Ox	Small mud clasts	None	Sparse	Present	Abundant	None	None	0
REF-C	4	A	09/27/15	11:55:59	96.1	64.1	0.6	Silt/Clay	Ox	Small mud clasts	None	Present	Sparse	Abundant	None	None	0
REF-C	4	B	09/27/15	11:57:05	86.3	57.6	0.5	Silt/Clay	Ox	Rope	None	Present	Present	Abundant	None	None	0
REF-C	5	A	09/27/15	11:48:46	93.5	62.3	0.6	Silt/Clay	Ox	Anthropogenic Debris	None	Present	Sparse	Present	Shrimp	None	0
REF-C	5	B	09/27/15	11:49:39	91.6	61.1	0.6	Silt/Clay	Ox	None	None	IND	IND	IND	IND	None	0

Location	Station	Replicate	Other Salient Features/Comment
Site	1	A	Loosely packed fine sediment is oxidized, light tan in color. SWI is pocked with small irregularities and low accumulations of sediment. Small tubes are barely visible on surface.
Site	1	C	Loosely packed fine sediment is oxidized, light tan in color. Some medium length tubes lying on surface. Large masses of sediment have fallen from prism onto SWI.
Site	1	D	Loosely packed fine sediment is oxidized, light tan in color. SWI is pocked with small irregularities and low accumulations of sediment. Large tubes visible against sediment surface. Large burrow near lasers.
Site	2	A	Loosely packed fine sediment is oxidized, light tan in color. SWI marked with shallow burrow depressions and long track marks.
Site	3	A	Loosely packed fine sediment is oxidized, light tan in color. Burrow openings apparent in SWI. Large shrimp between lasers.
Site	3	C	Loosely packed fine sediment is oxidized, light tan in color. Burrow openings apparent in SWI. Fauna just above lasers- small fish or shrimp. Tracks and small irregularities in sediment. Weak resuspension of material.
Site	4	A	Loosely packed fine sediment is oxidized, light tan in color. Burrow openings apparent in SWI, few are large. Shrimp at SWI. Many side by side paired tracks in sediment. Large tubes are visible, smaller tubes may not be visible at distance.
Site	5	A	Loosely packed fine sediment is oxidized, light tan in color. Burrow openings apparent in SWI, few are large. Side by side paired tracks in sediment. Large tubes are visible, smaller tubes may not be visible at distance.
Site	6	A	Loosely packed fine sediment is oxidized, light tan in color. Large burrow opening visible. Several shrimp at SWI. Large shell fragments are scant on SWI. Many small clasts, white and gray in color, scattered across SWI.
Site	7	A	Loosely packed fine sediment is oxidized, light tan in color. Burrow openings visible in SWI, one is moderately large. Many tracks visible. Shallow depression near center of image. Small tubes cover sediment surface.
Site	7	D	Loosely packed fine sediment is oxidized, light tan in color. Burrow openings visible in SWI, one is moderately large. Small gastropod above left laser. Shrimp at SWI. Small tubes cover sediment surface.
Site	8	A	Loosely packed fine sediment is oxidized, light tan in color. Many small burrow openings visible. Small tubes are visible throughout image in low density. Few small shrimp.
Site	8	C	Loosely packed fine sediment is oxidized, light tan in color. Many small burrow openings visible. Small tubes are visible throughout image in low density. SWI is heavily marked by small sets of tracks.

Location	Station	Replicate	Other Salient Features/Comment
Site	9	A	Loosely packed fine sediment is oxidized, light tan in color. Many small burrow openings visible. Small tubes are visible throughout image in low density. SWI is heavily marked by small sets of tracks.
Site	10	A	Loosely packed fine sediment is oxidized, light tan in color. Many small burrow openings visible. Small tubes are visible throughout image in low density. SWI is heavily marked by small sets of tracks. Small shrimp at SWI. Organisms blurry in water column.
Site	10	B	Loosely packed fine sediment is oxidized, light tan in color. Small tubes visible. Water column is cloudy with resuspended sediment. Single shrimp visible.
Site	11	A	Loosely packed fine sediment is oxidized, light tan in color. Small tubes visible. Large burrow in upper right. Water column is cloudy with resuspended sediment.
Site	11	B	Loosely packed fine sediment is oxidized, light tan in color. Small tubes visible. Water column is cloudy with resuspended sediment. Burrows visible in SWI.
Site	11	D	Loosely packed fine sediment is oxidized, light tan in color. Small tubes visible. Water column is cloudy with resuspended sediment. Few burrows visible in SWI. Shrimp.
Site	12	A	Loosely packed fine sediment is oxidized, light tan in color. Clusters of growth in patches. Small shrimp. Small shell fragments and rocks scattered across SWI.
Site	12	B	Very turbid water column. Lasers/benthic features are not visible.
Site	12	D	Very turbid water column. Lasers are not visible. Shell fragments and small tubes visible in upper right.
Site	13	A	Loosely packed fine sediment is oxidized, light tan in color. Dense tracks across SWI. Several medium burrows. Large burrow in upper right. Few tubes.
Site	13	C	Loosely packed fine sediment is oxidized, light tan in color. Small tracks across SWI. Small burrows visible. Single shrimp. Few tubes.
Site	13	D	Loosely packed fine sediment is oxidized, light tan in color. Large mud clasts in upper 1/3 of image from camera base sled. Small mud clasts across SWI. Many tubes in upper portion of image, fewer in lower half.
Site	14	A	Loosely packed fine sediment is oxidized, light tan in color. Small tracks across SWI. Small burrows visible. Small shrimp in lower left corner. Few tubes.

Location	Station	Replicate	Other Salient Features/Comment
Site	15	A	Loosely packed fine sediment is oxidized, light tan in color. Many tracks across SWI. Small burrows visible. Fish swimming in water column. Very small tubes visible on SWI. Shrimp in lower right.
Site	15	D	Loosely packed fine sediment is oxidized, light tan in color. Many tracks across SWI. Small burrows visible. Several shrimp visible in image. Very small tubes visible on SWI.
Site	16	A	Loosely packed fine sediment is oxidized, light tan in color. Abundant tracks cover SWI. Small tubes visible against SWI.
Site	17	A	Loosely packed fine sediment is oxidized, light tan in color. Abundant tracks cover SWI. Small tubes visible against SWI. Few reduced burrow mounds visible. Crab in lower right corner.
Site	17	B	Loosely packed fine sediment is oxidized, light tan in color. Abundant tracks cover SWI. Small tubes visible against SWI.
Site	18	A	Loosely packed fine sediment is oxidized, light tan in color. Abundant tracks cover SWI. Small tubes visible against SWI. Shrimp.
Site	18	B	Loosely packed fine sediment is oxidized, light tan in color. Abundant tracks cover SWI. Small tubes visible against SWI.
Site	19	A	Loosely packed fine sediment is oxidized, light tan in color. Abundant tracks cover SWI. Image is not in focus. Few small tubes visible
Site	19	B	Loosely packed fine sediment is oxidized, light tan in color. Abundant tracks cover SWI. Image is not in focus. Small tubes visible
Site	19	D	Loosely packed fine sediment is oxidized, light tan in color. Many tracks cover SWI. Image is not in focus. Small tubes visible. Several large burrow openings in SWI.
Site	20	A	Loosely packed fine sediment is oxidized, light tan in color. Many tracks cover SWI. Large burrow in center of image. Shrimp to far right.
Site	21	A	Loosely packed fine sediment is oxidized, light tan in color. Many tracks cover SWI. Small tubes and burrows visible.. Single small shell fragment at SWI.
Site	22	A	Loosely packed fine sediment is oxidized, light tan in color. Many thin tracks cover SWI. Small tubes and burrows visible. Large burrow in lower right.
Site	22	C	Loosely packed fine sediment is oxidized, light tan in color. Many tracks cover SWI. Small tubes and burrows visible.
Site	23	A	Loosely packed fine sediment is oxidized, light tan in color. Many tracks cover SWI. Small tubes and burrows visible. Small shrimp.

Location	Station	Replicate	Other Salient Features/Comment
Site	23	B	Loosely packed fine sediment is oxidized, light tan in color. Many tracks cover SWI. Small tubes and burrows visible. Small shrimp.
Site	23	C	Loosely packed fine sediment is oxidized, light tan in color. Many tracks cover SWI. Small tubes and burrows visible. Many shrimp at SWI.
Site	24	A	Loosely packed fine sediment is oxidized, light tan in color. Few burrow openings visible. SWI appears slightly slumped. Small clasts cover SWI. Shrimp.
Site	24	B	Loosely packed fine sediment is oxidized, light tan in color. Clusters of small mud clasts on surface. One large burrow on left. Small tubes, cluster lying on surface near right laser. Shrimp.
Site	24	C	Loosely packed fine sediment is oxidized, light tan in color. Visible portion of SWI is covered with a dense network of tracks. Tubes at SWI. Few burrows visible.
Site	25	A	Loosely packed fine sediment is oxidized, light tan in color. SWI is covered with a dense network of tracks. Tubes at SWI. Few burrows visible.
Site	26	A	Loosely packed fine sediment is oxidized, light tan in color. SWI is covered with a dense network of tracks. Tubes at SWI. Few burrows visible. Small bit of yellow algae visible, partially buried on surface. Few small shrimp at SWI.
Site	26	B	Loosely packed fine sediment is oxidized, light tan in color. Tracks and tubes at SWI. Few medium burrows visible at upper right.
Site	26	C	Loosely packed fine sediment is oxidized, light tan in color. Few tubes, tracks, and burrows visible. Turbid water column.
Site	27	A	Loosely packed fine sediment is oxidized, light tan in color. Tubes at SWI. Large burrow in lower portion of image. Shrimp at SWI.
Site	27	B	Loosely packed fine sediment is oxidized, light tan in color. Tubes at SWI. Shrimp at SWI. Yellow algae in lower right.
Site	27	C	Loosely packed fine sediment is oxidized, light tan in color. Set of tracks diagonally across image. Tubes at SWI. Shrimp at SWI.
Site	28	A	Loosely packed fine sediment is oxidized, light tan in color. Many tracks across SWI. Small shell fragment. Few medium burrows
Site	29	A	Loosely packed fine sediment is oxidized, light tan in color. Large clast in top right corner of image.

Location	Station	Replicate	Other Salient Features/Comment
Site	30	A	Loosely packed fine sediment is oxidized, light tan in color. Tracks at SWI. Large clast in top left corner of image. Large anemone at SWI.
REF-A	1	A	Loosely packed fine sediment is oxidized, light tan in color. Abundant tracks at SWI. Large burrow opening in upper right with tubes surrounding rim of burrow. Tubes visible at SWI.
REF-A	1	B	Loosely packed fine sediment is oxidized, light tan in color. Abundant tracks at SWI. Tubes visible at SWI. Several large burrows visible. Shrimp.
REF-A	1	C	Loosely packed fine sediment is oxidized, light tan in color. Tracks at SWI. Tubes visible at SWI. Several large burrows visible. Shrimp in upper right.
REF-A	2	A	Loosely packed fine sediment is oxidized, light tan in color. Tracks at SWI. Tubes visible at SWI. Three large burrows.
REF-A	2	B	Loosely packed fine sediment is oxidized, light tan in color. Tracks at SWI. Tubes visible at SWI. Shrimp in center of lasers.
REF-A	3	A	Loosely packed fine sediment is oxidized, light tan in color. Tracks at SWI. Tubes visible at SWI. Couple shrimp at SWI.
REF-A	3	B	Loosely packed fine sediment is oxidized, light tan in color. Many small burrow openings at SWI. Tubes visible at SWI. Tracks at SWI.
REF-A	3	C	Loosely packed fine sediment is oxidized, light tan in color. Few small burrow openings at SWI. Tubes visible at SWI. Series of tracks running diagonally from lower left to upper right of image.
REF-A	4	A	Loosely packed fine sediment is oxidized, light tan in color. Few small burrow openings at SWI. Tubes visible at SWI.
REF-A	5	A	Loosely packed fine sediment is oxidized, light tan in color. Few small burrow openings at SWI. Tubes visible at SWI. Few tracks.
REF-B	1	A	Loosely packed fine sediment is oxidized, light tan in color. Large burrow opening in top left corner of image. Small tubes visible against SWI. Small fecal coils. SWI is studded with many tracks.
REF-B	1	B	Loosely packed fine sediment is oxidized, light tan in color. Small tubes visible against SWI. Small tracks cross SWI.

Location	Station	Replicate	Other Salient Features/Comment
REF-B	1	C	Loosely packed fine sediment is oxidized, light tan in color. Burrows visible.. Small tubes visible against SWI. Small tracks cross SWI.
REF-B	2	A	Loosely packed fine sediment is oxidized, light tan in color. Burrows visible. Abundant small tubes. Few shrimp visible.
REF-B	2	B	Loosely packed fine sediment is oxidized, light tan in color. Many small burrows. Abundant small tubes. Few shrimp visible.
REF-B	2	D	Loosely packed fine sediment is oxidized, light tan in color. Few small burrows. Water column is clouded with resuspended sediment. Few shrimp visible.
REF-B	3	A	Loosely packed fine sediment is oxidized, light tan in color. Few tubes visible from distance. Many small burrows. Dense network of tracks. Few shrimp visible.
REF-B	3	B	Loosely packed fine sediment is oxidized, light tan in color. Small burrows in upper right, large burrow in lower right corner of image. Dense network of tracks. Few shrimp visible.
REF-B	3	C	Loosely packed fine sediment is oxidized, light tan in color. Few tracks. Single shrimp visible.
REF-B	4	A	Loosely packed fine sediment is oxidized, light tan in color. Rough uneven SWI with many small tracks. Large burrow opening to far left.
REF-B	4	C	Loosely packed fine sediment is oxidized, light tan in color. Rough uneven SWI with many small tracks. Large burrows to right half of image.
REF-B	5	A	Loosely packed fine sediment is oxidized, light tan in color. Rough uneven SWI with many small tracks. Small shrimp at SWI,
REF-B	5	B	Loosely packed fine sediment is oxidized, light tan in color. Rough uneven SWI with many small tracks. Small shrimp at SWI, large burrow on lower left corner.
REF-B	5	C	Loosely packed fine sediment is oxidized, light tan in color. Rough uneven SWI with many small tracks. Small shrimp at SWI.
REF-C	1	A	Loosely packed fine sediment is oxidized, light tan in color. SWI is very smooth, interrupted by tracks, small burrows. Large anemone visible in image.

Location	Station	Replicate	Other Salient Features/Comment
REF-C	1	B	Loosely packed fine sediment is oxidized, light tan in color. Small clasts deposited at SWI. Hydroid growth.
REF-C	2	A	Loosely packed fine sediment is oxidized, light tan in color. Small clasts deposited at SWI. Shrimp in center of image.
REF-C	2	D	Image is very cloudy. SWI is oxidized but no features visible. Large anemone visible.
REF-C	3	A	Loosely packed fine sediment is oxidized, light tan in color. Small clasts deposited at SWI. Abundant tracks cross SWI. Few large burrow openings visible.
REF-C	4	A	Loosely packed fine sediment is oxidized, light tan in color. Small clasts deposited at SWI. Abundant tracks cross SWI. Few large burrow openings visible.
REF-C	4	B	Loosely packed fine sediment is oxidized, light tan in color. Small clasts deposited at SWI. Abundant tracks cross SWI. Large rope crosses upper left corner of image.
REF-C	5	A	Loosely packed fine sediment is oxidized, light tan in color. Shrimp in image. Large square objected covered with mud drape in center of image.
REF-C	5	B	Image is very cloudy. SWI is oxidized but no features visible.

APPENDIX D

GRAIN SIZE SCALE FOR SEDIMENTS

Phi (Φ) Size	Size Range (mm)	Size Class (Wentworth Class)
<-1	>2	Gravel
0 to –1	1 to 2	Very coarse sand
1 to 0	0.5 to 1	Coarse sand
2 to 1	0.25 to 0.5	Medium sand
3 to 2	0.125 to 0.25	Fine sand
4 to 3	0.0625 to 0.125	Very fine sand
>4	<0.0625	Silt/clay